2mip

NASA TECHNICAL TRANSLATION NASA TT F-15,536

SPACE RESEARCH IN THE UKRAINE NO. 2, SPACE MECHANICS AND CONTROL SYSTEMS

Yu.A. Mitropol'skiy, ed.

Translation of Kosmicheskiye Issledovaniya na Ukraine. Vypusk 2, Kosmicheskaya Mekhanika i Upravlyayuschiye Sistemy, Kiev, "Naukova Dumka" Publisher, 1973, 95 pp.

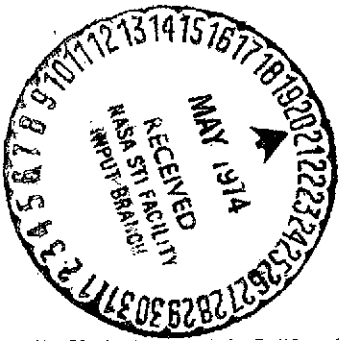

(NASA-TT-F-15536) SPACE RESEARCH IN THE UKRAINE. PART 2: SPACE MECHANICS AND CONTROL SYSTEMS (Kanner (Leo) Associates) 147 p HC $10.50 CSCL 22C

N74-22475

Unclas
G3/30 37889

NATIONAL AERONAUTICS AND SPACE ADMINISTRATION
WASHINGTON, D.C. 20546 MAY 1974

STANDARD TITLE PAGE

1. Report No. NASA TT F-15,536	2. Government Accession No.	3. Recipient's Catalog No.
4. Title and Subtitle SPACE RESEARCH IN THE UKRAINE. NO. 2, SPACE MECHANICS AND CONTROL SYSTEMS		5. Report Date May 1974 6. Performing Organization Code
7. Author(s) Yu. A. Mitropol'skiy, Editor		8. Performing Organization Report No. 10. Work Unit No.
9. Performing Organization Name and Address Leo Kanner Associates Redwood City, California 94063		11. Contract or Grant No. NASw-2481 13. Type of Report and Period Covered Translation
12. Sponsoring Agency Name and Address National Aeronautics and Space Administration, Washington, D.C. 20546		14. Sponsoring Agency Code

15. Supplementary Notes

Translation of Kosmicheskiye Issledovaniya na Ukraine. Vypusk 2, Kosmicheskaya Mekhanika i Upravlyayushchiye Sistemy, Kiev, "Naukova Dumka" Publisher, 1973, 95 pages

16. Abstract

This collection presents articles on urgent problems in space mechanics and the control of space objects. Discussed are problems of oscillations, stability, and stabilization of flight craft, and also trajectory problems of the injection of spacecraft into orbits, problems of the orbital attitude change of similar artificial earth satellites (AES), orientation of space flight craft, and the aerodynamics of AES.

17. Key Words (Selected by Author(s))	18. Distribution Statement
	Unclassified-Unlimited

19. Security Classif. (of this report)	20. Security Classif. (of this page)	21. No. of Pages	22. Price
Unclassified	Unclassified	147	10.50

NASA-HQ

Table of Contents

"Several problems in the aerodynamics of Interkosmos and Kosmos series satellites," B.M. Kovtunenko, A.I. Vasil'yeva, V.F. Kameko, Yu.T. Reznichenko, and E.P. Yaskevich, Kosmicheskiye issledovaniya na Ukraine [Space research in the Ukraine], No. 2, "Naukova dumka," Kiev, 1973, pp. 1 - 15.

A method for determining aerodynamic characteristics of a satellite in sun-synchronous orbit is presented, with allowance for the instantaneous position and orientation in orbit.

Based on the deceleration parameters of the AES Interkosmos-1, Interkosmos-4, Kosmos-166, and Kosmos-230, using local values of the coefficient C_x at the orbital perigee, the upper-atmospheric densities were determined in the altitude range h = 200 - 320 km corresponding to the mean level of solar activity. A comparison is given of the resulting densities with the data from the CIRA-65 model. The influence of the semiannual effect in the fluctuations of the upper-atmospheric density appeared in the experimental data.

Bibliography: 13 entries. Figures: 8. Tables: 3.

"Selection of extremal trajectories for the launch of AES from orbit," N.F. Gerasyuta, E.P. Kompaniyets, and A.A. Krasovskiy, Kosmicheskiye issledovaniya na Ukraine, No. 2, "Naukova dumka," Kiev, 1973, pp. 16-- 33.

A method for selecting control programs for a space object in the orbital departure section of AES providing, for specified fuel reserves onboard the object, the extremal value of some functional is proposed; the functional may be taken as the parameters of the endpoint of the powered section or the parameters of the initial orbit, or any other functional that depends on these parameters.

The analysis was conducted for the case of the Newtonian representation of the Earth gravity field potential with certain simplifications for the powered trajectory section.

Bibliography: 8 entries.

"Analysis of problems of spacecraft navigation and control," V.V. Gorbuntsov, V.G. Komarov, V.F. Lager', G.L. Madatov, and A.T. Onishchenko, Kosmicheskiye issledovaniya na Ukraine, No. 2, "Naukova dumka," Kiev, 1973, pp. 34 - 48.

A method of optimizing programming functions is described, based on the criterion of the maximum response, which consists of

constructing the absolutely-minimum Lyapunov-Bellman function as the envelope of a $(n - 1)$-parametric family of partial integrals traversing the point $(\overline{x}_0, t_0)$ of the phase space $X = \{x_n\}$.

Problems of optimizing the control for cases of spacecraft motion along elliptical orbits and when entering a planetary atmosphere are examined, using the Pontryagin principle of the maximum. The variational boundary value problem is solved with optimization of the functional within a certain interval of motion.

Bibliography: 10 entries. Figures: 2.

"Use of the finite-rotation vector in onboard digital computers for determining spacecraft orientation," A.P. Panov, Kosmicheskiye issledovaniya na Ukraine, No. 2, "Naukova dumka," Kiev, 1973, pp. 49 - 56.

The possibility of using in onboard digital computers the finite-rotation vector for determining the orientation of spacecraft (SC) based on readings of integrating rate transducers hard-mounted on the SC is examined.

It is shown that determining the SC orientation by using the finite-rotation vector is preferable from the standpoint of attaining the smallest volume of computations in the onboard digital computer, than the use of quaternions in the form of Rodrig-Hamilton parameters, since the gain in computation volume is nearly 30%.

Recursion algorithms of the first and second order of precision are presented for computation in the digital onboard computer of the projections of the finite-rotation vector, and error estimates of these algorithms are given.

Bibliography: 9 entries.

"Operating economy of spacecraft stabilization systems," N.F. Gerasyuta, Yu.D. Sheptun, and S.V. Yaroshevich, Kosmicheskiye issledovaniya na Ukraine, No. 2, "Naukova dumka," Kiev, 1973, pp. 57 - 69.

The possibility of increasing the operating economy of a relay system of orientation for a spacecraft moving outside the atmosphere with or without the presence of a constant perturbing moment is examined. Oscillations of the system are considered, with reference to the possible nonequality of the impulses of control moments produced per unit engagements of the actuators ($\Delta\omega \neq 0$). For the case when a perturbing moment is acting and $\Delta\omega \neq 0$, both

simple and complex natural oscillations can be established. The appropriate selection of $\Delta\omega$ minimizes the amount of energy expended.

Bibliography: 3 entries. Figures: 10.

"Problems of oscillations and the stability of motion of multi- /95
dimensional elastic and elastofluid controlled objects," A.I. Kukhtenko, V.V. Udilov, and B.A. Gudymenko, Kosmicheskiye issledovaniya na Ukraine, No. 2, "Naukova dumka," Kiev, 1973, pp. 70 - 87

The possibilities of using methods from the theory of the representation of groups and the method of decomposition in solving problems of the control of the motion of elastoliquid objects are discussed.

As an example illustrating the procedure of applying the theory of the representations of groups, the problem of the natural oscillations of an elastic orbital space station is examined. The forms of natural oscillations are presented by symmetry types; the multiplicities of natural frequencies are found and a decomposition (subdivision of the system into a series of subsystems) of a mathematical model of the control object is made, on the basis of symmetry properties.

Bibliography: 20 entries. Figures: 3.

"Analysis of natural oscillations of a spacecraft," N.F. Gerasyuta, Yu.D. Sheptun, and S.V. Yaroshevich, Kosmicheskiye issledovania na Ukraine, No. 2, "Naukova dumka," Kiev, 1973, pp. 88 - 106.

Oscillations of an aerodynamically unstable spacecraft with a relay jet orientation system, moving at the altitude h = 100 - 120 km, and acted on by a constant perturbing moment, are examined. The effect of the difference in the control impulses and atmospheric density on the nature of motion is investigated. The problem is solved by methods of point transformations and the theory of bifurcations. It is shown that with increase in atmospheric density, the multiplicity of complex oscillations decreases, and the sequence of the onset of bifurcation moments changes. The stability of simple and complex oscillations is proven; a comparison is made of the amounts of energy expended in orientation. It is shown that the energy consumption depends essentially on the difference of the impulses of the control instants.

Bibliography: 5 entries. Figures: 10. Tables: 2.

"Integration of Euler's kinematic equations," A.I. Tkachenko, Kosmicheskiye issledovaniya na Ukraine, No. 2, "Naukova dumka," Kiev, 1973, pp. 107 - 114.

The problem of computing the Euler angles characterizing the orientation of a spacecraft in space is discussed. First- and second-order algorithms are suggested for integrating the Euler kinematic equations.

"An algorithm for computing the trajectory of the injection of a space object into orbit," A.A. Krasovskiy and L.T. Gripp, Kosmicheskiye issledovaniya na Ukraine, No. 2, "Naukova dumka," Kiev, 1973, pp. 115 - 127.

A universal algorithm for the numerical integration of the equations of motion of a space object over the injection trajectory section is examined.

The algorithm is based on the method of successive approximations and the approximation of the right sides of the differential equations of motion by interpolational power polynomials. The trajectory elements were computed by using a reference trajectory specified in a simple analytic form.

Bibliography: 5 entries. Figures: 3.

"Analytic-numerical method of computing attitude changes of similar AES," A.A. Krasovskiy, Ye.I. Bushuyev, E.P. Kompaniyets, and A.A. Vasil'yeva, Kosmicheskiye issledovaniya na Ukraine, No. 2, "Naukova dumka," Kiev, 1973, pp. 128 - 140.

The motion of near Earth satellites for which the principal perturbing factors are the noncentrality of the Earth gravity field and the atmospheric drag is considered.

An analytic-numerical method of computing the orbital attitude changes is proposed, based on the equations of motion in osculating elements. Perturbations of the elements during a single revolution of the AES are determined by finite formulas, with reference to the second, third and fourth zonal harmonics of the expansion of the geopotential, and also with reference to the atmospheric drag, described by a dynamic model.

From preliminary estimates, the errors of the proposed method caused by the analytic representation of the perturbations of the orbital elements do not exceed 5%.

Bibliography: 8 entries. Figures: 1.

SEVERAL PROBLEMS IN THE AERODYNAMICS OF INTERKOSMOS AND KOSMOS SERIES SATELLITES

B.M. Kovtunenko, A.I. Vasil'yeva, V.F. Kameko, Yu.T. Reznichenko, and E.P. Yaskevich

Analysis of the parameters of sun-synchronized AES [artificial earth satellites] is of definite practical interest for aerodynamicists, since for this type of satellite the angle of attack is a slow-varying parameter and can be determined simply. As a consequence, full-scale values of aerodynamic characteristics and the density of the upper atmosphere can be determined more exactly. These AES include the satellites considered in the present article, Interkosmos-1, Interkosmos-4, Kosmos-166, and Kosmos-230, launched into orbit with the parameters indicated in Table 1. These satellites have identical geometrical shape (Fig. 1), formed by a prismatic body with spherical bases, eight solar battery panels mounted perpendicularly to the longitudinal axis of the body, and scientific equipment bays carried on a special platform. /3*

The main factor determining the ballistic lifetime and characteristics of the system of orientation of satellites with orbital altitude $h < 600$ km, is the aerodynamic action of the incident flow of rarified upper-atmospheric gas. The purpose of this article is the analysis of calculated and full-scale experimental data on the aerodynamics of Interkosmos satellites.

The aerodynamic characteristics of a body, dimensionless coefficients of surface forces, are calculated by integration over the surface of the body A of the forces acting at an elementary surface area, i.e., the overall forces and moment will be

$$\bar{P} = \int_A P_n \bar{n} dA + \int_A P_\tau \bar{\tau} dA + \int_A P_b \bar{b} dA;$$

$$\bar{M} = \int_A P_n [\bar{r}\bar{n}]\, dA + \int_A P_\tau [\bar{r}\bar{\tau}]\, dA + \int_A P_b [\bar{r}\bar{b}]\, dA,$$

where P_n, P_τ, and P_b are the normal, tangential, and binormal projections of the lift acting over the elementary area dA; $\bar{r}$ is the radius-vector of the elementary area.

In the case of the freely molecular streamlining regime when the Knudsen number $K_s \gg 1$ [1], the forces acting at dA do not

*Numbers in the margin indicate pagination in the foreign text.

depend on flow past the remaining surface and finding of the integrals is much simplified.

In calculating nonconvex bodies, of the type of Interkosmos series satellites, it is necessary to introduce a correction for the interference caused by the shading of some satellite structural members by others and for the repeated collisions of flow molecules with the surface.

The exact calculation of the aerodynamic characteristics of satellites is very difficult, since thus far full-scale parameters of the interaction of the incident flow of rarified gas with the surface are unknown. At the present time there are several interaction schemes [2, 3, 4] obtained on the basis of theoretical and laboratory investigations. One of the most common is the diffuse-mirror scheme [2], which was adapted in the calculations of the aerodynamic characteristics of Interkosmos satellites.

Limited full-scale experimental data [5, 6] indicate /4 generally in favor of the nearly diffuse character of the reflection of molecules from the satellite surface and the values of the coefficient of accommodation α_{ac} close to unity. Because of this, and with reference to the actual properties of satellite surfaces, in the calculations the values $\sigma_n = \sigma_\tau = \alpha_{ac} = 1$ were adopted, where σ_n and σ_τ are the coefficients of exchange of normal and tangential momentum.

TABLE 1.

Date	Satellite	Apogee, km	Perigee, km	Inclination of Orbit to the Equatorial Plane, Degrees	Period of Revolution, min
10/14/1969	Interkosmos-1	640	260	48.4	93.3
10/14/1970	Interkosmos-4	668	263	48.5	93.6
16/ 7 /1967	Kosmos-166	578	283	48.4	92.9
5 / 8 /1968	Kosmos-230	563	288	48.4	92.8

For the adopted scheme of interaction, the projections of the lift P_n, P_τ, and P_b are expressed by the following formulas [7]:

$$P_n = \left\{ \frac{\sin\alpha_i}{s\sqrt{\pi}} e^{-s^2\sin^2\alpha_i} + \left[\frac{1}{2s^2} + \sin^2\alpha_i \right] [1 + \operatorname{erf}(s\sin\alpha_i)] + \right.$$
$$\left. + \frac{1}{2s^2} \sqrt{\frac{T_w}{T_\infty}} e^{-s^2\sin^2\alpha_i} + \frac{\sqrt{\pi}}{2s} \sqrt{\frac{T_w}{T_\infty}} \sin\alpha_i [1 + \operatorname{erf}(s\sin\alpha_i)] \right\} \frac{\rho v^2}{2};$$
$$P_\tau = \left\{ \frac{\cos\alpha_i}{s\sqrt{\pi}} e^{-s^2\sin^2\alpha_i} + \sin\alpha_i \cos\alpha_i [1 + \operatorname{erf}(s\sin\alpha_i)] \right\} \frac{\rho v^2}{2};$$

$P_b = 0$ (the surface is assumed isotropic).

Here α_i is the local angle of attack of the area; $s = v/v_t$ is the ratio of the velocity of the incident flow to the most probable thermal velocity of the molecules in the flow; T_∞ is the temperature of the gas in the incident flow; T_W is the temperature of the surface of the body; and ρ is the density of the gas.

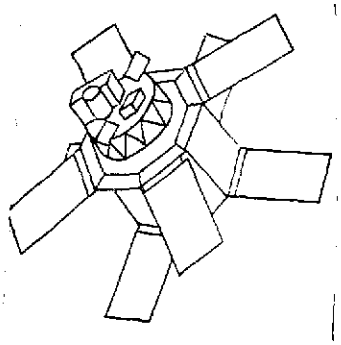

Fig. 1. General view of the satellites Interkosmos-1, Interkosmos-4, Kosmos-166, and Kosmos-230.

The effect of the nonsteady-state nature of flow past a satellite caused by oscillations relative to the center of mass with an angular velocity ω was not taken into account in the calculations, since the additional forces and moments induced thereby are of the order of $\sim\omega R/v$ compared to the steady characteristics [7] and are negligibly small in our case.

The calculated values of the drag coefficient of the satellites C_x given with respect to the area $A = 4.27\ m^2$, the coefficient of the aerodynamic moment relative to the center of mass m_z given with respect to the same area and to the length $L = 1.8$ m, and the coordinates of the center of pressure relative to the center mass l_d [illegible] calculated with allowance for the effect of shading as a function of the satellite angle of attack α are presented in Fig. 2. Here it was assumed that α is the angle between the direction of the longitudinal axis of the satellite Ox facing the Sun and the vector of satellite velocity $\bar{v}_0$ relative to the incident flow; the axis Oz relative to which the coefficient m_z was calculated is always perpendicular to the plane $\bar{v}_0 Ox$. Since the angle α does not determine uniquely the position of the satellite in the flow, the angle ϕ of rotation relative to the plane of the angle of attack was also introduced (Fig. 2). /5

To simulate the motion of a satellite in orbit in order to make an analysis of the aerodynamic forces and moments acting during flight, it is necessary to determine the values of the angle of attack α as a function of time. To do this, let us introduce the following rectangular right-handed coordinate systems:

-- the absolute system $Ax_a y_a z_a$; the axis Az_a coincides with the Earth axis and the direction to the North Star; the axis Ax_a is directed toward the point of the Vernal Equinox γ;

-- the terrestrial system $Ex_e y_e z_e$; the axis Ez_e is oriented from the center of the Earth along its axis of rotation toward the North Star; the axis Ex_e is oriented toward the point of intersection of the Greenwich Meridian with the equator; and

-- the orbital system $Cx_0 y_0 z_0$; the axis CY_0 is oriented from the center of the Earth to the satellite center of mass; the axis CX_0 lies in the orbital plane and is oriented in the direction of motion.

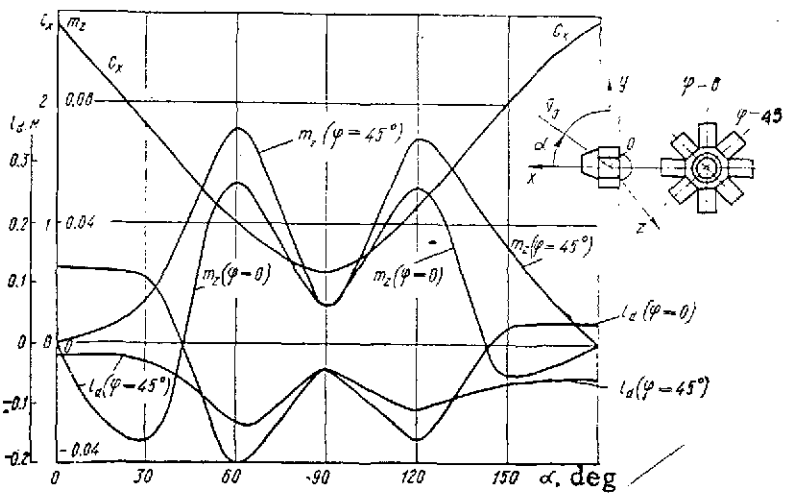

Fig. 2. Calculated values of the coefficient of aerodynamic drag C_x, the coefficient of aerodynamic moment m_z, and the coordinates of the center of pressure l_d as functions of the satellite angle of attack α.

The instantaneous values of the angle of attack α are determined by finding the projections of the vector $\bar{v}_0$ and the vector of direction toward the Sun $\bar{s}$ in the system $Cx_0 y_0 z_0$. The expressions for the projections of the vector $\bar{v}_0$ in the orbital system of coordinates are assumed to be analogous to those obtained in the study [8], according to which the vector $\bar{v}_0$ is defined by the ellipticity of the orbit and by the wind in the upper atmosphere:

$$\bar{v}_0 = \bar{v} + \bar{v}_r$$

Here $\bar{v}$ is the vector of the satellite velocity; $\bar{v}_r$ is the vector of satellite velocity relative to the rotating atmosphere; the projections of the vector $\bar{v}$ on the axes of the system $Cx_0 y_0 z_0$ are of the form

$$\bar{v}\left[\sqrt{\frac{\mu}{p}}(1+e\cos\nu);\ \sqrt{\frac{\mu}{p}}e\sin\nu;\ 0\right].$$

Neglecting the orbital precession in a revolution, we can represent the projections of the vector $\bar{v}_r$ on the axes of the system $Cx_0y_0z_0$

$$\bar{v}_r[-r(\omega_e+\sigma)\cos i;\ 0;\ -r(\omega_e+\sigma)\sin i\cos u].$$

The modulus of the vector $\bar{v}_0$ is

/6

$$v_0=\sqrt{\left[\sqrt{\frac{\mu}{p}}(1+e\cos\nu)-(\omega_e+\sigma)r\cos i\right]^2+\frac{\mu}{p}e^2\sin^2\nu+(\omega_e+\sigma)^2r^2\sin^2 i\cos^2 u}.$$

The direction cosines of the vector $\bar{v}_0$ in the system $Cx_0y_0z_0$ will be $\bar{v}(\beta_1;\beta_2;\beta_3)$, where

$$\beta_1=\frac{\sqrt{\frac{\mu}{p}}(1+e\cos\nu)-(\omega_e+\tau)r\cos i}{v_0};\quad \beta_2=\frac{\sqrt{\frac{\mu}{p}}e\sin\nu}{v_0};$$

$$\beta_3=\frac{(\omega_e+\sigma)r\sin i\cos u}{v_0};$$

e, i, and ν are the osculating elements of the orbit; ω_e is the angular rate of rotation of the Earth; σ is the "index of circulation" -- the angular velocity of the motion of air in the westerly direction relative to the Earth's surface; r is the modulus of the radius-vector of the satellite center of mass; p is the focal parameter; and μ is the gravitational constant of the Earth.

The position of the longitudinal satellite axis Ox, coinciding in our case with the vector of solar orientation $\bar{s}$ to a precision of $\pm 2^\circ$, is determined by two angles -- right ascension α_1 and declination δ. The direction cosines of vector $\bar{s}$ in the system $Ax_ay_az_a$ will be

$$s_x^A=\cos\delta\cos\alpha_1;$$

$$s_y^A=\cos\delta\sin\alpha_1;$$

$$s_z^A=\sin\delta.$$

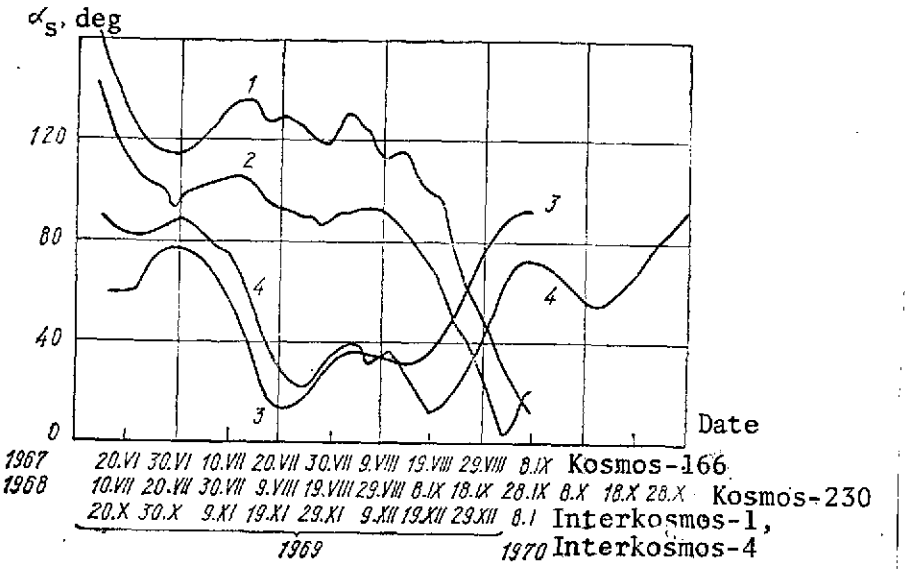

Fig. 3. Actual values of the satellite angles of attack in the orbital perigee:
1. Interkosmos-1
2. Interkosmos-4
3. Kosmos-166
4. Kosmos-230

The direction cosines of the vector $\bar{s}$ in the system $Ex_0y_ez_e$ are as follows:

$$s_x^e = \cos\delta\cos(\alpha_1 - \Omega_0);$$
$$s_y^e = \cos\delta\sin(\alpha_1 - \Omega_0);$$
$$s_z^e = \sin\delta,$$

where Ω_0 is Greenwich ephemeris time, $\Omega_0 = \left[\frac{S_0}{1+k} - (N+1) + t\right]\omega_e \times 3600$ /7

S_0 is the true stellar time of universal midnight; k is the correction for the difference between the stellar and mean solar times; N is the number of the time zone relative to which the time is reckoned; and t is the zone time.

The direction cosines s_i (i = x, y, z) of the vector $\bar{s}$ in the system $Cx_0y_0z_0$ will be

$$s_i^0 = \sigma_{j1}s_x^e + \sigma_{j2}s_y^e + \sigma_{j3}s_z^e,$$

where σ_{j1}, σ_{j2}, σ_{j3} (j = 1, 2, 3) are the elements of the matrix of the conversion from the terrestrial coordinate system to the orbital.

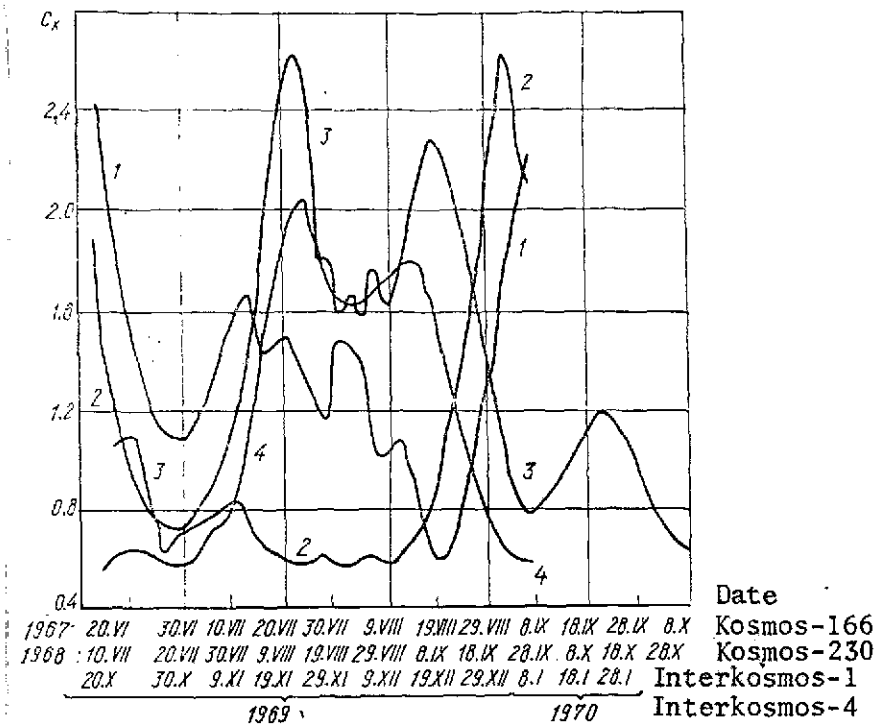

Fig. 4. Instantaneous values of the coefficient of aerodynamic drag in the orbital perigee:
1. Interkosmos-1
2. Interkosmos-4
3. Kosmos-166
4. Kosmos-230

The instantaneous value of the satellite angle of attack α is defined from the scalar product of the vector $\bar{v}_0$ and $\bar{s}$:

$$\alpha = \arccos(\beta_1 s_x^0 + \beta_2 s_y^0 + \beta_3 s_z^0).$$

Figure 3 presents the time-varying actual angles of attack α_s of the satellites Interkosmos-1, Interkosmos-4, Kosmos-166, and Kosmos-230 in the orbital perigee calculated by the method presented. Knowing the actual angles of attack permits the more exact determination of the instantaneous values of the aerodynamic characteristics. Figure 4 presents the instantaneous values of the coefficient C_x of the satellites under study in the orbital perigee, obtained from the data of the plots in Figs. 2 and 3. The drag coefficient C_x of the Interkosmos satellites is a smoothly varying function of the lifetime in the range of values 0.5-2.6; here the area of the midsection is assumed constant and equal to the area of the projection of the satellite onto a plane normal to the satellite axis of symmetry.

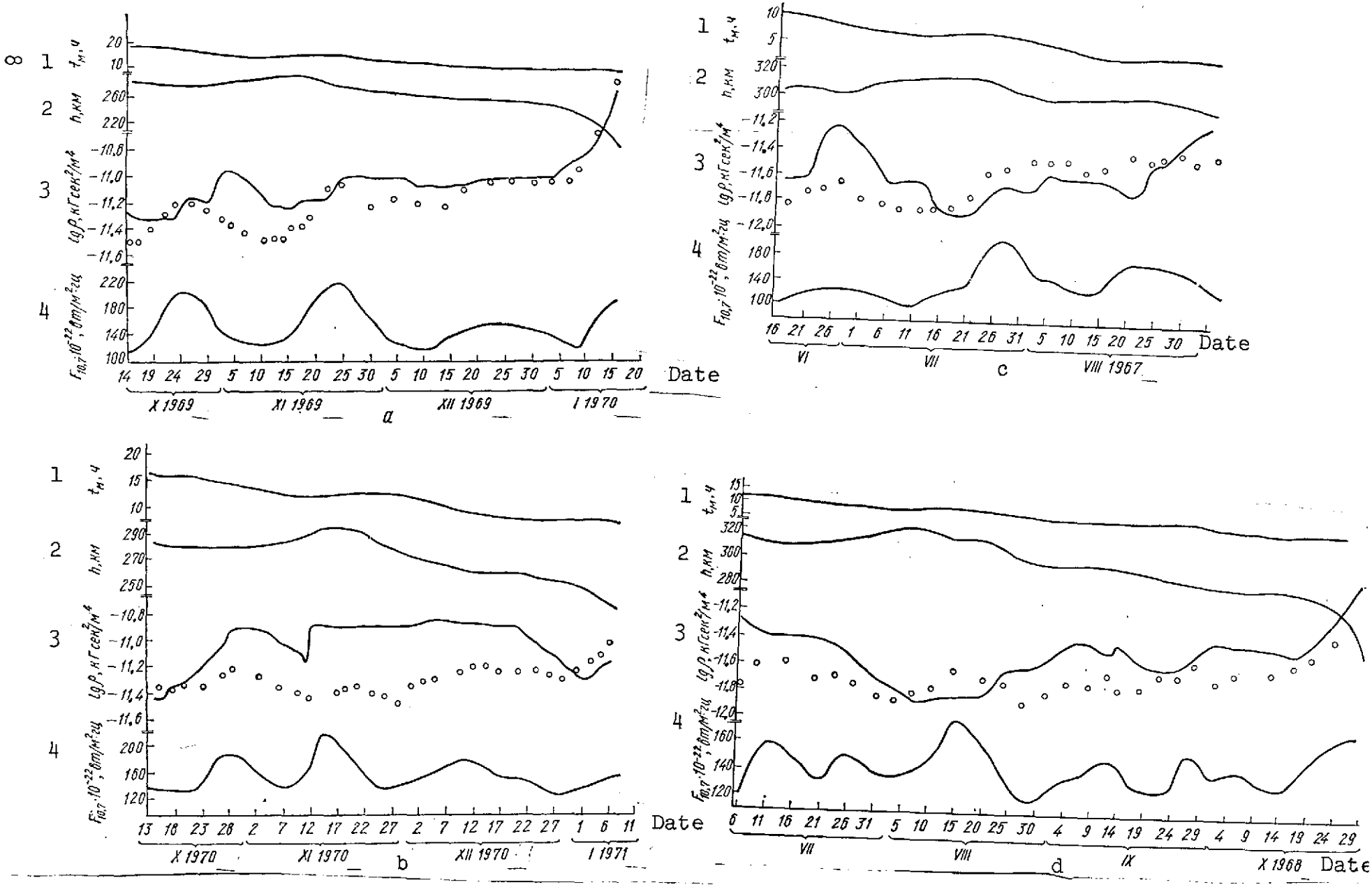

Fig. 5. Density of upper atmosphere from the data on the deceleration of the satellites Interkosmos-1 (a), Interkosmos-4 (b), Kosmos-166 (c), and Kosmos-230 (d) (O = corresponding densities according to the model CIRA-65). [Key on following page.]

Key to Fig. 5: 1. t_{lo}, hr
2. km
3. $kg \cdot sec^2/m^4$
4. $w/m^2 \cdot Hz$

Using the actual flight data of the satellites Interkosmos-1, /8
Interkosmos-4, Kosmos-166, and Kosmos-230, an analysis was made of the calculated and experimental aerodynamic characteristics. To do this, from the variation in the satellite orbital parameters, the density of the upper atmosphere was determined and compared with the data of the upper-atmospheric model CIRA-65; the actual momenta imparted to the orientation system of the Kosmos-230 satellite in flight were determined and compared with the calculated aerodynamic momentum; also compared was the actual lifetime of the satellites with their predicted values.

The upper-atmospheric density was determined by a method presented in the works [9, 10]. Figure 5 presents experimental values of the density ρ_{ex} obtained by using instantaneous values /9
of the coefficient C_x corresponding to the actual α_s (see Fig. 4), and also the altitudes above the Earth surface h, local time t_{lo}, and the index of solar activity $F_{10.7}$. Here also are presented, for comparison, the densities ρ_{CIRA} from the data of the CIRA-65 model, taken for the corresponding experimental values h, t_{lo}, and $F_{10.7}$. Here the effects associated with the geomagnetic activity and the semiannual variations in density were not taken into account.

The differences between the semiannual values ρ_{ex} and ρ_{CIRA} are accounted for mainly by the effect of semiannual variations, which are expressed by a density maximum in October-November and in April, and by a minumum in July and January [11]. The lifetimes of the satellites Interkosmos-1, Interkosmos-4, Kosmos-166, and /10
Kosmos-230 cover these characteristic periods (except for April). From the plots (Fig. 5) the mean relative deviations of ρ_{ex} from ρ_{CIRA} were determined, characterizing the semiannual fluctuations in density; the data are given in Table 2.

During the flight of the Interkosmos series satellites in the altitude range h ≈ 200 - 600 km, the main perturbing factor affecting motion relative to the center of mass is the aerodynamic moment. To maintain constant orientation toward the Sun, the satellites are equipped with an electric flywheel system of orientation, which continually compensates for the action of the perturbing aerodynamic moments, each time imparting to the satellite a momentum equal in magnitude and opposite in sense to the momentum of the external aerodynamic forces. For unloading of the flywheels, on board the satellites is a gas-jet system periodically compensating the momentum accumulated by the

TABLE 2.

Period Considered	Satellite	Mean Relative Deviation of Experimental Density Values from Model Values $(\rho_{CIRA} - \rho_{ex})/\rho_{ex}$
15 Jul - 24 Aug 1967	Kosmos-166	0.44
5-22 Aug 1968	Kosmos-230	0.32
1-29 Oct 1968	Kosmos-230	-0.35
27 Oct - 29 Nov 1969	Interkosmos-1	-0.38
21 Oct - 2 Nov 1970	Interkosmos-4	-0.59
10-16 Jan 1970	Interkosmos-1	0.09
1-7 Jan 1971	Interkosmos-4	0.28

flywheels. Thus, it was of interest to compare the actual momentum M_e^m communicated to the satellite by its gas-jet system, with the calculated momentum M_a^m of the external aerodynamic forces obtained for the actual parameters of satellite orbit and orientation. This comparison is made below for the example of the Kosmos-230 satellite.

Using the law of conservation of momentum [12], for a certain time interval $t_0 - t_k$ we can write the equation

$$\int_{t_0}^{t_k} M_{aer}\,dt = \sum_{i=1}^{n} M_{con}\,t_i,$$

where $M_{aer} = (1/2)m_z AL\rho v_0^2$ is the aerodynamic moment; $M_{con} = Rl$ is the control moment; t_i is the time during which the engine of the gas-jet system is operating at the i-th cut-in; $R = p_0 f_{cr} K_p \phi_l$ is the engine thrust; p_0 is the pressure in front of the nozzle; f_{cr} is the area of the nozzle critical section; K_p is the thrust coefficient; ϕ_l is the coefficient of losses in the nozzle; and l is the arm at which the engine thrust is applied relative to the center of mass.

The time t_i in some interval $t_0 - t_k$ is defined from the mean value of the pressure drop p_{av} in the cylinders of the gas-jet system on the assumption that a single nozzle is operating. Figure 6 presents the actual values of p for the Kosmos-230 satellites. The sawtooth nature of the variation in p is accounted for by fluctuations in the temperature T of the gas in the cylinders:

$$t_i = \frac{\dot{G}_{sp} R_g T}{\Delta p V_c}$$

where $\dot{G}_{sp}$ is the specific nozzle consumption per second, V_c is the cylinder capacity, and R_g is the gas constant.

Since the directions in which the engines of the gas-jet system act are at the angle $\pi/2$, and the direction of the action of the momentum vector is equiprobable, the experimental values of the momentum M_{ex} corresponding to the maximum Rl and the minimum $Rl\cos\frac{\pi}{4}$ control moment were determined (Fig. 7). The momentum due to the action of aerodynamic forces was integrated over the intervals $t_0 - t_k$; here the limiting deviations of the calculated values of the modulus of the coefficient m_z (see Fig. 2) corresponding to the angle of attack α_s at the perigee (see Fig. 3) were used. The density of the upper atmosphere was assumed according to the CIRA-65 model for the altitude $h_p + \lambda H$ (here h_p is the perigee altitude, H is the altitude of the homogeneous atmosphere, and λ is a coefficient that allows for the ellipticity of the orbit), the local time at the perigee, and actual level of solar activity $F_{10.7}$. The region of the possible calculated values M_a^m is given in Fig. 7. /11 /12

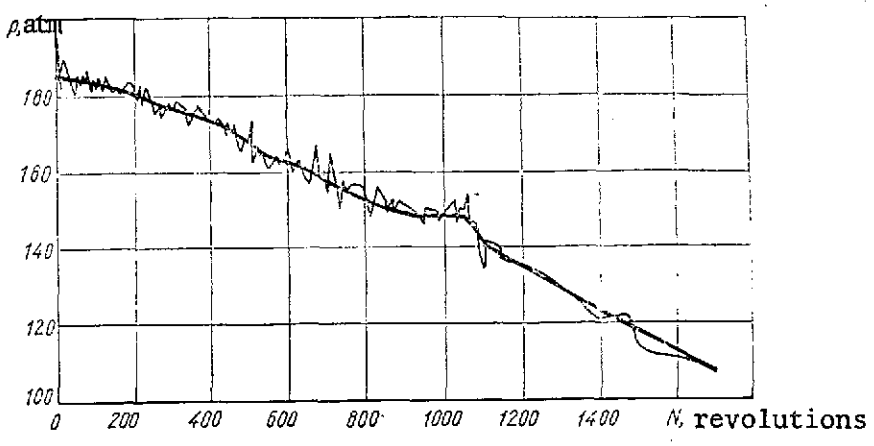

Fig. 6. Variation in actual pressure in cylinders of the gas-jet system of the Kosmos-230 satellite; the thicker line corresponds to the mean pressure.

From this figure it follows that in the period from 7 August to 18 September 1968, when the angles of attack α_s were small ($\alpha_s \lesssim 10$-$40°$), the regions of the values M_e^m and M_a^m coincided. In the periods from 27 July to 4 August, and from 20 September to 21 October, when the α_s values were 50-70°, and the calculated values of m_z had maxima, a deviation was observed; M_e^m was approximately 60 and (70-80)% of M_a^m, respectively. This deviation can be accounted for by the following causes.

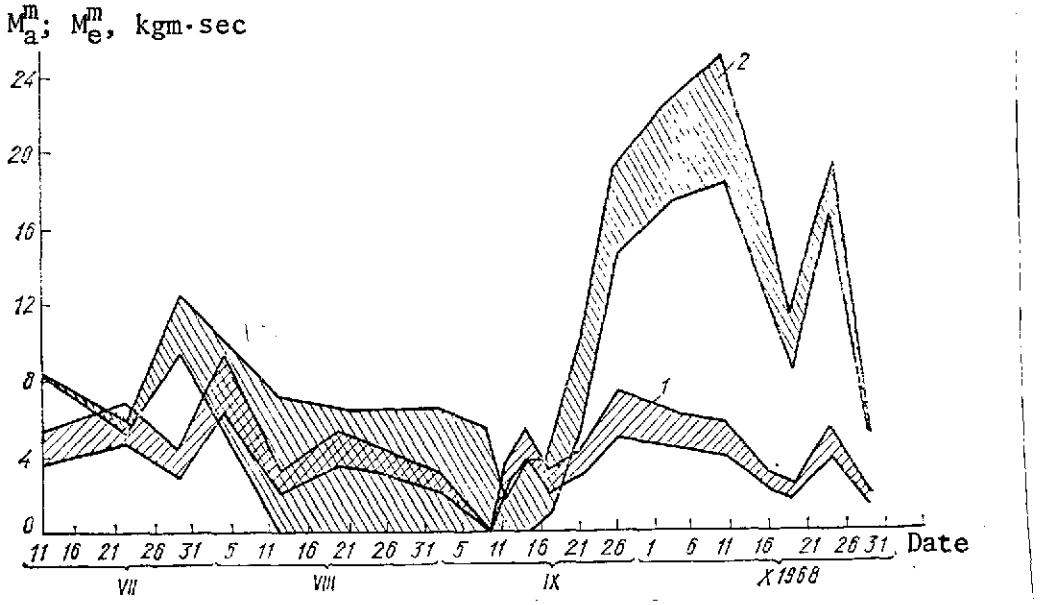

Fig. 7. Actual M_e^m and calculated M_a^m values of the momentum due to the action of aerodynamic forces of the Kosmos-230 satellite:
1. Region of possible actual values M_e^m;
2. Region of possible calculated values M_a^m.

1. Since the satellite is a body of complex configuration, molecules reflected from the surface undergo multiple collisions with the surface (interference effect). In the case of the Kosmos-230 satellite for which the angles of attack are in the region $\alpha_s \leq 90°$, the interference is characterized by the collision of reflected molecules with the reverse side of the solar batteries. This leads to the generation of a moment M_g that is opposite in sense to the perturbing aerodynamic moment and, as shown by estimates, is about 60% of M_{aer}. This ratio of M_{aer} and M_g is promoted by the relatively short distance between the satellite center of mass and the center of pressure ld calculated without allowance for interference (see Fig. 2).

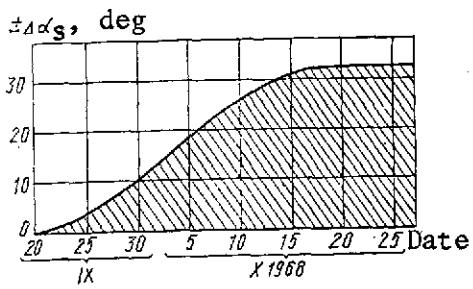

Fig. 8. Region of possible deviations of the angle of attack of the Kosmos-230 satellite in the penumbra of the Earth from the values α_s calculated without allowing for the shadowed section of the orbit.

2. The values of M_a^m (see Fig. 7) were calculated on the condition of flow past the satellite at the angle of attack α_s. This condition is not exactly fulfilled especially at the end of the lifetime when the orbit becomes weakly elliptical. When the satellite

passes the region of maximum aerodynamic head in the region of the orbital perigee, the values of α can differ appreciably from α_s. For example, on 7 October 1968 the angle of attack of Kosmos-230 was $\alpha_s = 57°$, and the change in α relative to α_s in the region of altitudes $h_p - (h_p + \lambda H)$ was $\pm 35°$. This reduces the averaged coefficient m_z in the perigee region by about 50%, and with reference to the averaging of the density leads to an approximately 25% reduction in M_a^m.

3. In the period from 20 September to 21 October 1968 (see Fig. 5 d), the local time at the point of perigee t_{lo} was $t_{lo} = 4.5 - 1.5$ hours, that is, the region of the perigee of the satellite orbit was in the shadow of the Earth. Over this section the satellite executed unoriented motion relative to the center of mass with the angular rate $\dot{\omega}$ equal to $0 \leq \omega \leq 0.5$ deg/sec. This also led to averaging, and in this time range, it also led to a decrease in the calculated value of m_z. The region of deviation of the angles of attack of Kosmos-230 in the shadow of the Earth from the α_s values calculated on the assumption of a nonshadowed section is shown in Fig. 8.

4. The scheme of reflection of the incident flow of rarified gas from the satellite surface was assumed to be completely diffuse. Actually, the parameters of full-scale interaction can differ from those adopted in this study, which can also account for the difference obtained in the values of M_e^m and M_a^m. The authors determined the values of M_a^m using the scheme of interaction given in [4], that allows for the dependence of the coefficients σ_s and σ_τ on the angle of inclination of the area to the flow. The resulting values exceeded the values of M_a^m given in Fig. 7 by a factor of three.

It was of interest to analyze (see Fig. 6) the drop in pressure p in the gas-jet system cylinders. The values of p_{av} in the region of the 560-th to 630th and 940-th to 1060-th revolutions have horizontal sections, indicating the absence during this period of aerodynamic perturbations. Actually, during this period the values of α_s were correspondingly 20-30° and 16-20°, for which m_z is small (see Fig. 2), and for certain angles ϕ the possibility that $m_z = 0$ is not precluded. /13

The precision of the calculation of aerodynamic forces as an integrated characteristic can be determined by comparing the actual ballistic lifetime of satellites with the calculated values.

TABLE 3.

Satellite	Ballistic Lifetime of Satellite in Orbit, Days		Relative Error, %
	Actual	Calculated	
Interkosmos-1	80	82	2.5
Kosmos-166	131	128	2.0
Kosmos-230	120	118	2.0

The calculated time was found by integrating the system of differential equations of the motion of the satellite center of mass in osculating parameters [13], on the assumption that the Earth gravity field corresponds to the potential of a three-axis nonsymmetric ellipsoid. In the calculations use was made of the values of the upper-atmospheric density from the data of the CIRA-65 model, corresponding to the daily values of the index $F_{10.7}$ and to the local time of the satellite track point. The coefficients of the satellite drag C_x at each instant of time corresponded to the actual angles of attack α_s. The calculation results are in Table 3.

The results of analyzing the actual parameters of the motion of Interkosmos series AES indicate the adequate reliability of calculated values of aerodynamic forces and moments obtained by using the wholly diffuse scheme of reflection ($\sigma_n = \sigma_\tau = \alpha_{ac} = 1$) and the upper-atmospheric model CIRA-65.

The authors are thankful to G.I. Zmiyevskaya for discussion of the results, and to N.M. Lukonin for assistance in the calculations.

REFERENCES

1. Shidlovskiy, V.P., Vvedeniye v dinamiku razreshennogo gaza [Introduction to the dynamics of rarified gases], "Nauka," Moscow, 1965.

2. Kogan, M.N., Dinamika razrezhennogo gaza [Dynamics of rarified gases], "Nauka," Moscow, 1967.

3. Barantsev, R.G., in the book Aerodinamika razrezhennykh gazov [Aerodynamics of rarified gases], Vol. 2, Leningrad State University Press, Leningrad, 1965.

4. Marov, M.Ya., G.I. Zmiyevskaya, and A.A. Pyarniuu, "Possibility of refining the parameters of flow interaction with surface and the variation of atmospheric density based on data on changes in satellite motion," Doklad na XIII sessii KOSPAR [Paper presented at the 13th session of COSPAR], Leningrad, 1970.

5. Beletskiy, V.V., Kosmicheskiye issledovaniya 8(2) (1970).

6. Mou, K., Raketnaya tekhnika i kosmonavtika 6(7) (1968).

7. Yaskevich, E.P., and Ye.I. Filatov, in the book: Gidromekhanika i teoriya uprugosti [Hydromechanics and the theory of elasticity], Vol. 6, Khar'kov State University Press, Khar'kov, 1967, p. 17.

8. Kameko, V.F., M.Ya. Marov, and E.P. Yaskevich, Kosmicheskiye issledovaniya 7(4) (1969).

9. King-Khili, D., Teoriya orbit iskusstvennykh sputnikov v atmosfere [Theory of the orbits of artificial statellites in the atmosphere], "Mir," Moscow, 1966.

10. Kameko, V.F., et al., Kosmicheskiye issledovaniya 9(3) (1971).

11. Jacchia, L.G., I.W. Slowey, and I.G. Campbell, "A study of the semiannual density variation in the upper atmosphere from 1958 to 1966, based on satellite drag analysis," COSPAR Meetings, Tokyo, May 1966, Smithsonian Institution Astrophysical Observatory, Cambridge, Massachusetts 02138.

12. Landau, L.D., and Ye.M. Lifshits, Mekhanika [Mechanics], "Nauka," Moscow, 1965.

13. Okhotsimskiy, D.Ye., T.Ye. Eneyev, and G.P. Taratynova, UFN 63(1) (1957).

SELECTION OF EXTREMAL TRAJECTORIES FOR THE LAUNCH OF AES FROM ORBIT

N.F. Gerasyuta, E.P. Kompaniyets, and A.A. Krasovskiy

Much attention at present is being given to the problems of determining extremal trajectories in space ballistics. In most studies the problem of the transfer from one given point in space to another along a trajectory ensuring the minimum fuel consumption is solved. As the optimized functional, use is made of the integral of the form $\int_{t_0}^{t_k} \dot{m} dt$, characterizing the consumption of mass during the flight, that is, essentially, for a specified engine operating regime the duration of the powered trajectory section is optimized. The boundary conditions at the boundary points in this case are assigned completely or some of them remain free. For incompletely assigned boundary conditions, also considered as an additional optimized functional are the parameters of motion at the left [1] or right [2-4] endpoints of integration (velocity, altitude, range, angle of inclination of the velocity vector, and so on) appearing in the coupling equation.

For the case when it is necessary to optimize a certain functional dependent on several or on all parameters of motion (altitude of apogee, altitude of perigee, orbital eccentricity, period of revolution, energy, etc.), the solution is considerably complicated and requires a very long time even when electronic computers are used. This article proposes a method for optimizing the trajectories of launch from orbit of AES, starting from the final target of injection into the assigned orbit. Any characteristic of the resulting orbit can be selected as the optimized functional (apogee altitude, perigee altitude, period of revolution, velocity at any point of the orbit, angular position of the perigee, focal parameter, etc.).

Formulation of the problem. The position of an object in space is completely characterized by six orbital elements (Ω, i, ω, a, e, and τ).

For individual cases (circular or parabolic orbits), several of these elements are meaningless.

In addition to these main elements, in celestial mechanics other quantities are also used, replacing them [5].

Hyperbolic Orbit	Elliptical Orbit
$\Omega,\ i,\ \omega,\ a,\ e,\ \tau;$	$\Omega,\ i,\ \omega,\ a,\ e,\ \tau;$
$\pi,\ h_\pi;$	$\pi,\ n,\ \varphi',\ \varepsilon;$
$\alpha_\tau,\ \beta_\tau,\ \gamma_\tau,\ P;$	$\alpha_\tau,\ \beta_\tau,\ \gamma_\tau,\ T,\ M_0;$
$\alpha'_\tau,\ \beta'_\tau,\ \gamma'_\tau$	$\alpha'_\tau,\ \beta'_\tau,\ \gamma'_\tau,\ h_\pi,\ h_a;$
	P

Here the substituting elements are written under each of the main elements that they can replace.

When space objects are launched, the assigned value of the orbital parameters on which the execution of the given mission depends must be ensured; the remaining parameters, obviously, can be selected arbitrarily.

Let us examine methods for ensuring assigned orbital parameters.

1. The parameters Ω, i, ω and their substituting elements determine the orientation of the orbital plane in space (Ω, i) and the orientation of the major axis in the orbital plane (ω). /15
The assigned values of these parameters for an assigned launch point ($\varphi_{\Gamma\delta}$, λ_0) can be ensured without energy expenditures as the result of selecting:

a. the instant of launch from Earth, and by varying this quantity in the range $0^h \leq t \leq 24^h$ we ensure any desired value of Ω from the range $0 \leq \Omega \leq 360°$;

b. the azimuth of the launch, and by varying this in the range $-90° \leq \psi_0 \leq +90°$ we can ensure any value of the parameter i from the range $(\pi - \varphi_{\Gamma 0}) \leq i \leq f_{\Gamma 0}$; and

c. the instant of launch from the parking orbit, and by varying the instant of launch from this orbit in the range $0 \leq t \leq t$, one can ensure any value of the parameter ω from the range $0 \leq \omega \leq 360°$.

2. The parameter τ and the elements replacing it determine the position of the satellite in orbit at the initial instant of time. The assigned value of this parameter can be ensured by using the intermediate orbit through selecting the corresponding revolution for the transfer to the assigned orbit.

3. The remaining elements (a, e) and their substituting elements (h_π, h_a, P, T, n, and φ') determine the dimensions of the orbit and its shape, and under otherwise equal conditions depend wholly on the parameters of the endpoint of the powered section of the trajectory of the satellite injection into orbit.

Therefore, the main requirement which the selection of the injection trajectory must satisfy is to find the optimal law of control of the launch vehicle flight ensuring the attainment of the assigned value of some functional of interest to us (a, e, h_π, h_a, ...), for minimum energy expenditures or determining the trajectory ensuring the extremal value of some functional (h_π, h_a, P, T, n, ϕ', etc.) for assigned energy expenditures.

Let us examine the motion of a spacecraft (SC) acted on by a planetary gravity field and the SC powerplant. We will assume that the SC has first been injected into a circular or elliptical orbit. At some instant of time it is necessary to execute a maneuver to perform an assigned mission: to leave the planetary sphere of attraction; to transfer to an elliptical orbit; to land on the planet's surface, etc.

Let us find the trajectory ensuring, for assigned kinematic parameters of the start of the trajectory, the extremal value of some functional I at the moment of engine cut-out, which we will assume to be given. The form of the functional I evidently will depend on the mission to be performed. Owing to reciprocity, the resulting solution will ensure also the attainment of the assigned value of functional I with minimum fuel consumption.

We will assume that the trajectory of the SC in space is defined if we obtain a closed system of differential equations describing the motion of the SC center of mass and if the initial conditions for the integration of this system ensuring the attainment of the extremal value of functional I are selected.

Let us examine the case when the maneuver of the SC occurs in the plane of the initial orbit defined by the parameters of SC motion at the initial instant of time. This assumption, without diminishing the generality of the results and without introducing fundamental and essential errors into the analysis, enables us to simplify our analysis and to select the extremal trajectories.

The system of equations adopted. Let us limit ourselves to the case when the mass of the rocket and the engine thrust are assigned functions of time.

We will solve the problem given the following simplifying assumptions:

1. the planet is a sphere with radially distributed density of mass;

2. the linear dimensions of the spacecraft are insignificant compared with its distance from the center of the planet;

3. the drag of the medium is absent;

4. the component of the thrust expended in control is negligibly small compared with the total thrust; and /16

5. the control system and the power unit operate ideally -- the vector of the engine thrust always coincides with the programmed vector.

The differential equations of motion in this case in the launch system of coordinates can be written as:

$$\left.\begin{aligned} \frac{dV_x}{dt} &= \frac{P}{m}\cos\varphi - g_x, \\ \frac{dV_y}{dt} &= \frac{P}{m}\sin\varphi - g_y, \\ \frac{dx}{dt} &= V_x, \\ \frac{dy}{dt} &= V_y. \end{aligned}\right\} \tag{1}$$

The system will be closed if the dependence of the parameters P, m, and ϕ on the time, and the dependence of the parameters g_x and g_y on the coordinates are assigned.

The projections of the acceleration of the force of gravity onto the axes Ox and Oy can be represented as:

$$\begin{aligned} g_x &= g_0 \frac{xR^2}{[(R+y)^2 + x^2]^{3/2}}, \\ g_y &= g_0 \frac{(R+y)R^2}{[(R+y)^2 + x^2]^{3/2}}, \end{aligned} \tag{2}$$

or

$$\begin{aligned} g_x &= k\frac{x}{[(R+y)^2 + x^2]^{3/2}}, \\ g_y &= k\frac{R+y}{[(R+y)^2 + x^2]^{3/2}}. \end{aligned} \tag{3}$$

Considering that in solving these problems the extent of the powered section of the trajectory of the launch from orbit is assumed to be more or less restricted, in order to facilitate the solution of the problem, let us simplify the expressions for g_x and g_y. We will expand them in series in neighborhoods of the point (0,0) and, by limiting ourselves to the terms containing x and y to the first power, we will get the approximate formulas:

$$g_x = g_0 \frac{x}{R},$$
$$g_y = g_0 - 2g_0 \frac{y}{R}. \qquad (4)$$

Equation of extremal trajectory. The trajectory of a SC is described by four first-order differential equations:

$$\left.\begin{aligned}
\omega_1 &= \dot{V}_x - \frac{P}{m}\cos\varphi + k\frac{x}{[(R+y)^2+x^2]^{3/2}} = 0,\\
\omega_2 &= \dot{V}_y - \frac{P}{m}\sin\varphi + k\frac{R+y}{[(R+y)^2+x^2]^{3/2}} = 0,\\
\omega_3 &= \dot{x} - V_x = 0,\\
\omega_4 &= \dot{y} - V_y = 0,
\end{aligned}\right\} \qquad (5)$$

which are differential equations of coupling between the parameters V_x, V_y, x, y, and ϕ. These equations include one independent variable g, five dependent variables V_x, V_y, x, y, and ϕ, therefore, have a single degree of freedom. Thus, for any assigned system of initial conditions x_0, y_0, V_{x0}, and V_{y0}, there is an infinite set of possible trajectories differing by a law of control of SC attitude in space ϕ arbitrarily assigned for each of them.

Suppose that at the initial instant of time $t - t_0$ the kinematic /17 parameters of motion of the variable-mass point m_0 are assigned:

$$x_0,\ y_0,\ V_{x0},\ V_{y0}. \qquad (6)$$

If over the time interval $|t_0, t_k|$ the law of control ϕ of the SC attitude in space is assigned, the trajectory of the object is determined uniquely, since in this case we have the unique solution

$$\left.\begin{aligned}
x &= \psi_1(x_0;\ y_0;\ V_{x0};\ V_{y0};\ \varphi),\\
y &= \psi_2(x_0;\ y_0;\ V_{x0};\ V_{y0};\ \varphi),\\
V_x &= \psi_3(x_0;\ y_0;\ V_{x0};\ V_{y0};\ \varphi),\\
V_y &= \psi_4(x_0;\ y_0;\ V_{x0};\ V_{y0};\ \varphi).
\end{aligned}\right\} \qquad (7)$$

It is required, among all controls ϕ transferring the SC from a point with parameters x_0, y_0, V_{x0} and V_{y0}, to the point in space x_k, y_k, V_{xk} and V_{yk}, not explicitly assigned, to find the control ϕ that provides the extremum for some functional

$$I = f(x_k;\ y_k;\ V_{xk};\ V_{yk}), \tag{8}$$

dependent on the kinematic parameters of motion at the endpoint of the powered trajectory section. We will call the trajectory satisfying this condition the extremal trajectory.

In determining the extremal trajectory, we will not specify what the functional I is. We will leave it in the general form (8), assuming that first derivatives of this functional exist and that they are continuous over the time interval $|t_0, t_k|$.

Let us solve the problem for the arbitrary extremum of functional (8). To do this, let us examine a new functional:

$$F = I + \int_{t_0}^{t_k} H dt = f(x;\ y;\ V_x;\ V_y) + \int_{t_0}^{t_k} H dt. \tag{9}$$

Here, the integrand function will be of the form

$$H = \lambda_1\omega_1 + \lambda_2\omega_2 + \lambda_3\omega_3 + \lambda_4\omega_4, \tag{10}$$

where λ_1, λ_2, λ_3 and λ_4 are certain, thus far undetermined, functions of time; ω_1, ω_2, ω_3, and ω_4 are determined according to (5).

By virtue of condition (5), functional (9) is equivalent to functional (8), since the integrand H tends to zero for any values of the parameters λ_i.

Obviously, variations of these functionals will also coincide. Let q_i stand for the functions $q_i = x, y, V_x, V_y, \phi$ being varied and let us take the first variation of functional (9):

$$\delta F = \sum_{i=1}^{5} \frac{\partial I}{\partial q_i}\delta q_i \Bigg|_{t=t_0}^{t=t_k} + \int_{t_0}^{t_k} \sum_{i=1}^{5} \left(\frac{\partial H}{\partial q_i}\delta q_i + \frac{\partial H}{\partial \dot{q}_i}\delta \dot{q}_i \right) dt + H dt \Bigg|_{t=t_0}^{t=t_k}. \tag{11}$$

Integrating by parts, we get:

$$\delta F = \sum_{i=1}^{5} \frac{\partial I}{\partial q_i} \delta q_i \Bigg|_{t=t_0}^{t=t_k} + \left[\left(H - \sum_{i=1}^{5} \frac{\partial H}{\partial \dot{q}_i} \dot{q}_1 \right) \delta t + \sum_{i=1}^{5} \frac{\partial H}{\partial \dot{q}_i} \delta q_i \right] \Bigg|_{t=t_0}^{t=t_k} + \sum_{i=1}^{5} \int_{t_0}^{t_k} \left[\frac{\partial H}{\partial q_i} - \frac{d}{dt} \left(\frac{\partial H}{\partial \dot{q}_i} \right) \right] \delta q_i dt. \tag{12}$$

Let us make an analysis of the variation of functional F.

The first term in expression (11) can be rewritten as:

$$\delta Q = \sum_{i=1}^{5} \frac{\partial I}{\partial q_i} \delta q_i \Bigg|_{t=t_0}^{t=t_k} = \frac{\partial I}{\partial V_{x0}} \delta V_{x0} + \frac{\partial I}{\partial V_{y0}} \delta V_{y0} + \frac{\partial I}{\partial x_0} \delta x_0 + \frac{\partial I}{\partial y_0} \delta y_0 + \frac{\partial I}{\partial V_{xk}} \delta V_{xk} + \frac{\partial I}{\partial V_{yk}} \delta V_{yk} + \frac{\partial I}{\partial x_k} \delta x_k + \frac{\partial I}{\partial y_k} \delta y_k + \frac{\partial I}{\partial \varphi_0} \delta \varphi_0 + \frac{\partial I}{\partial \varphi_k} \delta \varphi_k. \tag{13}$$

At the initial instant of time $t = t_0$, the values of the functions being varied are assigned, and therefore their variations are equal to zero:

$$\delta V_{x0} = \delta V_{y0} = \delta x_0 = \delta y_0 = 0. \tag{14}$$

Assuming that function I does not depend explicitly on the pitch program, we can write the equality:

$$\partial I / \partial \phi = 0 \tag{15}$$

for the entire interval of integration.

Therefore, expression (12) becomes simplified,

$$\delta Q = \frac{\partial I}{\partial V_{xk}} \delta V_{xk} + \frac{\partial I}{\partial V_{yk}} \delta V_{yk} + \frac{\partial I}{\partial x_k} \delta x_k + \frac{\partial I}{\partial y_k} \delta y_k. \tag{16}$$

Let us examine the second term in expression (12):

$$\left[\left(H - \sum_{i=1}^{5} \frac{\partial H}{\partial \dot{q}_i} \dot{q}_i \right) \delta t + \sum_{i=1}^{5} \frac{\partial H}{\partial \dot{q}_i} \delta q_i \right] \Bigg|_{t=t_0}^{t=t_k} = \left[\left(H - \sum_{i=1}^{5} \frac{\partial H}{\partial \dot{q}_i} \dot{q}_i \right) \delta t \right] \Bigg|_{t=t_0}^{t=t_k} + \sum_{i=1}^{5} \frac{\partial H}{\partial \dot{q}_i} \delta q_i \Bigg|_{t=t_k} - \sum_{i=1}^{5} \frac{\partial H}{\partial \dot{q}_i} \delta q_i \Bigg|_{t=t_0}. \tag{17}$$

Since the length of the interval of integration $|t_0, t_k|$ is assigned, the variation δt must be equal to zero:

$$\delta t = 0 \tag{18}$$

With reference to conditions (14), (15), and (17), we can rewrite the second term in expression (12) as:

$$\left[\left(H - \sum_{i=1}^{5} \frac{\partial H}{\partial \dot{q}_i} \dot{q}_i\right) \delta t + \sum_{i=1}^{5} \frac{\partial H}{\partial \dot{q}_i} \delta q_i\right]\Bigg|_{t=t_0}^{t=t_k} = \sum_{i=1}^{5} \frac{\partial H}{\partial \dot{q}_i} \delta q_i \Bigg|_{t=t_k} =$$
$$= \frac{\partial H}{\partial \dot{V}_{xk}} \delta V_{xk} + \frac{\partial H}{\partial \dot{V}_{yk}} \delta V_{yk} + \frac{\partial H}{\partial \dot{x}_k} \delta x_k + \frac{\partial H}{\partial \dot{y}_k} \delta y_k + \frac{\partial H}{\partial \dot{\varphi}_k} \delta \varphi_k. \tag{19}$$

Since the function H does not depend explicitly on the derivative $\dot{\phi}$, obviously, the equality

$$\frac{\partial H}{\partial \dot{\varphi}_k} = 0. \tag{20}$$

obtains.

Let us determine the derivatives $\frac{\partial H}{\partial \dot{V}_{xk}}$, $\frac{\partial H}{\partial \dot{V}_{yk}}$, $\frac{\partial H}{\partial \dot{x}_k}$, and $\frac{\partial H}{\partial \dot{y}_k}$, by using (10) and (5):

$$\begin{aligned} \frac{\partial H}{\partial \dot{V}_{xk}} &= \lambda_{1k}; \quad \frac{\partial H}{\partial \dot{x}_k} = \lambda_{3k}; \\ \frac{\partial H}{\partial \dot{V}_{yk}} &= \lambda_{2k}; \quad \frac{\partial H}{\partial \dot{y}_k} = \lambda_{4k}. \end{aligned} \tag{21}$$

From expressions (12) - (21), it follows that the variation of the functional (9) will be of the form: /19

$$\begin{aligned} \delta F = &\left(\frac{\partial I}{\partial V_{xk}} \delta V_{xk} + \frac{\partial I}{\partial V_{yk}} \delta V_{yk} + \frac{\partial I}{\partial x_k} \delta x_k + \frac{\partial I}{\partial y_k} \delta y_k\right) + \\ &+ (\lambda_{1k} \delta V_{xk} + \lambda_{2k} \delta V_{yk} + \lambda_{3k} \delta x_k + \lambda_{4k} \delta y_k) + \\ &+ \sum_{i=1}^{5} \int_{t_0}^{t_k} \left[\frac{\partial H}{\partial q_i} - \frac{d}{dt}\left(\frac{\partial H}{\partial \dot{q}_i}\right)\right] \delta q_i dt, \end{aligned} \tag{22}$$

where $\frac{\partial I}{\partial V_{xk}}$, $\frac{\partial I}{\partial V_{yk}}$, $\frac{\partial I}{\partial x_k}$, and $\frac{\partial I}{\partial y_k}$ are the derivatives of the functional being optimized with respect to the corresponding functions at the

instant of the endpoint of the powered section ($t = t_k$); λ_{1k}, λ_{2k}, λ_{3k}, and λ_{4k} are the values of the functions λ_i at the endpoint of the powered section.

By grouping the terms in expression (22) containing identical variations of the functions δV_x, δV_y, δx, and δy, we get:

$$\delta F = \left(\frac{\partial I}{\partial V_{xk}} + \lambda_{1k}\right)\delta V_{xk} + \left(\frac{\partial I}{\partial V_{yk}} + \lambda_{2k}\right)\delta V_{yk} + \left(\frac{\partial I}{\partial x_k} + \lambda_{3k}\right)\delta x_k + \\ + \left(\frac{\partial I}{\partial y_k} + \lambda_{4k}\right)\delta y_k + \sum_{i=1}^{5}\int_{t_0}^{t_k}\left[\frac{\partial H}{\partial q_i} - \frac{d}{dt}\left(\frac{\partial H}{\partial \dot{q}_i}\right)\right]\delta q_i dt. \tag{23}$$

Assuming that there is an internal extremum for expression (23), let us find it from the condition:

$$\delta F = 0 \tag{24}$$

For variation (24) to approach zero, it is necessary that the functions q_i (V_x, V_y, x, y, ϕ) being varied satisfy the Euler-Lagrange equations:

$$\frac{\partial H}{\partial q_i} - \frac{d}{dt}\left(\frac{\partial H}{\partial \dot{q}_i}\right) = 0, \tag{25}$$

and the Lagrangian multipliers (λ_i) will be selected so that at the right endpoint of integration the following relations are satisfied:

$$\lambda_{1k} = -\frac{\partial I}{\partial V_{xk}}, \quad \lambda_{3k} = -\frac{\partial I}{\partial x_k}, \\ \lambda_{2k} = -\frac{\partial I}{\partial V_{yk}}, \quad \lambda_{4k} = -\frac{\partial I}{\partial y_k}. \tag{26}$$

The system of equations (25) is a necessary condition for the extremum of functional (9).

The Euler-Lagrange equations (25) for functional (9) depend on the form of the coupling equations. For coupling equations (5), they can be written as:

$$\dot{\lambda}_1 + \lambda_3 = 0, \tag{27}$$
$$\dot{\lambda}_2 + \lambda_4 = 0, \tag{28}$$

$$\dot{\lambda}_3 - \frac{k}{r^5}[\lambda_1 (r^2 - 3x^2) - 3\lambda_2 x (R + y)] = 0, \tag{29}$$

$$\dot{\lambda}_4 - \frac{k}{r^5}\{\lambda_2 [r^2 - 3 (R + y)^2] - 3\lambda_1 x (R + y)\} = 0, \tag{30}$$

$$\frac{P}{m}(\lambda_1 \sin\varphi - \lambda_2 \cos\varphi) = 0. \tag{31}$$

By solving equation (31), we find:

$$\varphi = \operatorname{arctg}\frac{\lambda_2}{\lambda_1}. \tag{32}$$

The system of equations of the extremal trajectory can be written as: /20

$$\begin{aligned}
V_x &= \frac{P}{m}\cos\varphi - k\frac{x}{[(R + y)^2 + x^2]^{3/2}},\\
\dot{V}_y &= \frac{P}{m}\sin\varphi - k\frac{R + y}{[(R + y)^2 + x^2]^{3/2}},\\
\dot{x} &= V_x,\\
\dot{y} &= V_y,\\
\dot{\lambda}_1 &= -\lambda_3,\\
\dot{\lambda}_2 &= -\lambda_4,\\
\dot{\lambda}_3 &= \frac{k}{r^5}[\lambda_1 (r^2 - 3x^2) - 3\lambda_2 x (R + y)],\\
\dot{\lambda}_4 &= \frac{k}{r^5}\{\lambda_2 [r^2 - 3 (R + y)^2 - 3\lambda_1 x (R + y)\},\\
\varphi &= \operatorname{arctg}\frac{\lambda_2}{\lambda_1},\\
P &= P (t),\\
m &= m (t).
\end{aligned} \tag{33}$$

The system of equations (33), together with the initial conditions of motion of the variable-mass point at the initial instant of time (6) and the boundary conditions at the right endpoint (26) gives the complete solution to the problem formulated. Here, the pitch program $\phi = \phi(t)$, defined by Eq. (32), cannot be obtained in explicit form, since the system of linear differential equations (27) - (30) with variable coefficients (x, y) is not solvable in explicit form with respect to the Lagrangian multipliers λ_i. To find the extremal trajectory, we must select the initial values of the Lagrangian multipliers λ_{0i}, which at the endpoint of the integration interval ensure the boundary conditions (26). The Lagrangian multipliers λ_{0i} can be selected by using any iterative methods.

In practice, the extent of the powered trajectory section is limited in the number of cases. Then finding the extremal trajectory is simplified owing to the possibility of introducing simplifications into the coupling equations (5). Let us examine the same problem of determining this trajectory of the variable-mass point in a central gravitational field that furnishes an extremum to the functional

$$I = f(x_k;\ y_k;\ V_{xk};\ V_{yk}), \tag{34}$$

dependent on the kinematic parameters of motion at the endpoint of the powered trajectory section. We will also assume that the time interval $|t_0, t_k|$ in which we seek the extremal trajectory is specified.

Let us replace the differential coupling equations (5) with the corresponding simplified equations:

$$\left.\begin{aligned}
\omega_1 &= \dot{V}_x - \frac{P}{m}\cos\rho + \nu^2 x = 0,\\
\omega_2 &= \dot{V}_y - \frac{P}{m}\sin\varphi + g_0 - 2\nu^2 y = 0,\\
\omega_3 &= \dot{x} - V_x = 0,\\
\omega_4 &= \dot{y} - V_y = 0,
\end{aligned}\right\} \tag{35}$$

where $\nu^2 = g_0/R$.

By bringing into consideration the equivalent functional: /21

$$F = I + \int_{t_0}^{t_k} H dt = I + \int_{t_0}^{t_k} \sum_{i=1}^{4} \lambda_i \omega_i dt \tag{36}$$

and following the same reasoning that was given above, we obtain the result that a necessary condition for the extremum of functional (36) (the approach to zero of the first variation) requires that the functions $q_i(V_x, V_y, x, y, \phi)$ and λ_i $(i = 1, 2, 3, 4)$ satisfy the Euler-Lagrange equations:

$$\frac{\partial H}{\partial q_i} - \frac{d}{dt}\left(\frac{\partial H}{\partial \dot{q}_i}\right) = 0. \tag{37}$$

Let us simultaneously obtain the boundary conditions at the right endpoint of integration t_k:

$$\lambda_{1k} = -\frac{\partial I}{\partial V_{xk}}, \quad \lambda_{3k} = -\frac{\partial I}{\partial x_k},$$
$$\lambda_{2k} = -\frac{\partial I}{\partial V_{yk}}, \quad \lambda_{4k} = -\frac{\partial I}{\partial y_k}. \tag{38}$$

The Euler-Lagrange equations for functional (36) can be written as:

$$\lambda_1 = -\lambda_3, \tag{39}$$
$$\lambda_2 = -\lambda_4, \tag{40}$$
$$\lambda_3 = \nu^2\lambda_1, \tag{41}$$
$$\lambda_4 = -2\nu^2\lambda_2, \tag{42}$$
$$\frac{P}{m}\lambda_1 \sin\varphi - \frac{P}{m}\lambda_2 \cos\varphi = 0. \tag{43}$$

From Eq. (43), we get the optimal pitch program:

$$\varphi = \operatorname{arctg}\frac{\lambda_2}{\lambda_1}. \tag{44}$$

Equations (39) - (42) are a system of linear differential equations with constant coefficients and can be integrated.

By integrating Eqs. (39) and (40), and by using Eqs. (41) and (42), we get:

$$\ddot{\lambda}_1 = -\lambda_3 = -\lambda_1\nu^2, \tag{45}$$
$$\ddot{\lambda}_2 = -\lambda_4 = 2\lambda_2\nu^2. \tag{46}$$

By setting up the corresponding characteristic equations

$$p_1^2 = -\nu^2, \tag{47}$$
$$p_2^2 = 2\nu^2 \tag{48}$$

and by solving them, we get the roots of the characteristic equations:

$$p_{11} = i\nu, \quad p_{12} = -i\nu, \tag{49}$$
$$p_{21} = \sqrt{2}\nu, \quad p_{22} = -\sqrt{2}\nu. \tag{50}$$

The general solutions of the homogeneous differential equations (45) and (46) can be represented as:

$$\lambda_1 = f_1 \cos \nu t + f_2 \sin \nu t, \tag{51}$$

$$\lambda_2 = f_3 e^{\omega t} + f_4 e^{-\omega t}, \tag{52}$$

where f_1, f_2, f_3, and f_4 are certain constant coefficients; $\omega = \sqrt{2}\nu$.

With reference to (39) and (40), we get the expressions for λ_3 and λ_4: /22

$$\lambda_3 = f_1 \nu \sin \nu t - f_2 \nu \cos \nu t, \tag{53}$$

$$\lambda_4 = -f_3 \omega e^{\omega t} + f_4 \omega e^{-\omega t}. \tag{54}$$

Let us define the constants f_1, f_2, f_3, and f_4 in Eqs. (51) - (54). Using the boundary conditions at the right endpoint of integration (38), for the Lagrangian multipliers we can write:

$$\left.\begin{aligned}
\lambda_{1k} &= -\frac{\partial I}{\partial V_{xk}} = f_1 \cos \nu t_k + f_2 \sin \nu t_k, \\
\lambda_{2k} &= -\frac{\partial I}{\partial V_{yk}} = f_3 e^{\omega t_k} + f_4 e^{-\omega t_k}, \\
\lambda_{3k} &= -\frac{\partial I}{\partial x_k} = f_1 \nu \sin \nu t_k - f_2 \nu \cos \nu t_k, \\
\lambda_{4k} &= -\frac{\partial I}{\partial y_k} = -f_3 \omega e^{\omega t_k} + f_4 \omega e^{-\omega t_k}.
\end{aligned}\right\} \tag{55}$$

By solving the system of equations (55) for f_i, we get:

$$\left.\begin{aligned}
f_1 &= \frac{-\frac{\partial I}{\partial V_{xk}} \nu \cos \nu t_k - \frac{\partial I}{\partial x_k} \sin \nu t_k}{\nu}, \\
f_2 &= \frac{-\frac{\partial I}{\partial V_{xk}} \nu \sin \nu t_k + \frac{\partial I}{\partial x_k} \cos \nu t_k}{\nu}, \\
f_3 &= \frac{-\frac{\partial I}{\partial V_{yk}} \omega + \frac{\partial I}{\partial y_k}}{2\omega e^{\omega t_k}}, \\
f_4 &= \frac{-\frac{\partial I}{\partial V_{yk}} \omega - \frac{\partial I}{\partial y_k}}{2\omega e^{-\omega t_k}}.
\end{aligned}\right\} \tag{56}$$

The optimal pitch system (44) providing an extremum for functional (36), with reference to expressions (51), (52), and (56), can be represented as the following function:

$$\varphi = \operatorname{arctg}\left\{\frac{1}{\sqrt{2}}\left[\frac{\frac{\partial I}{\partial V_{yk}}\omega \operatorname{ch}\omega(t_k - t) + \frac{\partial I}{\partial y_k}\operatorname{sh}\omega(t_k - t)}{\frac{\partial I}{\partial V_{xk}}\nu\cos\nu(t_k - t) + \frac{\partial I}{\partial x_k}\sin\nu(t_k - t)}\right]\right\}. \qquad (57)$$

The expression for the optimal pitch program, given the simplified representation of the Earth's gravitational field, is analogous to the results obtained by D.B. Okhotsimskiy and T.M. Eneyev in solving the problem of determining the optimal control $\phi(t)$ ensuring maximum level-flight velocity V_k at the end of the powered section at a specified altitude h_k [1], and is a generalization of the results they obtained for an arbitrarily assigned functional, dependent on kinematic parameters of the end of the powered trajectory section.

In this case, the system of equations of the extremal trajectory and the final relations can be written as:

$$\left.\begin{aligned}
\dot{V}_x &= \frac{P}{m}\cos\varphi - \nu^2 x,\\
\dot{V}_y &= \frac{P}{m}\sin\varphi - g_0 + 2\nu^2 y,\\
\dot{x} &= V_x,\\
\dot{y} &= V_y,\\
\varphi &= \operatorname{arctg}\left\{\frac{1}{\sqrt{2}}\left[\frac{\frac{\partial I}{\partial V_{yk}}\omega \operatorname{ch}\omega(t_k - t) + \frac{\partial I}{\partial y_k}\operatorname{sh}\omega(t_k - t)}{\frac{\partial I}{\partial V_{xk}}\nu\cos\nu(t_k - t) + \frac{\partial I}{\partial x_k}\sin\nu(t_k - t)}\right]\right\},\\
P &= P(t),\\
m &= m(t),\\
\nu &= \sqrt{\frac{g_0}{R}},\\
\omega &= \sqrt{2}\nu.
\end{aligned}\right\} \qquad (58)$$

/23

The system of equations (58), given the initial conditions defining the motion of the variable-mass material point at the instant t_0 (6), wholly defines the extremal trajectory of this point.

Further simplification of the equations of the extremal pitch program providing an extremum for the functional of the type (8) can be made for the plane-parallel field by the method given above. In this case the formula for determining the optimal pitch program is of the form:

$$\operatorname{tg}\varphi = \frac{\frac{\partial I}{\partial V_{yk}} + \frac{\partial I}{\partial y_k}(t_k - t)}{\frac{\partial I}{\partial V_{xk}} + \frac{\partial I}{\partial x_k}(t_k - t)}. \tag{59}$$

Expression (59) is analogous to the results given in the studies [1, 6-8].

Legendre-Klebsch condition. To evaluate the maximum or minimum value of the functional for the extremal trajectory, just as in finding the maximum (minimum) of functions, we must determine the sign of the second variation. The Legendre-Klebsch condition is a supplementary necessary condition for the existence of the extremum and determines its form.

As assumed above, the functional

$$F = I + \int_{t_0}^{t_k} H(V_x, V_y, x, y)\,dt \tag{60}$$

is linear relative to the first derivatives and obtaining the second variation, and therefore, any evaluations concerning the maximum or minimum of the functional achieved on this extremal trajectory does not appear possible.

It is shown in the work [2] that in solving problems of finding the optimal trajectories of SC, one must include among the functions being varied the controls u of the magnitude and direction of the thrust vector. Here a necessary condition for the maximum value of the extremum of the functional is that along the extremal between the nodal points the inequalities

$$e = \sum_{i,k=1}^{n} \frac{\partial^2 F}{\partial \eta_i \partial \eta_k} \delta\eta_i \delta\eta_k \leqslant 0, \tag{61}$$

be satisfied, and a necessary condition for the minimum value of the extremum of the functional is that along the extremal between nodal points the inequalities

$$e = \sum_{i,k=1}^{n} \frac{\partial^2 F}{\partial \eta_i \partial \eta_k} \delta\eta_i \delta\eta_k \geqslant 0, \tag{62}$$

be satisfied, where n is the number of functions being varied, η_i and η_k are the functions being varied.

The absence of the equality sign corresponds to the strengthened Legendre-Klebsch condition.

In our case, for optimization, the Legendre-Klebsch condition e-function can be written as: /24

$$e = \sum_{i,k=1}^{5} \frac{\partial^2 F}{\partial \eta_i \partial \eta_k} \delta\eta_i \delta\eta_k, \tag{63}$$

where $\eta_1 = V_x$, $\eta_2 = V_y$, $\eta_3 = x$, $\eta_4 = y$, and $\eta_5 = \phi$.

Extending expression (63) with reference to (60), (5), and (10), and assuming that only the first derivatives of functional (60) exist, continuous over the segment $|t_0, t_k|$, we get:

$$e = (\lambda_1 \cos\varphi + \lambda_2 \sin\varphi)(\delta\varphi)^2. \tag{64}$$

With reference to the Euler-Lagrange equation (31), we will have:

$$e = \frac{\lambda_1}{\cos\varphi} \quad \text{or} \quad e = \frac{\lambda_2}{\sin\varphi}. \tag{65}$$

Based on expressions (61) - (65), we can make the following conclusions:

1) the optimal pitch programs providing a maximum for functional (60) must satisfy over the segment $|t_0, t_k|$ the condition:

$$\frac{\lambda_1}{\cos\varphi} \leqslant 0 \quad \text{or} \quad \frac{\lambda_2}{\sin\varphi} \leqslant 0; \tag{66}$$

2) optimal pitch programs providing a minimum for functional (60) must satisfy over the segment $|t_0, t_k|$ the condition:

$$\frac{\lambda_1}{\cos\varphi} \geqslant 0 \quad \text{or} \quad \frac{\lambda_2}{\sin\varphi} \geqslant 0. \tag{67}$$

From conditions (66) and (67) it follows that:

1) in the acceleration of the SC, when the pitch program over the time interval $|t_0, t_k|$ lies within the range

$-\frac{\pi}{2} \leqslant \varphi \leqslant +\frac{\pi}{2}$, the maximum value of functional (60) is realized when:

$$\lambda_1 \leq 0 \tag{68}$$

and the minimum -- when:

$$\lambda_1 \geq 0 \tag{69}$$

independently of the form of the function I to be optimized (whether it is the apogee altitude, the velocity at the end of the powered section, the energy, the semi-major axis, the period of revolution, eccentricity, etc.);

2) in solving problems in space ballistics associated with the deceleration of a SC (launch from orbit, transfer from a high-altitude circular orbit to an elliptical orbit with minimum perigee altitude, etc.), when the pitch program over the time interval $|t_0, t_k|$ lies within the range $\frac{\pi}{2} \leqslant \varphi \leqslant \frac{3}{2}\pi$, the maximum value of functional (60) is provided when:

$$\lambda_1 \geq 0 \tag{70}$$

and the minimum -- when:

$$\lambda_1 \leq 0 \tag{71}$$

3) when the pitch program ϕ passes through zero or $\pi/2$, the parameter λ_2 must also reverse its sign, i.e., it must pass through zero.

REFERENCES

1. Okhotsimskiy, D.Ye. and T.M. Eneyev, UFN, LXIII(1) (1957).

2. Tarasov, Ye.V., Optimal'nyye rezhimy poleta letatel'nykh apparatov [Optimal aircraft flight regimes], Oborongiz, Moscow, 1963.

3. Ponomarev, V.M., Teoriya upravleniya dvizheniyem kosmicheskikh apparatov [Theory of spacecraft control], "Nauka," Moscow, 1965.

4. Ostoslavskiy, I.V., Issledovaniya po dinamike poleta [Studies in flight dynamics], "Mashinostroyeniye," Moscow, 1965. /25

5. Duboshin, G.N., Nebesnaya mekhanika. Osnovnyye zadachi i metodi [Celestial mechanics. Fundamental problems and methods], Fizmatgiz, Moscow, 1963.

6. Lawden, D.F., "Dynamic problems of interplanetary flight," Aeronautics Quarterly 6 (1955).

7. Lawden, D.F., Aeronaut. Acta 1 (1955).

8. Fried, B.D., Jet Propulsion 27(6) (1957).

ANALYSIS OF PROBLEMS OF SPACECRAFT NAVIGATION AND CONTROL

V.V. Gorbuntsov, V.G. Komarov, V.F. Lager', G.L. Madatov, and A.T. Onishchenko

Trajectories of spacecraft can be divided naturally into sections that are specific as to the nature of motion, and control tasks and methods.

The first (powered) section, along which motion occurs near a planet with sustainer engines functioning, differs by its high energy indicators for a relatively short flight duration. These characteristics of the powered section lead to the necessity of energy optimization of control with the presence of a series of constraints on the trajectory and the control system.

Numerous problems in optimizing programmed motion (maximum response, minimization of fuel consumption, etc.) can be reduced to the Mayer variational problem. The shortcoming of classical methods of solving the problem is the necessity of setting up an auxiliary system of differential equations, whether the Euler-Lagrange equations in the problem with unconstrained variations, or the Hamiltonian system of equations in the principle of the maximum with constrained variations [5].

The method of dynamic programming yields numerical algorithms that lack this shortcoming, but their realization in the general case requires the storage of cumbersome tables. The problem of reducing dimensionality usually requires in each case an individual examination and some computational art. The sequential procedure presented below -- the method of envelopes -- in several cases of practical importance is more economical than the classical algorithm of dynamic programming.

The second (passive) section is marked by a long duration and low energy outlays. Here the problem of determining trajectory emerges to the fore. Regardless of whether this problem is solved on Earth (trajectory calculations) or in an onboard digital computer (onboard navigation), requirements of high operating economy and precision are imposed on the algorithms.

Most known algorithms for the operational calculation of trajectories, for example, trajectories of the class Earth- Moon-Earth [3, 9, 10], yield only an approximate solution to the constrained three-body problem. The methods presented below for determining the parameters of the motion of spacecraft (SC) over the passive flight section in the gravitational field of several

attracting centers -- the method of independent actions and the method of imaginary masses -- are convenient for the operational solution of both the constrained and the unconstrained n-body problem, are economical, and are not inferior in precision to methods of numerical integration.

The method of independent actions is based on the approximation of the true trajectory of the object of interest in the n-body problem by a sequence of geometrical sums of unperturbed trajectories in the two-body problem, calculated on the assumption that the object of interest is in isolated interaction with each attracting body of the system. In the method of imaginary masses, the true trajectory of the object of interest is approximated by a sequence of sections of unperturbed trajectories in the two-body problem relative to some variable imaginary attracting mass. In both methods, calculation of the true trajectory reduces to determining at the calculation step the parameters of the motion of the object from the final relations of the theory of Keplerian orbits. /26

A special place among problems of control over the passive section is occupied by problems of optimization of the control of the motion of an object around the center of mass. Here the main requirement is usually the minimum energy outlays while ensuring the required precision and operating economy of the algorithms from the standpoint of instrumental realization.

Finally, the last section -- the section of descent onto a planet, just as the powered section, imposes increased requirements on the programs of the control system, since a number of requirements that are technically difficult to achieve and contradictory, aimed at ensuring the viability of the object in the difficult conditions of motion, are imposed on the trajectory of the object. The solution of these problems often reduces to complicated nonstandard variational problems. Applying the principle of the maximum [5] gives a positive result when solving a broad class of these problems.

The method of envelopes. Let us examine the proposed procedure for optimization with the example of the solution to the problem of maximum response for a second-order object ($n = 2$):

$$\begin{aligned} &\dot{\bar{x}} = \bar{f}(x, u, t), \\ &\bar{x}(t_0) = \bar{x}^0, \ u \in U, \end{aligned} \tag{1}$$

where $\bar{x} = \{x_1, x_2\}$ are the phase coordinates of the object; u is a scalar control, where we will first assume the set U of admissible controls to coincide with the space of smooth functions; $\bar{f} = \{f_1, f_2\}$ is a vector function, differentiable and continuous together with its derivatives, such that:

$$\frac{\partial^2 f_1}{\partial u^2} \cdot \frac{\partial f_2}{\partial u} - \frac{\partial f_1}{\partial u} \cdot \frac{\partial^2 f_2}{\partial u^2} \neq 0. \tag{2}$$

Further, we will assume that for a fixed $\bar{x}$ and t, the set of vectors $\bar{f}(u, \bar{C})$ is convex. It is required to select the control u(t) so that the object occupies, in the minimum time T, the position where $L(\bar{x})$ is some single-valued function:

$$\bar{x}(T) \in \{\bar{x}_L : L(\bar{x}) = 0\}. \tag{3}$$

Let us introduce into consideration the time interval $\Delta t > 0$ sufficiently small so that, by preserving the required precision of the calculations, we can assume over the interval $[t_{i-1} = t_i - \Delta t, t_i]$ that the right sides of Eqs. (1) are constant and equal to $\bar{f}(\bar{x}_{i-1}(t_{i-1}), u_{i-1}(t_{i-1}), t_{i-1})$. Let us write:

$$\bar{x}_1 = \bar{x}^0 + \bar{f}_0(\bar{x}^0, u_0, t_0)\Delta t. \tag{4}$$

With the variation $u_0 \in U$, the end of vector $\bar{x}_1$ describes some curve in phase space, which is the locus of points attained at the time instant $t_1 = t_0 + \Delta t$. By considering each point of the curve thus obtained as the initial point for the subsequent motion, let us write the two-parameter family of curves:

$$i = 2;\ \bar{x}_i(\bar{x}^0, u_0, u_{i-1}) = \bar{x}_{i-1}(\bar{x}^0, u_0) + \bar{f}_i(\bar{x}_{i-1}, u_{i-1}, t_{i-1})\Delta t. \tag{5}$$

The locus of phase space attained at the instant $t_i = t_0 + i\Delta t$ can be obtained, by constructing the envelope of the family (5):

$$i = 2;\ \bar{x}_i(\bar{x}^0, u_0) = \bar{x}_i(\bar{x}^0, u_0, u_{i-1}^*(u_0)), \tag{6}$$

where the control $u_i^*(u_0)$ transferring the object from curve (4) to envelope (6) is defined from the equations [6][1]: /27

$$i = 2;\ \Phi(\bar{x}^0, u_0, u_{i-1}) \equiv \left|\left(\frac{\partial \bar{x}_i}{\partial u_0} \frac{\partial \bar{x}_i}{\partial u_{i-1}}\right)\right| = 0. \tag{7}$$

Expressions (5) - (7) can be written for any $i \geq n$.

[1]The possible nonuniqueness of the solution to Eq. (7) does not play an essential role here, since the selection of the corresponding values u_{i-1}^* is usually determined during the actual process of solving a specific problem.

Let us show that the controls given by the solution to Eq. (7) are optimal. As we know, an extremal trajectory must satisfy not only Eqs. (1), but also the Euler-Lagrange equations:

$$\frac{d}{dt}\left(\frac{\partial F}{\partial \dot{x}_k}\right) - \frac{\partial F}{\partial x_k} = 0, \qquad k = 1, 2, \ldots, n+1, \tag{8}$$

where the expanded function F for this problem is of the form:

$$F = (\bar{\lambda}(\dot{\bar{x}} - \bar{f})), \tag{9}$$

$\bar{\lambda} = \{\lambda_1(t), \lambda_2(t)\}$ is a vector whose components are variable cofactors.

After uncomplicated transformations, system (8) can be represented as:

$$(A)^T\bar{\lambda} = 0 \tag{10}$$

For n = 2, the matrix (A) is of the form

$$(A) = \left(\frac{\partial \bar{f}}{\partial u}\ \frac{d}{dt}\left(\frac{d\bar{f}}{\partial u}\right) - \left(\frac{\partial \bar{f}}{\partial \bar{x}}\right)^T \frac{\partial \bar{f}}{\partial u}\right). \tag{11}$$

In order for the system of homogeneous equations (10) to have a nontrivial solution, it is necessary that $|A| = 0$, from whence we get the differential equation to find the u(t). In particular, when n = 2, we have

$$\Phi(\dot{u}, u, \bar{x}, t) \equiv \left| \begin{pmatrix} \frac{\partial f_1}{\partial u} & \frac{d}{dt}\left(\frac{\partial f_1}{\partial u}\right) - \left(\frac{\partial f_1}{\partial \bar{x}}\right)\frac{\partial \bar{f}}{\partial u} \\ \frac{\partial f_2}{\partial u} & \frac{d}{dt}\left(\frac{\partial f_2}{\partial u}\right) - \left(\frac{\partial f_2}{\partial \bar{x}}\right)\frac{\partial \bar{f}}{\partial u} \end{pmatrix} \right| = 0. \tag{12}$$

Using relation (5), let us rewrite (7) as:

$$\left| \left(\frac{\partial \bar{f}}{\partial u} + \left(\frac{\partial \bar{f}}{\partial \bar{x}}\right)\frac{\partial \bar{f}}{\partial u}\Delta t \quad \frac{\partial \bar{f}}{\partial u} + \frac{d}{dt}\left(\frac{\partial \bar{f}}{\partial u}\right)\Delta t\right) \right| = 0. \tag{13}$$

Combining the columns on the determinant thus obtained and then letting Δt approach zero, we arrive at relation (12). Thus, Eq. (12) is equivalent to Eq. (7) and the value of the control given by it is optimal. Here the surfaces (in the case n = 2,

they are curves) (6) are the surfaces of the level of a Bellman function min T. For the problem of dimensionality n = 3, 4, ..., we can get an equation analogous to (7):

$$\Phi(\bar{x}^0, u_0, u_1, \ldots, u_{n-2}, u_{i-1}) \equiv \left|\left(\frac{\partial \bar{f}}{\partial u_0} \quad \frac{\partial \bar{f}}{\partial u_1} \cdots \quad \cdots \frac{\partial \bar{f}}{\partial u_{n-2}} \quad \frac{\partial \bar{f}}{\partial u_{i-1}}\right)\right| = 0 \qquad (14)$$

defining the optimal control at the i-th ($i \geq n$) step $u^*_{i-1} = u^*_{i-1}(u_0, u_1, \ldots, u_{n-2})$, as a function of n - 1 independent parameters characterizing the specific extremal; for example, the values of the controls for the first n - 1 steps can be these parameters. At each step i = 1, 2, ..., let us directly calculate $\frac{\partial \bar{x}_i}{\partial u_{i-1}} = \frac{\partial \bar{x}_{i-1}}{\partial u_{i-1}} \Delta t$ and $\left(\frac{\partial \bar{x}_i}{\partial \bar{x}_{i-1}}\right) = (I) + \left(\frac{\partial \bar{x}_{i-1}}{\partial \bar{x}_{i-1}}\right) \Delta t$. The remaining /28 derivatives $\partial x_i / \partial u_k$, k = 0, 1, ..., n - 2 appearing in expression (14) are defined by the recursion formula $\frac{\partial \bar{x}_i}{\partial u_k} = \left(\frac{\partial \bar{x}_i}{\partial \bar{x}_{i-1}}\right) \frac{\partial \bar{x}_{i-1}}{\partial u_k}$, using the values of the same derivatives calculated for the preceding step.

The procedure is repeated for successive i up to some i = m at which:

$$\min_i \operatorname{mix}_{u_0, \ldots, u_{n-2}} \delta(\bar{x}_i, \bar{x}_L), \qquad (15)$$

is attained, where δ is the minimum distance (for example, in the sense $|\bar{x}_i - \bar{x}_L|$ from the i-th envelope to the points of the surface $L(\bar{x}_L) = 0$.

Using the m envelope surfaces thus obtained, let us construct the optimal control u*(t) in the form of the sequence $u_{m-1}, u_{m-2}, \ldots$, traversing the envelope in the reverse direction beginning from the point x_m given by (15), as is usually [2] done in algorithms of dynamic programming.

Computing the envelopes requires storage of (n - 1)-dimensional tables, i.e., the dimensionality of the problem is reduced by one compared to the classical algorithm of dynamic programming. In several cases the advantage here proves to be quite substantial, in spite of the necessity of computing at each step n^2 derivatives $(\partial \bar{f}/\partial \bar{x})$ and n derivatives $\partial \bar{f}/\partial u$. Additional advantages of this

method are provided by the fact that in most practical problems the envelopes are deliberately quite smooth surfaces and their approximation poses no difficulties.

Let us note that when we use, instead of (7), Eq. (12) directly obtained from the Euler-Lagrange equations, the computational advantages are lost owing to the necessity of additionally computing the derivatives of higher orders (for example, even for n = 3, instead of n(n + 1) = 12 first-order derivatives, we would have to compute (n/2)(n + 2) (n + 3) = 45 second-order derivatives and as many third-order derivatives.

In conclusion, let us consider the problem when the set U does not coincide with the space of smooth functions, and we will assume that

$$U = \{u:\ a \leqslant u \leqslant b,\ a \neq b\}.$$

is given. In this case, with reference to property (3), the optimal control at each step is defined as u^*_{i-1}, if Eq. (14) yields $u^*_{i-1} \in U$, and $u^{**}_{i-1} = \{u: \min_{u_{i-1} \in U} |u_{i-1} - u^*_{i-1}|\}$, if $u^*_{i-1} \notin U$.

The method of independent actions. Let us examine a system of n material points with masses m_i (i = 1, 2, ..., n). For an arbitrary instant of time t_0, let us assume that their positions $\bar{r}_{i0}$ and velocities $\bar{v}_{i0}$ are known with respect to some inertial rectangular coordinate system Oxyz. It is required to determine the parameters of the motion of each material point of the system at an arbitrary instant of time t from known initial conditions.

The equations of motion of each j-th point (j = 1, 2, ..., n) considered in the system in the selected coordinate system are of the form:

$$\ddot{\bar{r}}_j = -\sum_{i=1}^{n} k_i \frac{\bar{r}_{ji}}{r^3_{ji}},$$

$$\left.\begin{aligned} \bar{r}_{ji} &= \bar{r}_j - \bar{r}_i, \qquad i, j = 1, 2, \ldots, n, \\ k_i &= fm_i, \end{aligned}\right\} \tag{16}$$

/29

where f is the gravitational constant.

Let us define the trajectory of motion of the j-th point over some time interval (t, t + Δt) with a hodograph, which describes the linear combination of radii-vectors of the instantaneous positions of this point on trajectories defined by the equations:

$$\ddot{(\bar{\rho}_j)}_i = -k_i \frac{\bar{\rho}_{ji}}{\rho_{ji}^3},$$
$$\bar{\rho}_{ji} = (\bar{\rho}_j)_i - (\bar{\rho}_i)_j, \qquad i \neq j. \tag{17}$$

Here, at the time t_s of the beginning of the s-th step of the computation, the following conditions are satisfied:

$$(\bar{\rho}_j)_i|_s = \bar{r}_j(t_s) = \bar{r}_{js}, \quad (\bar{\rho}_i)_j|_s = \bar{r}_i(t_s) = \bar{r}_{is},$$
$$(\bar{v}_j)_i|_s = \bar{v}_j(t_s) = \bar{v}_{js}, \quad (\bar{v}_i)_j|_s = \bar{v}_i(t_s) = \bar{v}_{is},$$

where $(\bar{\rho}_j)_i$, $(\bar{v}_j)_i$, $(\bar{\rho}_i)_j$, and $(\bar{v}_i)_j$ are the instantaneous values of the radii-vectors and velocities of the j-th and i-th points, respectively, in the selected coordinate system when they are in isolated interaction.

We will select the computation step Δt_s from the condition that the inequality

$$|\bar{r}_j - (\bar{\rho}_j)_i|_s \ll |\bar{r}_j - \bar{r}_i|_s, \qquad i \neq j.$$

is satisfied.

This enables us, with reference to (17), to write the equation of motion of the j-th point of the system as a computation step in the form:

$$\ddot{\bar{r}}_j = -\sum_{i=1}^{r} k_i \frac{\bar{\rho}_{ji}}{\rho_{ji}^3}. \tag{18}$$

The solution of Eq. (18) is of the form:

$$\bar{r}_j = \sum_{\substack{i=1 \\ i \neq j}}^{n} (\bar{\rho}_j)_i - (n-2)[\bar{r}_{js} + \bar{v}_{js}(t - t_s)], \tag{19}$$

$$\bar{v}_j = \sum_{\substack{i=1 \\ i \neq j}}^{n} (\bar{v}_j)_i - (n-2)\bar{v}_{js}, \tag{20}$$

$$t_s \leqslant t \leqslant t_s + \Delta t.$$

The parameters $(\bar{\rho}_j)_i$ are defined from the final relations of the theory of Keplerian orbits [1].

The method of fictitious masses. The formulation of the problem is analogous to the foregoing. Let us imagine the desired motion of the point m_j as occurring under the influence of one attracting point with fictitious variable mass M_j. We define the position of the point M_j in the selected coordinate system by the vector $\bar{R}_j$ (Fig. 1), and the position of the point m_j relative to M_j -- by the vector

$$\bar{\rho}_j = \bar{r}_j - \bar{R}_j. \tag{21}$$

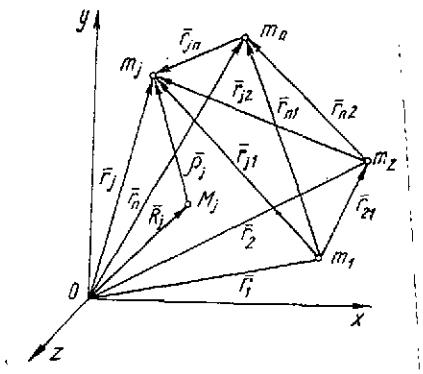

Fig. 1. System of n material points with fictitious mass.

We can write the equation of motion of the point m_j relative to M_j as the equation of a two-body problem:

$$\ddot{\bar{\rho}}_j = -f\frac{M_j + m_j}{\rho_j^3}\bar{\rho}_j. \tag{22}$$

Considering that:

$$\ddot{\bar{\rho}}_j = \ddot{\bar{r}}_j + \ddot{\bar{R}}_j,$$

we get /30

$$\ddot{\bar{r}}_j = \ddot{\bar{R}}_j - f\frac{M_j + m_j}{\rho_j^3}\bar{\rho}_j. \tag{23}$$

Combined examination of Eqs. (16) and (23) leads to the relation:

$$\ddot{\bar{R}}_j - f\frac{M_j + m_j}{\rho_j^3}\bar{\rho}_j = -\sum_{i=1}^{n} k_i \frac{\bar{r}_{ji}}{r_{ji}^3}, \qquad i \neq j. \tag{24}$$

Parameters M_j and $\bar{R}_j$ are functions of k_i and $\bar{r}_{ji}$, however at the computation step Δt_s they can be regarded as constant, by setting ρ_j as the variable. Then Eqs. (23) and (24) are reduced to, respectively:

$$\ddot{\bar{r}}_j = \ddot{\bar{\rho}}_j = -f\frac{M_j + m_j}{\rho_j^3}\bar{\rho}_j, \tag{25}$$

$$\frac{M_j + m_j}{\rho_j^3}\bar{\rho}_j = \sum_{i=1}^{n} m_i \frac{\bar{r}_{ji}}{r_{ji}^3}. \tag{26}$$

Let us define M_j and $\bar{R}_j$. Denoting:

$$\sum_{i=1}^{n} m_i \frac{\bar{r}_{ji}}{r_{ji}^3} = \bar{B}_j, \quad |\bar{B}_j| = B_j,$$

based on (21) and (26) we get:

$$\bar{R}_j = \bar{r}_j - \frac{\bar{B}_j}{B_j} \sqrt{\frac{M_j + m_j}{B_j}}. \tag{27}$$

To find M_j, let us use the conditions defined by the continuity of the gravitational potential. These conditions are analogous to the conditions for the constrained three-body problem (10) and are of the form:

1) $M_j = m_i$ when $r_{ji} = 0$;

2) $\partial M_j / \partial r_{ji} = 0$ when $r_{ji} = 0$, $i \neq j$

3) $\partial^2 M_j / \partial r^2_{ji} = 0$ when $r_{ji} = r_{jk}\left(\frac{m_i}{m_k}\right)^{\frac{2}{5}} \approx r_{i\,s.a}$

$k = 1, 2, \ldots, n; \quad i \neq k; \quad m_i \ll m_k.$

where $r_{i\,s.a}$ is the radius of the sphere of action of point m_i relative to the point m_j, which is the main attracting center for m_i. For example, for the actual system Sun (m_1), Earth (m_2), Moon (m_3), and SC (m_4), condition 3 can be represented as:

3') $\frac{\partial^2 M_4}{\partial r_{42}^2} = 0$ when $r_{42} = r_{41}\left(\frac{m_2}{m_1}\right)^{\frac{2}{5}} \approx r_{2\,s.a}$

3") $\frac{\partial^2 M_4}{\partial r_{43}^2} = 0$ when $r_{43} = r_{42}\left(\frac{m_3}{m_2}\right)^{\frac{2}{5}} \approx r_{3\,s.a}$

where in the case 3', in determining the radius of the Earth's (m_2) sphere of action, the principal attracting center is the Sun (m_1), and in the case 3", in determining the radius of the sphere of action of the Moon (m_3), the Earth is the main attracting center.

The relation for M_j, which in the general case is of the form:

$$M_j = \frac{\sum_{i=1}^{n} (m_i^p / r_{ji}^q)}{\sum_{i=1}^{n} (m_i^{p-1} / r_{ji}^q)}, \qquad i \neq j \tag{28}$$

satisfies conditions 1) and 2), where p and q are positive integers satisfying the inequalities /31

$$p \geq 0, \quad q \geq 1 \tag{29}$$

To satisfy condition 3), by virtue of Eq. (28), the following relation must obtain:

$$r_{jl}^{q} = \frac{q-1}{q+1} \cdot \frac{m_l^{p-1}}{\sum_{l=1}^{n} \frac{m_l^{p-1}}{r_{jl}^{q}}}, \quad l = 1, 2, \ldots, n; \quad i \neq j \neq l. \tag{30}$$

Considering that in actual problems, the sphere of action of point m_l is defined in the gravitational field of one principal attracting center $m_K >> m_l$, without allowing for the small perturbations of actions of the remaining system points, we can write relation (30) as:

$$r_{jl} = \left(\frac{q-1}{q+1}\right)^{\frac{1}{q}} \left(\frac{m_l}{m_k}\right)^{\frac{p-1}{q}} r_{jk}. \tag{31}$$

Relation (31) satisfies condition 3) for:

$$\left(\frac{q-1}{q+1}\right)^{\frac{1}{q}} = 1, \tag{32}$$

$$\frac{p-1}{q} = \frac{2}{5}. \tag{33}$$

Based on (29) and (33), the values of q must be multiples of 5, and (32) is satisfied as $q \to \infty$. When $q = 5$ or $q = 10$, the error of computation based on formula (31) is the limits at which condition 3) is satisfied, equal to 0.08 and 0.02, respectively. As shown by experiment, for the values $p = 3$ and $q = 5$, a high precision of calculation can be achieved.

Optimal algorithm for the stabilization of the motion of an artificial satellite in orbit. As the criterion of optimality, let us examine the functional

$$I = \int_{t_0}^{t_k} |u| \, dt,$$

equivalent to the energy expenditure in control.

If the motion of the artificial satellite of a planet (ASP) is defined by system 1, where the control u appears linearly, then with reference to the constraints:

$$1-u^2\leqslant 0, \tag{34}$$

$$a^2-\bar{x}^2\leqslant 0 \tag{35}$$

the problem can be solved by using the constrained principle of the maximum [4]. In this formulation, this problem is a generalization of the known solutions [4, 5], since here instead of the constraints on control (34), we consider the requirements imposed on the precision of control (35).

In this case, application of the mathematical apparatus of the constrained principle of the maximum is simplified, since the optimal trajectories only touch the boundaries of the domain (35) of the admissible changes in phase coordinates. Thus, to the necessary conditions of the principle of the maximum [5] are added only the conditions of discontinuity at the point of tangency for conjugate variables.

Bearing in mind that the ASP is acted on by perturbing moments, which by their nature of change are either close to a constant, or else proportional to the phase coordinate, it is precisely these two types of moments that have been examined as the right sides of the system.

The following results were obtained. The optimal algorithm of stabilization for ASP is a piecewise-constant function; the optimal phase trajectories are piecewise-smooth functions and form convex closed domains. The nodal points at these trajectories correspond to the points of control surface switching. /32

Figure 2 is a phase portrait of the optimal trajectory for the case when a moment of the form $M = A_1\bar{x} + A_2$ acts on the ASP, where $A_1 > 0$ and $A_2 > 0$.

The phase plane is divided into two domains: Ω_1 and Ω_2. The domain Ω_1 lies to the right of the curve ABCDE. If the phase coordinates of the ASP lie in this domain, the control must be switched on and $u = -1$. The domain Ω_2 lies to the left of the curve ABCDE. The initial position of the ASP corresponds to this domain, the control is absent, and $u = 0$. The curve ABCDE is the switching line.

The resulting algorithm of the stabilization of an ASP that is optimal for the case when perturbing moments of these kinds act on the satellite can be used also in setting up the stabilization algorithms for more complicated kinds of perturbing moments.

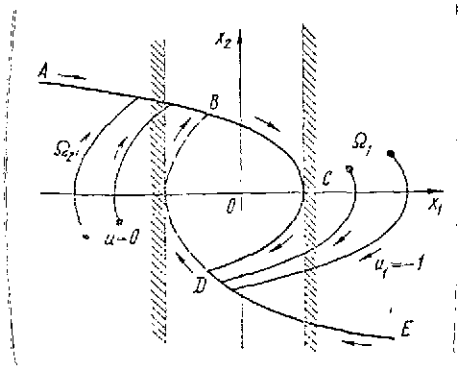

Fig. 2. Phase portrait of optimal trajectory.

Problems of optimal control with functionals dependent on intermediate values of coordinates. In the classical formulation, these variational problems were first presented in the studies [7, 8]. Their application to the solution of variational problems of descent into a planetary atmosphere led to the necessity of analyzing complex multidimensional boundary value problems that are not amenable to the analysis being examined here. This complexity was caused by the nonlinearities of the differential equations of motion of the ASP and by the use therein of functions of the aerodynamic characteristics of the ASP that cannot be analytically represented.

Analysis of problems of this type was carried out for simplified equations of motion of an ASP. It was assumed that the planet is a sphere with a Newtonian central potential; the atmospheric density is an exponential function of altitude; the extent of the descent trajectory is small compared with the planetary radius; and the aerodynamic characteristics are constant. The system of equations of motion of the ASP was reduced to the form:

$$\left.\begin{aligned}
\frac{dv}{d\rho} &= -\varkappa_1 \frac{v}{\sqrt{1-w^2}},\\
\frac{dw}{d\rho} &= \varkappa_2 u_1,\\
\frac{du}{d\rho} &= \frac{\varkappa_2}{w\sqrt{1-w^2}} u_2,\\
\frac{d\chi}{d\rho} &= -\frac{1}{\beta R}\cdot\frac{w}{\rho\sqrt{1-w^2}},\\
\frac{d\varepsilon}{d\rho} &= \frac{1}{\beta R}\cdot\frac{w}{\rho\sqrt{1-w^2}}\cdot\frac{\pi-(u+\varepsilon)}{\frac{\pi}{2}-\chi},\\
\frac{dt}{d\rho} &= \frac{1}{\beta\sqrt{\xi R}}\cdot\frac{1}{\rho\sqrt{v(1-w^2)}},
\end{aligned}\right\} \qquad (36)$$

where ρ is the density of the planetary atmosphere; κ_1 and κ_2 are the aerodynamic coefficients; R is the mean planetary radius; ξ is the acceleration due to the force of gravity; v, w, u, χ, ε, and t define three coordinates of the ASP center of mass and three components of the velocity vector of the center of mass in the coordinate system associated with the planet and with its origin at the center of attraction. The controls u_1 and u_2 are

associated by the relation $u_1^2 + u_2^2 = 1$. The functional being optimized for these problems is represented as: /33

$$I = f(\rho_1, v_1, \ldots, t_1), \tag{37}$$

where the parameters $v_1, \ldots t_1$ correspond to the intermediate value ρ_1 (which in the general case can be determined).

Analysis of the system (36) in several cases makes it possible for a specific form of functional (37) to obtain an approximate analytic solution of the optimal problem and to investigate its main features.

As an example, let us consider the motion of an ASP in the vertical plane; we will select the control from the condition of the minimum

$$I = -\frac{1}{\beta R}\int_{\rho_0}^{\rho_1} \frac{\omega}{\rho\sqrt{1-\omega^2}}\,d\rho = \chi_1 - \chi_0,$$

where ρ_1 is an assigned quantity in the interval $|\rho_0 - \rho_k|$. The equations of motion in this case will be of the form:

$$\left.\begin{aligned}
\frac{dv}{d\rho} &= -\varkappa_1 \frac{v}{\sqrt{1-\omega^2}},\\
\frac{d\omega}{d\rho} &= \varkappa_2 u_1,\\
\frac{d\chi}{d\rho} &= -\frac{1}{\beta R}\frac{\omega}{\rho\sqrt{1-\omega^2}},\\
\frac{dt}{d\rho} &= \frac{1}{\rho\sqrt{\xi R}}\frac{1}{\rho\sqrt{v(1-\omega^2)}}
\end{aligned}\right| \quad \text{for } |u_1| \leqslant 1. \tag{38}$$

We will seek the solution for the following initial and final conditions:

$$v(\rho_0) = C_1, \quad \omega(\rho_0) = C_2,$$
$$\chi(\rho_0) = C_3, \quad \chi(\rho_K) = C_5, \quad t(\rho_0) = C_4,$$

where C_1, C_2, C_3, C_4, and C_5 are constants.

From the necessary conditions of optimality [7] we get the result that the optimal law of variation of control is the piecewise-constant function:

$$u_1 = \operatorname{sign}\psi$$

where the function ψ continuous over $|\rho_0 - \rho_k|$ and equal to zero at the endpoint is defined from the solution to the differential equation:

$$\frac{d\psi}{d\rho} = -(1-\lambda)\frac{d\chi}{d\rho}/\omega(1-\omega^2) \text{ on } [\rho_0 \div \rho_1],$$

$$\frac{d\psi}{d\rho} = \lambda\frac{d\chi}{d\rho}/\omega(1-\omega^2) \text{ on } [\rho_1 \div \rho_K],$$

$$\lambda = \text{const.}$$

Analysis of this equation shows that there is only one point of a change in the sign of the function ψ and, therefore, control u_1 has one switching point. We note that for the resulting control the first three equations of system (38) are integrated to completion, and the last -- in quadratures.

REFERENCES

1. Balk, M.B., Elementy dinamiki kosmicheskogo poleta [Elements of space flight dynamics], "Nauka," Moscow, 1965.

2. Bellman, R., and S. Dreyfus, Prikladnyye zadachi dinamicheskogo programmirovaniya [Applied problems of dynamic programming], "Nauka," Moscow, 1965.

3. Yegorov, V.A., UFN 63(1a) (1957).

4. Leytman, Dzh., Vvedeniye v teoriyu optimal'nogo upravleniya [Introduction to the theory of optimal control], "Nauka," Moscow, 1968.

5. Pontryagin, L.S. et al., Matematicheskaya teoriya optimal'nykh protsessov [Mathematical theory of optimal processes], Fizmatgiz, Moscow, 1961.

6. Finikov, S.P., Differentsial'naya geometriya [Differential geometry], Moscow State University Press, Moscow, 1961.

7. Troitskiy, V.A., PMM 26(6) (1962). /34

8. Troitskiy, V.A., "Variational problems of the optimization of control processes with functionals dependent on intermediate values of the coordinates," DAN SSSR 149(2) (1963).

9. Byrnes, D.V., and H.L. Hooper, AIAA Paper, No. 1062 (1970) (Russian translation,EI, Astronavtika i raketodinamika, No. 2 (1971)).

10. Shaikh, N.A., Astronaut. acta 12(3) (1966) (Russian translation, EI, Astronavtika i raketodinamika, No. 6 (1967)).

USE OF THE FINITE-ROTATION VECTOR IN ONBOARD DIGITAL COMPUTERS FOR DETERMINING SPACECRAFT ORIENTATION

A.P. Panov

The problem of determining the orientation of spacecraft (SC) relative to inertial space using digital onboard computers (DOC) is one of the most specific problems solved on board a SC with integrating rate transducers hard-mounted on the SC body [1].

The specific details of the problem include the fact that the primary integrated information on the SC attitude does not permit the use of ordinary mathematical methods for the numerical integration of differential equations of the SC attitude and requires the use in the DOC of special algorithms. This specific feature is aggravated by the fact that the algorithms used for these purposes must ensure the determination of the SC orientation with a minimum volume of computations and occupy a minimum volume in the DOC storage.

There are several computational algorithms for determining the orientation of a SC using the three Eulerian angles, the four Rodrig-Hamilton parameters (RH) -- quaternions, the four Keill-Klein parameters, and the four direction cosines [2-5]. Here the highest preference [4-8] is given to the use in the DOC of algorithms for computing the parameters RH, since they require the smallest volume of computations for realization.

The orientation of the SC can also be determined by using the finite-rotation vector. Use of the finite-rotation vector in the DOC instead of the RH parameters reduces the volume of computations by 30%, since in this case it is sufficient to compute only three parameters -- the projections of the finite-rotation vector.

As we know from the theory of finite rotations of a solid [9], the finite-rotation vector has the direction of the unit vector of the axis of rotation $\bar{e}$, equal in magnitude to the doubled tangent of half the angle of rotation χ and is of the form:

$$\bar{\vartheta} = 2\bar{e}\operatorname{tg}\frac{\chi}{2}. \qquad (1)$$

The vector ϑ uniquely determines the position of the body relative to a fixed (inertial) coordinate system, and from its projections onto the axes of the trihedron Oxyz fixed to the rotating body we can find the direction cosines.

Actually, between the projections of the finite-rotation vector and the RH parameters [9] there is a relationship, which can be written in matrical form as:

$$\bar{\vartheta} = \frac{2}{\lambda_0}\lambda, \tag{2}$$

where

$$\vartheta = \begin{bmatrix} \vartheta_x \\ \vartheta_y \\ \vartheta_z \end{bmatrix}, \tag{3}$$

/35

$$\lambda = \begin{bmatrix} \lambda_x \\ \lambda_y \\ \lambda_z \end{bmatrix}, \tag{4}$$

$$\lambda_0 = \sqrt{1 - (\lambda_x^2 + \lambda_y^2 + \lambda_z^2)}. \tag{5}$$

On the other hand, the matrix of the direction cosines

$$L = \begin{bmatrix} l_{xX} & l_{xY} & l_{xZ} \\ l_{yX} & l_{yY} & l_{yZ} \\ l_{zX} & l_{zY} & l_{zZ} \end{bmatrix}, \tag{6}$$

characterizing the orientation of the trihedron Oxyz relative to the inertial trihedron O_1XYZ can be expressed also in terms of the parameters RH:

$$L = \begin{bmatrix} \lambda_0^2 + \lambda_x^2 - \lambda_y^2 - \lambda_z^2, & 2(\lambda_0\lambda_z + \lambda_x\lambda_y), & 2(-\lambda_0\lambda_y + \lambda_x\lambda_z), \\ 2(-\lambda_0\lambda_z + \lambda_y\lambda_x), & \lambda_0^2 + \lambda_y^2 - \lambda_z^2 - \lambda_x^2, & 2(\lambda_0\lambda_x + \lambda_y\lambda_z), \\ 2(\lambda_0\lambda_y + \lambda_z\lambda_x), & 2(-\lambda_0\lambda_x + \lambda_z\lambda_y), & \lambda_0^2 + \lambda_z^2 - \lambda_x^2 - \lambda_y^2 \end{bmatrix}. \tag{7}$$

The joint solution of (2) and (7) is the matrix **L** in terms of the projections of the finite-rotation vector:

$$L = \lambda_0^2 P, \tag{8}$$

where

$$\lambda_0^2 = \frac{1}{1 + \frac{1}{4}(\vartheta_x^2 + \vartheta_y^2 + \vartheta_z^2)}; \tag{9}$$

$$P = \begin{bmatrix} 1 + \frac{1}{4}(\vartheta_x^2 - \vartheta_y^2 - \vartheta_z^2), & \vartheta_z + \frac{1}{2}\vartheta_x\vartheta_y, & -\vartheta_y + \frac{1}{2}\vartheta_z\vartheta_x, \\ -\vartheta_z + \frac{1}{2}\vartheta_x\vartheta_y, & 1 + \frac{1}{4}(-\vartheta_x^2 + \vartheta_y^2 - \vartheta_z^2), & \vartheta_x + \frac{1}{2}\vartheta_y\vartheta_z, \\ \vartheta_y + \frac{1}{2}\vartheta_z\vartheta_x, & -\vartheta_x + \frac{1}{2}\vartheta_y\vartheta_z, & 1 + \frac{1}{4}(\vartheta_z^2 - \vartheta_x^2 - \vartheta_y^2) \end{bmatrix} \tag{10}$$

To compute matrix (7), it is required to perform ten multiplication and 21 operations of the addition and shift type in the DOC, and the computation of matrix (10) together with (9) can be carried out by performing six multiplication operations, one division operation, and 29 operations of the addition and shift type. Computation of matrix **L** based on (8) requires the additional performance of nine multiplication operations. We note that the matrix **L** is required generally for the linear transformation of vectors, for example, for computing the projections of the vector of the apparent velocity onto the axes of the inertial coordinate system:

$$W = L^T w, \tag{11}$$

where **w** is the matrix-column consisting of the projections of the apparent velocity on the fixed axes:

$$w = \begin{bmatrix} w_x \\ w_y \\ w_z \end{bmatrix}, \tag{12}$$

and $\mathbf{L}^T$ is the transposed matrix **L**.

In this case, the operations in the separate computation of (8) and (10) need not be carried out, but computations using the formula: /36

$$W = \lambda_0^2 (P^T w), \tag{13}$$

can be performed at once, and because of this, to solve the part of the problem associated with determining the orientation, it is sufficient to perform nine multiplications, one division, and 29 operations of the addition and shift type.

As we can see, from the standpoint of the volume of computations required in solving linear programming problems in the DOC, the parameters RH and the projections of the finite-rotation vector are approximately equivalent. To solve the problem of determining the direction cosines of the axis of the SC finite rotation providing the alignment of the fixed axes of the SC with the coordinate system specified in inertial space, the parameters RH and the projections of the finite-rotation vector are also equivalent, since:

$$\frac{1}{2\sqrt{\lambda_x^2 + \lambda_y^2 + \lambda_z^2}} \lambda = \frac{1}{\sqrt{\vartheta_x^2 + \vartheta_y^2 + \vartheta_z^2}} \vartheta. \tag{14}$$

The preference for using the vector representation of the SC orientation in the DOC compared with the parameters RH is manifested only after constructing algorithms for computing the projections of the finite-rotation vector.

Suppose that from the primary data integrating transducers information on the SC angular motion arrives at the DOC in discrete form:

$$\Theta = \begin{bmatrix} \Theta_x \\ \Theta_y \\ \Theta_z \end{bmatrix} = \int_{t_h}^{t_h+H} \omega dt, \tag{15}$$

where ω is the matrix-column consisting of the projections of the vector of the absolute angular rate of rotation of the SC onto the axes of the fixed trihedron:

$$\omega = \begin{bmatrix} \omega_x \\ \omega_y \\ \omega_z \end{bmatrix}, \tag{16}$$

H is the time step of discretization, and t_h is the arbitrary instant of time, where $\Theta_i << 1$ (i = x, y, z).

Since the primary data (15) does not reflect the nature of motion of the SC within the time interval H, we will assume that it was obtained during one small finite rotation, which is the resultant of all rotations made by the SC in actuality during the time H. We can show that given this assumption, the information (15) will reflect this small resultant rotation with an error that can reach a value of the order of $O(H^3)$ or $O(\Theta^3)$, owing to the noncommutativity of the finite-rotation components [5, 9].

Then the projections of the vector of the small finite rotation $\Delta\bar{\theta}$ can be represented in terms of the information (15) as:

$$\Delta\theta = \frac{\ell}{\chi} \operatorname{tg} \frac{\chi}{2} \Theta, \tag{17}$$

where

$$\chi = \sqrt{\Theta_x^2 + \Theta_y^2 + \Theta_z^2}, \tag{18}$$

whence, after expanding tg $\chi/2$ in a power series, we get, with the error $(1/4)\chi^2\Theta$:

$$\Delta\theta = \Theta \tag{19}$$

We denote the matrix of the projections of the finite-rotation vector determining the SC orientation at the beginning of step H by: /37

$$\theta_h = \begin{bmatrix} \theta_{x,h} \\ \theta_{y,h} \\ \theta_{z,h} \end{bmatrix}. \tag{20}$$

According to the rule of addition of finite rotations [9], we obtain an algorithm for computing the projections of the vector of the rotation that is the resultant of the rotations $\bar{\theta}_h$ and $\Delta\bar{\theta}$:

$$\vartheta = \left(1 - \frac{1}{4}\Theta^T\theta_h\right)^{-1} \cdot \left(\Theta + \theta_h - \frac{1}{2}\breve{\Theta}\theta_h\right). \tag{21}$$

Here Θ^T is the transposed matrix Θ, and $\breve{\Theta}$ is the skew-symmetric matrix, of the form:

$$\breve{\Theta} = \begin{bmatrix} 0 & -\Theta_z & \Theta_y \\ \Theta_z & 0 & -\Theta_x \\ -\Theta_y & \Theta_x & 0 \end{bmatrix}. \tag{22}$$

Here we note that the error of algorithm (21) is wholly defined by the error of equality (19) and by the error of the non-commutativity of the information (15).

For a DOC not performing operations of division, from (21) we can get algorithms of any order of precision. Replacing the fractional part in (21) by a power series, for example, we get the first-order algorithm:

$$\vartheta = \left(1 + \frac{1}{4}\Theta^T\theta_h\right)\left(\theta_h + \Theta - \frac{1}{2}\breve{\Theta}\theta_h\right) \tag{23}$$

with the estimate of the error in the step:

$$\delta\vartheta = \frac{1}{16}\left(\Theta^T\theta_h\right)^2\theta_h; \tag{24}$$

the second-order algorithm:

$$\vartheta = \left| 1 + \frac{1}{4}\Theta^{\mathrm{T}}\vartheta_h + \frac{1}{16}(\Theta^{\mathrm{T}}\vartheta_h)^2 \right| \left| \vartheta_h + \Theta - \frac{1}{2}\Theta[\vartheta_h] \right| \tag{25}$$

with the estimate of the error for the step:

$$\delta\vartheta = \frac{1}{64}(\Theta^{\mathrm{T}}\vartheta_h)^3 + \frac{1}{4}[\Theta[\Theta\vartheta]]\Theta + 0(H^3). \tag{26}$$

we can easily also form algorithms of the third and higher orders of precision, however they require that we obtain primary information not containing the noncommutativity error.

In scalar notation, algorithms (23) and (25) are of the form, respectively:

$$\vartheta_x = (1+k)\left[\vartheta_{x,h} + \Theta_x - \frac{1}{2}(\Theta_y\vartheta_{z,h} - \Theta_z\vartheta_{y,h})\right] \quad (x, y, z), \tag{27}$$

$$\vartheta_x = (1+k+k^2)\left[\vartheta_{x,h} + \Theta_x - \frac{1}{2}(\Theta_y\vartheta_{z,h} - \Theta_z\vartheta_{y,h})\right] \quad (x, y, z), \tag{28}$$

where $$k = \frac{1}{4}(\Theta_x\vartheta_{x,h} + \Theta_y\vartheta_{y,h} + \Theta_z\vartheta_{z,h});$$

(x, y, z) is the symbol of cyclic permutation.

For comparison, let us write the algorithms for computing the parameters RH [5]:

first-order algorithm

$$\lambda_x = \lambda_{x,h} + \frac{1}{2}(\Theta_x\lambda_{0,h} + \Theta_z\lambda_{y,h} - \Theta_y\lambda_{z,h}),$$
$$\lambda_0 = \lambda_{0,h} - \frac{1}{2}(\Theta_x\lambda_{x,h} + \Theta_y\lambda_{z,h} - \Theta_z\lambda_{y,h}) \quad (x, y, z); \tag{29}$$

second-order algorithm

/38

$$\lambda_x = \left(1 - \frac{1}{8}\Theta^2\right)\lambda_{x,h} + \frac{1}{2}(\Theta_x\lambda_{0,h} + \Theta_z\lambda_{y,h} - \Theta_y\lambda_{z,h}),$$
$$\lambda_0 = \left(1 - \frac{1}{8}\Theta^2\right)\lambda_{0,h} - \frac{1}{2}(\Theta_x\lambda_{x,h} + \Theta_y\lambda_{y,h} + \Theta_z\lambda_{z,h}) \quad (x, y, z), \tag{30}$$

where $$\Theta^2 = \Theta_x^2 + \Theta_y^2 + \Theta_z^2.$$

As we can see, the first-order algorithms (27) and (29), from the standpoint of the required volume of computations, are equivalent, however algorithm (27) yields an economy in the DOC storage used.

Use of algorithm (28) instead of algorithm (30) provides, when carried out in the DOC, besides the advantage in the volume of the required storage, also a savings in the volume of computations, saving six operations of multiplication and six operations of the addition or shift type in each step, which is 30% of the total volume of computations using algorithm (30).

REFERENCES

1. "Inertial systems without gyrostabilized platform," Voprosy raketnoy tekhniki [Problems of rocket technology], No. 1, 1967.

2. Savazh, P.G., Mekhanika, No. 1 (1968).

3. Bolanskiy, Ye.D., and V.D. Furman, Kosmicheskiye issledovaniya 8(6)(1970).

4. Wilcox, I.C., IEEE Trans. on Aerospace and Electronic Systems, AES-3,5, 1967.

5. Tkachenko, A.I., in the book Matematicheskoye obespecheniye ETsVM [Mathematical basis for digital computers], Vol. 1, published by the Institute of Cybernetics of the Ukrainian SSR Academy of Sciences, Kiev, 1970.

6. Tkachenko, A.I., Kibernetika i vychisletel'naya tekhnika [Cybernetics and computers], Vol. 5, "Naukova dumka," Kiev, 1970.

7. Ikes, B.P., Raketnaya tekhnika i kosmonavtika 8(1) (1970).

8. Bezhko, A.P. et al., Inzhenernyy zhurnal, Mekhanika tverdogo tela, No. 1 (1971).

9. Lur'ye, A.I., Analiticheskaya mekhanika [Analytic mechanics], Fizmatgiz, Moscow, 1961.

OPERATING ECONOMY OF SPACECRAFT STABILIZATION SYSTEMS

N.F. Gerasyuta, Yu.D. Sheptun, and S.V. Yaroshevich

Natural oscillations of spacecraft outside the atmosphere when acted on by a constant perturbing moment have been examined by E.V. Gaushus [1, 2]. It is assumed that the orientation of spacecraft is performed with a relay system, whose actuators produce impulses of controlling moments that are equal in magnitude.

Actual motion must differ from that considered above owing to the inequality of the control impulses, which can be due to the imprecision of the manufacture of actuators or provided for deliberately.

The inequality of the impulses of controlling moments can be expressed mathematically by writing dimensionless equations of motion as follows:

$$\ddot{\varphi} = \varkappa + L,$$

$$\varkappa = \begin{cases} -\delta_1 & \text{for } j \geqslant 1;\ j > m \text{ and } \frac{dj}{d\tau} < 0, \\ 0 & \text{for } |j| \leqslant m;\ 1 > |j| > m \text{ and } \frac{dj}{d\tau} > 0, \\ +\delta_2 & \text{for } j \leqslant -1;\ j < -m \text{ and } \frac{dj}{d\tau} > 0, \end{cases}$$

$$j = T\dot{\varphi} + \varphi,\ \delta_1 \neq \delta_2.$$

Here ϕ and κ are the controlled and controlling parameters; L is the coefficient of the perturbing moment; and T and m are the controller parameters. /39

The equation of the phase trajectory of a spacecraft is of the form:

$$\dot{\varphi}^2 - \dot{\varphi}_0^2 = 2(\varkappa + L)(\varphi - \varphi_0).$$

The phase trajectory in the plane $(\phi, \dot{\phi})$ is shown in Fig. 1. The changes in the angular velocity of the craft when actuators are switched on are characterized by the quantities $\omega_1 = |\dot{\varphi}_{i+1} - \dot{\varphi}_i|$ and $\omega_2 = |\dot{\varphi}_{i+3} - \dot{\varphi}_{i+2}|$. If $\delta_1 \neq \delta_2$, then $\omega_1 \neq \omega_2$, and $\Delta\omega = \omega_2 - \omega_1 \neq 0$.

Let us review the oscillational motions of the system and examine the possible method of reducing the amount of energy expended by the actuators of the system during regulation for the case when there is no perturbing moment (L = 0).

Suppose $\omega_2 > \omega_1$ and $\omega_2 - \omega_1 = \Delta\omega$. Let us limit ourselves to the case when $\Delta\omega < \omega_1$. The phase trajectory of the possible motions of the system is shown in Fig. 2. Let us call the motions characterized by the trajectory sections 123 and 34567 the single-impulse and double-impulse cycles, respectively. Let us select as the segment without contact the segment of the line of the inclusion MM, for whose points the condition

$$0 < V < \omega_2, \quad V = \dot{\varphi}. \tag{1}$$

is satisfied.

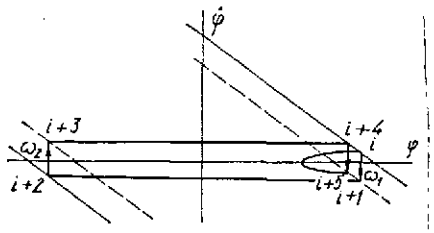

Fig. 1. Example of phase trajectory of perturbing motion ($L \neq 0$).

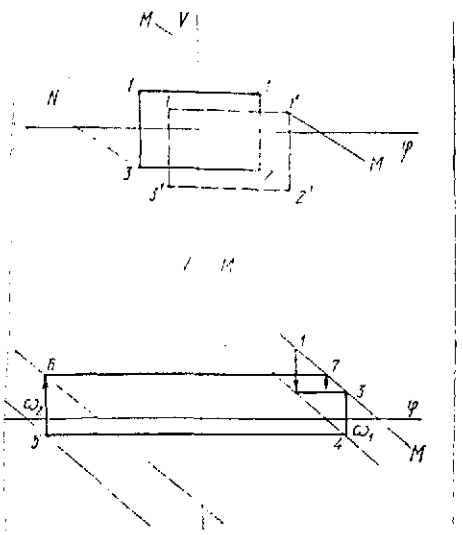

Fig. 2. Phase trajectory of the motion of a spacecraft when $L = 0$, $\Delta\omega \neq 0$.

Let us construct the point transformation of segment (1) into itself. The transformation is defined by the recursion function

$$f(V) = \begin{cases} \alpha(V) = V + \Delta\omega & \text{for } V < \omega_1, \\ \beta(V) = V - \Delta\omega & \text{for } V > \omega_1. \end{cases}$$

The transformations defined by the recursion functions $\alpha(V)$ (corresponding to the double-impulse cycle) and $\beta(V)$ (corresponding to the single-impulse cycle) are denoted by T_α and T_β. The form of the recursion functions $\alpha(V)$ and $\beta(V)$ is shown in Fig. 3; $\alpha(V)$ and $\beta(V)$ are straight lines parallel to the bisector of the right angle, and therefore the simple transformations T_α and T_β do not have fixed points. The fixed points are possible in complex n-multiple transformations of the form $\Pi_n = T_\alpha^{n-1} T_\beta$, with the recursion formula:

$$f_n(V) = \alpha_{n-1}[\beta(V)] = V + (n-1)\Delta\omega - \omega_1,$$

$n = 2, 3, \ldots,$

if

$$\omega_1/\Delta\omega = n - 1. \tag{2}$$

Any point of the segment (1) (the coordinates of the fixed points are random in nature) is a fixed point.

When condition (2) is satisfied, the control system performs a natural-oscillatory motion; during the period of the natural oscillations one single-impulse and (n - 1) double-impulse cycles occur. The ordinate of the initial point of the first double-impulse cycle following the single-impulse cycle will always satisfy the condition $0 \leq V_0 \leq \Delta\omega$. In the general case, the function $f_n'(V)$ describes the mapping of a circle into itself, induced by the rotation of each point of the circle by the same angle. Therefore, to each rational $\omega_1/\Delta\omega$ there corresponds the corresponding fixed points of this mapping of the corresponding multiples, that is, closed phase trajectories of different complexities, and corresponding to the irrational $\omega_1/\Delta\omega$, there correspond the closed invariant trajectories. /40

The ordinate V_0 continuously changes in the range $0 < V_0 < \Delta\omega$; during the control process, motions are induced that are characterized by the transformations $\Pi_n = T_\alpha^{n-1}T_\beta$, $\Pi_{n+1} = T_\alpha^n T_\beta$. We can show a $V_\Gamma = \mu\Delta\omega$ such that when $V_0 < V_\Gamma$, the transformation Π_{n+1} occurs, and when $V_0 > V_\Gamma$ -- the transformation Π_n occurs.

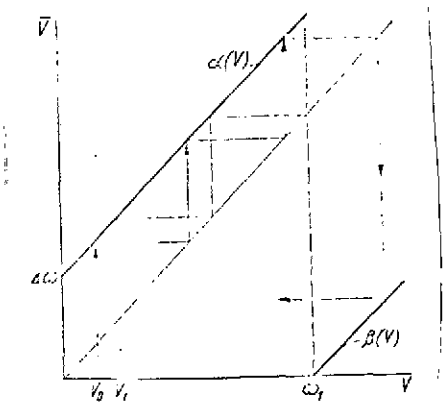

Fig. 3. The Koenigs-Lamereaux plot (L = 0).

The duration of the sequence m - 1 (m = n + 1 or m = n) of double-impulse cycles and one single-impulse cycle is defined by the sum:

$$t_\Sigma = t_0 + \sum_{i=1}^{m-1} t_i = \frac{\omega_1 T}{V_0} + \sum_{i=1}^{m-1}\left(\frac{2\Delta - \omega_1 T}{\omega_1 - V_0 - (i-1)\Delta\omega} + \frac{2\Delta - \omega_2 T}{V_0 + i\Delta\omega}\right)$$

where $t_0(t_i)$ is the duration of the single-impulse (double-impulse) cycle, respectively.

The duration of the sequence of cycles t_Σ depends essentially on the ordinate of the initial point of the first cycle. This function, plotted for the values of the parameters $\omega_2 = 2$, $\omega_1 = 1.63$, $T = 0.3$, and $\Delta = 1$ is illustrated by Fig. 4.

Let us compare the amount of energy expended by the actuators when $\omega_1 = \omega_2$ and $\omega_1 \neq \omega_2$. We know [2] that for an $\omega_1 = \omega_2$ and $V_0 = \omega_1/2$, we have the largest number of on-switchings of the actuators and the largest energy outlay over the final time interval. This case, as a rule, is used as the calculation

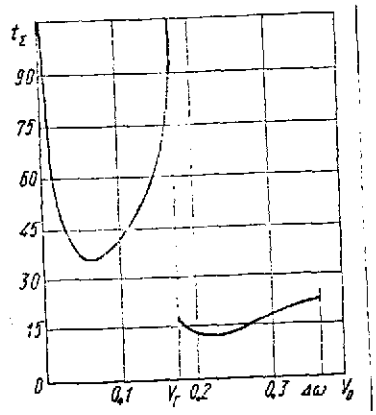

Fig. 4. Dependence of the duration of the series of cycles t_Σ on the ordinate of the initial point.

case when determining the required energy reserve. For comparison, let us examine the ratio $q = Q/Q_c$, where Q and Q_c are the energy outlays during the time τ for $\omega_1 \neq \omega_2$, and $\omega_1 = \omega_2 = \omega$, respectively. In determining Q_c, we will assume that $\omega = \inf(\omega_1\omega_2)$ and that the natural oscillations of the system are symmetrical.

The values of q corresponding to the different values of $\Delta\omega$ and calculated for $\omega_1 = 1.67$, $T = 0.3$, $\omega_2 = \omega_1 + \Delta\omega$, and $\tau = 10$, are presented below:

$\Delta\omega$	5% ω_1	10% ω_1	15% ω_1
q	0.38	0.42	0.22

The quantity V_0 was selected for each $\Delta\omega$ by using the plot $t_\Sigma = t_\Sigma(V_0)$ so that during the flight time τ the sequence consisting of (m - 1) double-impulse and one single-impulse cycles occurred, whose duration was a minimum, $t_\Sigma = t_{\Sigma\,\min}$. The time $\tau = 810$ corresponded to $t \approx 5400$ sec (the time of one revolution of the satellite around the Earth). For the selected ω_1 and ω_2, during the time $\tau = 810$, 100 - 150 engagements of the actuators occurs; 20-30 series of cycles with the duration $t_\Sigma = t_\Sigma(V_0)$ are observed. Therefore, when $\Delta\omega \neq 0$, the energy outlays are appreciably less than in the case $\Delta\omega = 0$. /41

Let us examine the motion and estimate the energy consumption for stabilization of the spacecraft when acted on by a perturbing moment. Following the work [1], we will conduct the analysis of motion in the phase plane (U,x) where $U = T\dot{\phi} + \phi$; $x = \dot{\phi} + LT$. Then the equation of the phase trajectory can be written as $x^2 - x_0^2 = 2(\kappa + L)(U - U_0)$. The phase trajectory is shown in Fig. 5.

Selecting as the segment without contact the line

$$U = 1 - \omega_1 T; \quad -T/2 - LT < x < T/2 - LT,$$

we get the following equations for the recursion function:

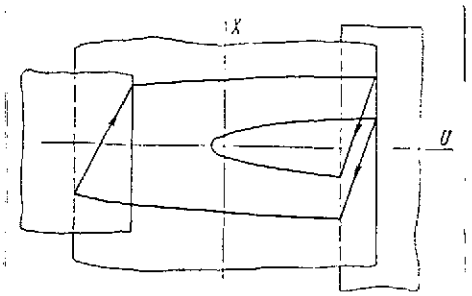

Fig. 5. Example of phase trajectory of the motion of a spacecraft in the plane (U,x), (L ≠ 0.

$$f(x)=\begin{cases}\Theta(x)=\sqrt{x^2+2L\omega_1 T}-\omega_1 \text{ for } x>-\sqrt{E_1},\\ \gamma(x)=\sqrt{(\omega_2-\sqrt{x^2-E_1})^2+E_2}-\omega_2 \text{ for } x<-\sqrt{E_1},\end{cases}$$
$$E_1=2L(2-\omega_1 T),\quad E_2=2L(2-\omega_2 T). \tag{3}$$

The transformations defined by the functions $\Theta(x)$, $\gamma(y)$, will be denoted by T_Θ and T_γ, respectively. We will conduct our analysis for the fixed value $\omega_1 > 2(2\sqrt{L} - LT)$, for which the function $\Theta(x)$ has no fixed point (the spacecraft oscillations are produced by engaging both actuators).

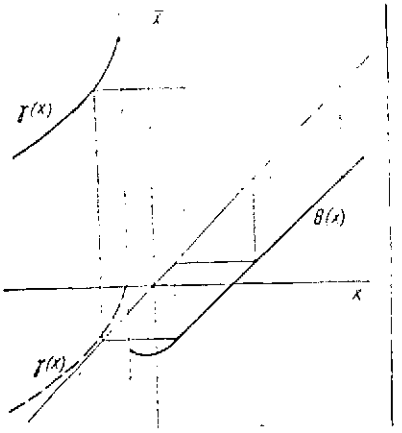

Fig. 6. Koenigs-Lamereaux plot for the point transformation Π_m (L ≠ 0).

Let us examine the effect of the parameter $\Delta\omega$ on the nature of the motion, by varying ω_2 in the range $0 \leq \omega_2 \leq (2/T)$. Suppose $\omega_2 >> \omega_1$. Then the following motions are possible, corresponding to the point transformations

$\Pi_m = T_\Theta^{m-2} T_\gamma T_\Theta$ (m = 1, 2, 3,...) with the recursion functions $f_m = \Theta_{m-2}\{\gamma[\Theta(x)]\}$.

The diagram of the transformation Π_m is in Fig. 3. With decrease in ω_2, the transformation Π_m successively changes into the transformations Π_{m-1}, Π_{m-2}, ..., $\Pi_{m-\ell} = T_\Theta^{m-\ell-2} T_\gamma T_\Theta$ (ℓ = 1, 2, ..., m - 2). If ℓ = m - 2, we have $\Pi_2 = T_\Theta T_\gamma$, which with further increase in ω_2 changes into the transformations

For some value ω_2, the multiple fixed point of the simple transformation $\gamma(x)$ is produced. The function $\gamma(x)$ corresponding to the moment at which the fixed point appears is shown in Fig. 6 with a dashed line. /42

The equation of the bifurcation curve $\omega_2 = \omega_2(L)$ can be obtained by solving the system of equations:

$$\gamma(C) - C = 0,$$
$$\left.\frac{d\gamma}{dx}\right|_{x=C} = 1.$$

In the following, the multiple fixed point splits into two (larger and smaller); the larger fixed point disappears when the equality $\gamma[-\sqrt{E_1}] = -\sqrt{E_1}$, from whence:

$$\omega_2 = LT + \sqrt{L^2T^2 + (\omega_1 - \sqrt{E_1})^2 - 4L}.$$

The coordinate C_M of the second fixed point decreases to the value

$$C_M = \sqrt{E_2} - \omega_1. \tag{4}$$

If $\omega_2 \leqslant \omega_2^* = \sqrt{C_M^2 - E_1}$, where ω_2^* is the value for which equality (4) is satisfied, the transformation T_γ is impossible; motion commences, whose phase trajectory is illustrated by Fig. 7. Analysis of this motion is conveniently done by adopting as the segment without contact the line

$$U = -1 + \omega_2 T, \quad \sqrt{E_2} - \omega_1 \leqslant x \leqslant 0 \tag{5}$$

The recursion formulas written with respect to the segment (5) are analogous to the functions f(x) (3). Analysis of this point transformation will not differ from the analysis of the transformation $\Pi_m = T_\Theta^{m-1} T_\gamma$. Therefore in the following we will limit ourselves to considering the oscillations characterized by the recursion functions f(x).

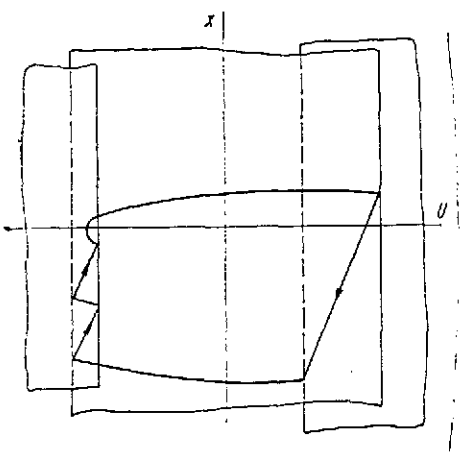

Fig. 7. Example of the phase trajectory of spacecraft motion, if $\omega_2 < \sqrt{C_M^2 - E_1}$.

We will make the analysis of the stability of the periodic motions of the system. The stability of simple fixed points of the transformation T_Θ according to the Koenigs theorem follows from the fact that for any values of the system parameters and any values of x, the condition [3]

$$\lambda_\Theta = \frac{d\Theta(x)}{dx} = \frac{x}{\sqrt{x^2 + 2L\omega_1 T}} < 1.$$

is satisfied.

The multiple fixed point of the simple transformation T_γ

is semistable, since:

$$\lambda_\gamma = \frac{d\gamma(x)}{dx} = 1.$$

The larger fixed point a_1 of this transformation is always unstable ($\lambda_\gamma > 1$). The value of λ_γ for the part a_2 continuously decreases with decrease in ω_2, and therefore, the point can become unstable only when $\lambda_\gamma < -1$.

Let us find the λ_γ for the smallest coordinate of the point a_2:

$$\lambda_\gamma = \frac{d\gamma}{dx}\Big|_{x=C_M} = \frac{[\omega_2 - \sqrt{(\sqrt{E_2}-\omega_1)^2 - E_1}]\,(\sqrt{E_2}-\omega_1)}{\sqrt{[\omega_2 - \sqrt{(\sqrt{E_2}-\omega_1)^2 - E_1}]^2 + E_2}\cdot\sqrt{(\sqrt{E_1}-\omega_1)^2 - E_1}}.$$

From the equations of the fixed point $\gamma(x) = x$, we get: /43

$$-\omega_1 + \sqrt{[\omega_2 - \sqrt{(\sqrt{E_2}-\omega_1)^2 - E_1}]^2 + E_2} = \sqrt{E_2} - \omega_1,$$
$$\omega_2 - \sqrt{(\sqrt{E_2}-\omega_1)^2 - E_1} = 0,$$

whence $\lambda_\gamma|_{x=C_m} = 0$ and, therefore, the point a_2 is always stable.

For the complex transformations Π_m and Π_n, the functions λ_m and λ_n are defined by the formulas [1]:

$$\lambda_m = \frac{df_m}{dx} = \frac{d\gamma[\Theta(x)]}{dx}\prod_{i=1}^{m-2}\frac{d\Theta[f_i(x)]}{dx},$$

$$\lambda_n = \frac{df_n}{dx} = \frac{d\Theta}{dx}\prod_{i=1}^{n-1}\frac{d\gamma[f_i(x)]}{dx}.$$

Here $f_i(x) = \gamma_{i-1}[\Theta(x)]$.

Analysis shows that λ_m and λ_n take on extremal values when $x = C_0$, where C_0 is the coordinate of the fixed point corresponding to the parameter $\omega_2 = 0$.

If $\omega_2 = 0$, then $\gamma(x)$ degenerates into $\Theta(x)$ and, therefore,

$$\lambda_m|_{x=C_0} = \lambda_n|_{x=C_0} = \prod_{i=1}^{n}\frac{d\Theta}{dx}[F_i(x)].$$

Here $F_i = \Theta_{i-1}[\theta(x_0)]$.

Since $\left|\frac{d\theta}{dx}\right| < 1$ for any values of x, then $|\lambda_m|_{x=c_*} = \lambda_n|_{x=c_*} < 1$.

This implies that with change in ω_2, the fixed points of the transformations Π_m and Π_n do not change their stability. Here the larger fixed point is always unstable, and the smaller is always stable.

Let us examine the change in the complex oscillations of a spacecraft for the example of the transformation Π_m. The function $f_m^{\Theta}(x)$ is defined in the interval $\sup[-f_m^{\Theta}(-\sqrt{E_1})], -\sqrt{E_1} \leq x \leq \inf[f_m^{-\Theta}(-\sqrt{E_1})], S]$, where S can be found from the equation $\Theta(S) = -\sqrt{E_1}$.

With decrease in ω_2, the structure of the phase trajectories bringing about the transformation Π_m changes. The instants of change of structure (bifurcation moments) are defined by the generalized equation:

$$\Theta_K\{\gamma[\Theta(r)]\} = R, \tag{6}$$

where K, r, and R take on the values m - 1, 0 and $-\sqrt{E_1}$ at the moment of inception of the transformation Π_m; m - 1, $-\sqrt{E_1}$, and $-\sqrt{E_1}$ at the moment that the fixed point of the transformation Π_{m+1} disappears; m - 2, $-x_1$ and x_1 when the double fixed point appears, from which subsequently the points a_1 and a_2 emerge ($a_1 > a_2$); m - 2, S and S with the disappearance of the point a_1; m - 2, 0, and $-\sqrt{E_1}$ at the moment of the inception of the transformation Π_{m-1}; m - 2, $-\sqrt{E_1}$, and $-\sqrt{E_1}$ for the disappearance of the point a_2.

By solving Eq. (6) for the parameter ω_2, we get the generalized equation of the bifurcation curves:

$$\omega_2 = (M + L) + \sqrt{(M + LT)^2 - N - M^2 - 4L}, \tag{7}$$

where $M = \sqrt{[\Theta(r)]^2 - E_1}$, and $N = \omega_1 + \bar{\Theta}_K(R)$.

The function $\bar{\Theta}(R)$ realizes a transformation that is the inverse of $\Theta(R)$. Using Eq. (7), we can plot bifurcation curves $\omega_2 = \omega_2(L)$ that enable us to determine the nature of the oscillatory motions of the spacecraft for assigned system parameters.

As an example, in Fig. 8 are shown the functions $\omega_2 = \omega_2(L)$ calculated for the transformation Π_2. The change of complex /44

oscillations of other kinds occurs analogously. An exception is represented by the oscillations corresponding to transformations Π_n.

The value of the function $f_n(x)$ at the moment of inception depends on ω_2 and varies with change in ω_2. The function $f_n(x)$ is defined for the values of x belonging to the interval:

$$\sup[-\bar{f}_{n-1}(-\sqrt{E_1}),\ -\sqrt{E_1}] \leqslant x \leqslant \inf[\bar{f}_{n-1}(-\sqrt{E_1}),\ S].$$

If $\phi_{0n} > 0$, then with decrease in ω_2 the multiple point of transformation Π_n is formed, which divides into two fixed points a_1 and a_2 (larger and smaller). The later fixed point disappears when the condition $a_1 = \inf[\bar{f}_{n-1}(-\sqrt{E_1}),\ \phi]$ is satisfied, which is equivalent to the condition of the simultaneous observance of the equalities $f_n(a_1) - a_1 = 0$ and $f_{n-1}(a_1) + \sqrt{E_1} = 0$. Cancelling out a_1, we get $f_{n-1}[\gamma(-\sqrt{E_1})] = -\sqrt{E_1}$ or $f_n(\phi) = \phi$, where $\phi_n = \gamma(-\sqrt{E_1})$.

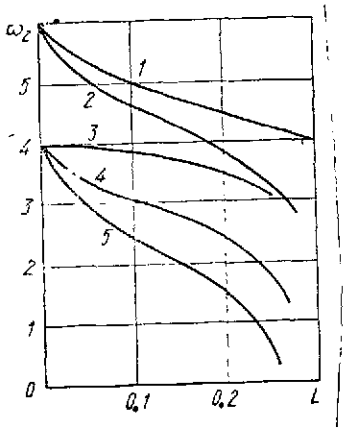

Fig. 8. Bifurcation curves of the point transformation Π_2:
1. Function $\omega_2(L)$ for the moment of inception of the transformation $\Pi_2 = T_\gamma T_\theta$; 2. as above, for the moment of the disappearance of the fixed point of the transformation $\Pi_3 = T_\gamma T_\theta^2$; 3. as above for the moment of the appearance of the fixed points of the transformation Π_2; 4. moment of inception of the transformation $\Pi_3 = T_\gamma^2 T_\theta$; 5. moment of the disappearance of the transformation Π_2.

If $\phi_n \leq 0$, then there is no multiple and larger fixed points in the transformation Π_n. The smaller fixed point is initiated at the instant B_n^γ when the equality $f_n(\phi) = \phi$ is satisfied.

Using the Koenigs-Lamereaux plot and the generalized equation (6), we can establish the sequence of the occurrence of the bifurcation instants, by showing that this sequence depends on ϕ_n.

If $\phi_n > \sqrt{E_1}$, the disappearance of the smaller fixed point of the transformation Π_{n-1} occurs earlier than the appearance of the multiple fixed point of the transformation Π_n.

If $\phi_n < \sqrt{E_1}$, then the disappearance of the smaller fixed point of the transformation Π_{n-1} is preceded by the appearance of the multiple fixed point and by the disappearance of the larger fixed point of the transformation Π_n. In the latter case, the existence, for the same value of ω_2, of fixed points of two neighboring transformations Π_n and Π_{n-1} is possible.

Let us examine the dependence of the energy expenditure in the orientation of the spacecraft on the difference $\Delta\omega = \omega_1 - \omega_2$; we conduct our analysis for the point transformations of the type Π_n, assuming $L > 0$.

In the periodic motions corresponding to the fixed points of the transformations $\Pi_n = T_\Theta T_\gamma^{n-1}$, the number of engagements of the actuators producing negative control impulses is one greater than the number of engagements of the actuators producing positive control pulses. Hence there follows the formula for determining the period of natural oscillations:

$$T_a = \frac{1}{L}[\omega_1 + (n-1)\Delta\omega], \tag{8}$$

where n is the cycle multiplicity.

We will assume that the energy outlay in a single engagement is $q_1 = r\omega_1$, and $q_2 = r\omega_2$ (r is the coefficient of proportionality). Then the energy outlay during the flight time t ($t >> T_a$) will be defined by the formula:

$$Q = \frac{r[n\omega_1 + (n-1)\omega_2]t}{T_a}.$$

With reference to relation (8), we get: /45

$$Q = \frac{r[n\omega_1 + (n-1)\omega_2]tL}{\omega_1 + (n-1)\Delta\omega}.$$

If $\omega_1 = \omega_2$, then $Q = Q_0 = r(2n_0 - 1)tL$, where n_0 is the cycle multiplicity when $\omega_1 = \omega_2$. Then the relative energy outlay will be:

$$\bar{Q} = \frac{Q}{Q_0} = \frac{n\omega_1 + (n-1)\omega_2}{[\omega_1 + (n-1)\Delta\omega](2n_0 - 1)}.$$

Figure 9 shows the dependence of the relative outlay on the parameter ω_2 (ω_1 = const). The function $\bar{Q}(\omega_2)$ is discontinuous

for the values ω_2 corresponding to the transition of oscillatory motions from one type to another (from the transformation Π_n to the transformation Π_{n-1}). Here the number n and the outlay change in jumplike fashion.

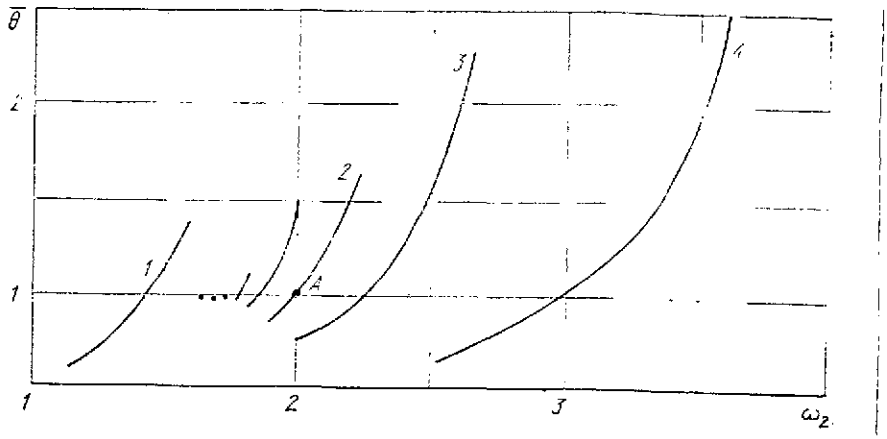

Fig. 9. Plot of relative energy expenditure:
1. Function $\bar{Q}(\omega_2)$ for the transformation T_γ;
2. as above, for the transformation $\Pi_4 = T_\gamma^3 T_\theta$;
3. as above, for the transformation $\Pi_3 = T_\gamma^2 T_\theta$;
4. as above, for the transformation $\Pi_2 = T_\Gamma T_\theta$.

The function $\bar{Q}(\omega_2)$ is calculated for the value $\omega_1 = 2$, $L = \text{const} > 0$. Therefore point A (see Fig. 9) characterizes the relative expenditure if the actuators produce upon engagement the same control impulses; the number of engagements in the closed cycle when $\omega_1 = \omega_2 = 2$ will be $n_0 = 7$, and the relative expenditure $\bar{Q} = 1$. The variation with time of the spacecraft angular coordinate $\phi = \phi(t)$ is shown in Fig. 10 a.

If $\omega_2 = 1$ and 2, then as follows from Fig. 9, the oscillations are characterized by the simple transformation T_γ; the phase trajectory closes in two engagements of the actuators. The relative expenditure is much smaller than in the case $\omega_2 = 2$ ($\bar{Q} = 0.6$). The plot of the variation in the angular coordinate for $\omega_2 = 1$ and 2 is shown in Fig. 10 b. /46

This analysis affords the following conclusions.

1. When the dynamics of the spacecraft outside the atmosphere is analyzed, it is useful to allow for the inequality of the impulses of the control moments ($\Delta\omega \neq 0$) produced by different actuators of the control system.

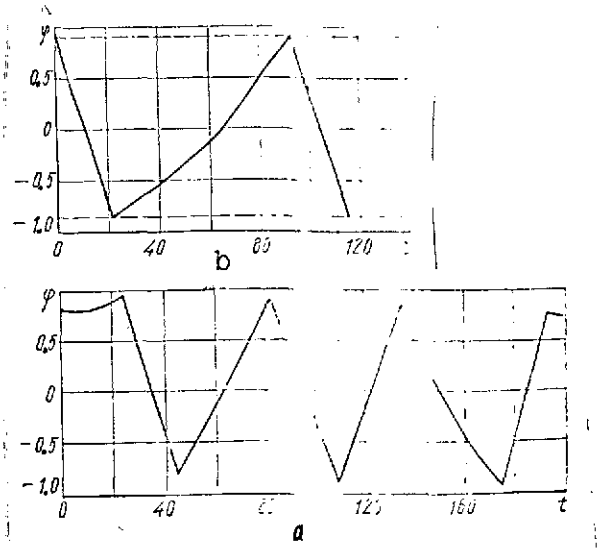

Fig. 10. Plot of the variation with time of the spacecraft angular coordinate.
a. $\omega_2 = \omega_1 = 2$
b. $\omega_2 = 1, 2$.

2. If the perturbing moment is absent and $\Delta\omega \neq 0$ is ensured, simple natural oscillations are impossible -- alternation of open double-impulse cycles with one single-impulse cycle occurs. Complex natural oscillations are established if the difference of the control impulses is a multiple of the magnitude of a single impulse. Control systems in which the control impulses are not equal to each other are somewhat more economical (by a factor of 1.5 and higher) than systems with equal impulses.

3. For the case of the action of a perturbing moment and $\Delta\omega \neq 0$, establishment of both simple and complex natural oscillations is possible. The appropriate selection of $\Delta\omega$ minimizes the amount of energy expended -- the energy outlays in spacecraft orientation can be reduced by 1.5-2 times.

REFERENCES

1. Gaushus, E.V., Avtomatika i telemekhanika 9/10 (1968).

2. Gaushus, E.V., in the book: Iskusstvenniye sputniki Zemli [Artificial Earth satellites], Vol. 16, USSR Academy of Sciences Press, Moscow, 1963.

3. Andronov, A.A., A.A. Vutt, and S.E. Khaykin, Teoriya kolebaniy [Theory of oscillations], Gostekhizdat, Moscow, 1954.

PROBLEMS OF OSCILLATIONS AND THE STABILITY OF MOTION OF MULTIDIMENSIONAL ELASTIC AND ELASTOFLUID CONTROLLED OBJECTS

A.I. Kukhtenko, V.V. Udilov, and B.A. Gudymenko

Allowing for the elasticity of a structure and the oscillations of a fluid in the cavities of a flight craft leads to various problems in the analysis of oscillations and the stability of motion becoming essentially multidimensional. Let us examine the possibility of using methods from the theory of the representations of groups and the method of decomposition in solving problems of the control of the motion of elastofluid objects.

Application of the theory of group representations in solving problems in the stabilization of elastic spacecraft. The theory of linear representations of groups can prove of much assistance in the study of multidimensional elastic space objects [1]. The methods of the theory of linear representations of groups prove applicable in those cases when the dynamic system under analysis is symmetric. Here, by system symmetry we mean the invariance of its mathematical model relative to a specific group of linear transformations. Orbital space stations of the type described in the work [2], as well as cluster type flight craft [3] can be classified as symmetric space objects. Solving a number of problems (analysis of the frequency spectrum, of the stability of motion, and of optimality) associated with automatic control of this class of objects is fraught with serious computational difficulties brought about by the multidimensionality of these problems. However, the presence of the properties of symmetry of the system under study enables us to reduce the initial multidimensional problem to a series of problems of much smaller dimensionality, although to solve the latter, if they still prove to be multidimensional, we have to seek other ways of overcoming the "curse of multidimensionality." One such approach, known by the designation method of decomposition, is described in the second part of this article.

Realization of the decomposition of problems emerging in the analysis of symmetric dynamical systems can be achieved by different methods, based on the theory of the linear representations of groups. One such method (the "elementary cell" method) as applied to the analysis of frequency equations of complex rod systems has been described in the work [4]. Essentially, the method consists of isolating in the initial rod system its smallest part, which when acted on by different elements of the symmetry group the entire system can be "constructed." For the elementary cell thus isolated, additional coupling equations are sought and frequency equations are set up by known methods. The fullest description of the elementary cell method is to be found in the work [5]. /47

Another approach to achieving the decomposition of linear ordinary differential equations, quadratic forms, and boundary value problems corresponding to the natural oscillations of complex rod systems, based on the method of projection operators known from the theory of linear representations of groups, is developed in the works [6] – [10].

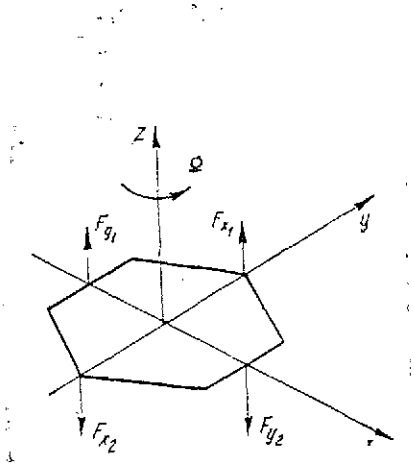

Fig. 1. Configuration of a station with the form of a regular hexagonal.

In order to actually demonstrate the method of allowing for the symmetry properties and to recognize all that can be achieved by applying group theory, let us examine the supporting rod system of an orbital space station (Fig. 1). The system for stabilizing the toroidal space station is examined in the work [2]. Our consideration includes the analysis of the symmetry of the control object and the structure of the equations of its elastic oscillations, and also finding all the simplifications that can be achieved owing to the symmetry of the object, in the problem of its automatic stabilization.

Let us first consider the properties of the object's symmetry. We will use the equations of motions of a deformable body in the Lur'ye form for the mathematical description of the control object [11].

Let us assume that the object of control (Fig. 1) consists of six monotypical rods rigidly connected to each other, each of which is given flexural rigidity in the plane xz and torsional rigidity. Let us fix the axis s with the k-th rod, with the origin of reference at the middle of the rod and oriented along its axis of symmetry. We let a stand for rod length.

The formulation of the equations of motion of a deformable body in the Lur'ye form is based on the assignment to the system of functions approximating the vector of elastic displacements. In the selection of these functions, the properties of the object's symmetry are also used.

The vertical displacement of the points of the elastic axis and the angles of rotation of the sections relative to the s axis of the k-th rod can be written as:

$$w_k(s,t) = A_1(s)\,w_k^+(t) + A_2(s)\,w_k^-(t) + A_3(s)\,\varphi_k^+(t) + A_4(s)\,\varphi_k^-(t), \quad (1)$$

$$\theta_k(s,t) = A_5(s)\,\theta_k^+(t) + A_6(s)\,\theta_k^-(t). \quad (2)$$

The functions $A_\ell(s)$ ($\ell = 1, \ldots, 6$) can always be selected so that the following relations are satisfied:

$$\left.\begin{aligned} &w_k(s,t)\big|_{s=-a/2} = w_k^+(t), \quad w_k(s,t)\big|_{s=a/2} = w_k^-(t), \\ &\frac{\partial w_k(s,t)}{\partial s}\bigg|_{s=-a/2} = \varphi_k^+(t), \quad \frac{\partial w_k(s,t)}{\partial s}\bigg|_{s=a/2} = \varphi_k^-(t), \\ &\theta_k(s,t)\big|_{s=-a/2} = \theta_k^+(t), \quad \theta_k(s,t)\big|_{s=a/2} = \theta_k^-(t). \end{aligned}\right\} \quad (3)$$

This can be achieved by interpolation by the beam functions or by the Hermitian polynomials. In the latter case, the functions $A_\ell(s)$ are of the form: /48

$$\left.\begin{aligned} &A_1(s) = 2\left(1 + \frac{s}{a}\right)\left(\frac{1}{2} - \frac{s}{a}\right)^2, \quad A_2(s) = 2\left(1 - \frac{s}{a}\right)\left(\frac{1}{2} + \frac{s}{a}\right)^2, \\ &A_3(s) = \left(s + \frac{a}{2}\right)\left(\frac{s}{a} - \frac{1}{2}\right)^2, \quad A_4(s) = \left(s - \frac{a}{2}\right)\left(\frac{s}{a} + \frac{1}{2}\right)^2, \\ &A_5(s) = \frac{1}{2}\left(1 - \frac{2s}{a}\right), \quad A_6(s) = \frac{1}{2}\left(1 + \frac{2s}{a}\right). \end{aligned}\right\} \quad (4)$$

Let $w_k(t)$ stand for the vertical displacement of the k-th assembly, $p_k(t)$ -- for the angle of rotation relative to the radial direction, and $q_k(t)$ -- for the angle of rotation relative to the tangential direction (Fig. 2). Then we have the relations:

$$\left.\begin{aligned} &\theta_k^+ = \frac{\sqrt{3}}{2}q_k - \frac{1}{2}p_k, \quad \varphi_k^+ = \frac{1}{2}q_k + \frac{\sqrt{3}}{2}p_k, \quad w_k^+ = w_k, \\ &\theta_k^- = \frac{\sqrt{3}}{2}q_{k+1} + \frac{1}{2}p_{k+1}, \quad \varphi_k^- = -\frac{1}{2}q_{k+1} + \frac{\sqrt{3}}{2}p_{k+1}, \quad w_k^- = w_{k+1}. \end{aligned}\right\} \quad (5)$$

Using these relations, let us express the deflection function (1) and the angles of torsion (2) in terms of the coordinates of the assemblies:

$$\left.\begin{aligned} w_k(s,t) = {} & A_1(s)\,w_k + A_2(s)\,w_{k+1} + \frac{1}{2}A_3(s)\,q_k - \frac{1}{2}A_4(s)\,q_{k+1} + \\ & + \frac{\sqrt{3}}{2}A_3(s)\,p_k + \frac{\sqrt{3}}{2}A_4(s)\,p_{k+1}, \end{aligned}\right. \quad (6)$$

$$\left.\theta_k(s,t) = \frac{\sqrt{3}}{2}A_5(s)\,q_k + \frac{\sqrt{3}}{2}A_6(s)\,q_{k+1} - \frac{1}{2}A_5(s)\,p_k + \frac{1}{2}A_6(s)\,p_{k+1}.\right. \quad (7)$$

The functions (6) and (7) constructed in this way allow us to satisfy the conditions of continuity of vertical displacements and the angles of rotation of the assemblies relative to the radial and tangential directions.

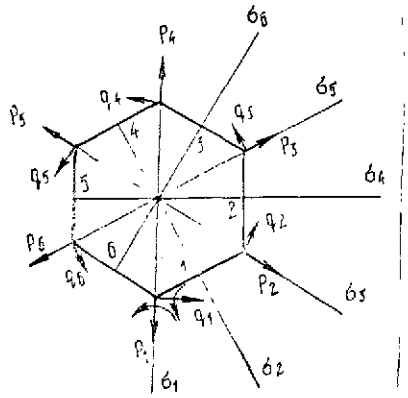

Fig. 2. System of coordinates associated with the station.

Let us convert from the coordinates p_k, q_k, and w_k to other coordinates, called symmetric coordinates. These coordinates can be constructed by the method of projection operators [1]. Use of symmetrical coordinates in the expansions (6) and (7) leads to a simplification of the equations of motion of a deformable body. Symmetric coordinates are close to normal coordinates, and some of them can even coincide with the normal coordinates. Also important is the fact that seeking for the symmetrical coordinates is based on the symmetry properties of the system. Let us examine these properties in more detail.

The construction shown in Fig. 1 has six planes of symmetry σ_k ($k = 1, \ldots, 6$), whose traces are shown in Fig. 2, and also a sixth-order axis of symmetry, which coincides with the z axis. The presence of the sixth-order symmetry axis implies that the construction coincides with itself for rotations about its axis by the angles $\pi k/3$ ($k = 1, \ldots, 6$). These elements of symmetry give rise to 12 operations: six rotations $\hat{C}_6^k$ ($k = 1, \ldots, 6$) relative to the z axis, and six reflections $\hat{\sigma}_k$ ($k = 1, \ldots, 6$). The set of rotations $\hat{C}_6^k$ and reflections $\hat{\sigma}$ forms the group C_{6v}. The unit of the group here will be rotation about the z axis by 0 or 360°. The order of this group is 12.

Now let us construct any unitary representation of the group C_{6v}. To do this, let us note that the functions p_k, q_k, and w_k can be considered as the coordinates of the 18-dimensional vector x in the basis of unit vectors: /49

$$e_k^p = (\underbrace{0 \ldots 1}_{k} \ldots 0), \quad e_k^q = (\underbrace{0 \ldots 1}_{6+k} \ldots 0), \quad e_k^w = (\underbrace{0 \ldots 1}_{12+k} \ldots 0). \tag{8}$$

Thus, in the 18-dimensional vector space L we have the representation of vector x in the form:

$$x = \sum_{k=1}^{6} (p_k e_k^p + q_k e_k^q + w_k e_k^w). \qquad (9)$$

Let us define in L the operators $\hat{C}_6^k$ and $\hat{\sigma}_k$ (k = 1, ..., 6) as follows:

$$\begin{aligned} &\hat{C}_6^k e_l^p = e_{k+l}^p, \quad \hat{C}_6^k e_l^q = e_{k+l}^q, \quad \hat{C}_6^k e_l^w = e_{k+l}^w, \\ &\hat{\sigma}_k e_l^p = -e_{k-l+2}^p, \quad \hat{\sigma}_k e_l^q = e_{k-l+2}^q, \quad \hat{\sigma}_k e_l^w = e_{k-l+2}^w. \end{aligned} \qquad (10)$$

In the expressions (10), we assume that

Relations (10) map the transformations of the basis unit vectors (8) generated by the operations of the symmetry of group C_{6v}. It is not difficult to verify that the set of operators $\hat{C}_6^k, \hat{\sigma}_k$ forms the unitary representation of the group C_{6v} in the basis (8). Knowing the unitary representation of the group, and also the tables of its nonreducible representations, which are presented, for example, in the work [1], we can expand the space L into the direct sum of eight orthogonal subspaces:

$$L = \sum_{\alpha=1}^{6} \sum_{\gamma=1}^{s_\alpha} \oplus E_{\alpha\gamma} \qquad (11)$$

and find the basis unit vectors $\{e_{\alpha\beta\gamma}\}$ ($\beta = 1, \ldots, m_\alpha$) of each of the subspaces $E_{\alpha\gamma}$. Corresponding to the expansion (11) is the representation of vector x in the basis $e_{\alpha\beta\gamma}$ ($\alpha = 1, \ldots, q$; $\beta = 1, \ldots, m_\alpha$; $\gamma = 1, \ldots, s_\alpha$), referred to as canonical:

$$x = \sum_{\alpha=1}^{q} \sum_{\beta=1}^{m_\alpha} \sum_{\gamma=1}^{s_\alpha} q_{\alpha\beta\gamma} e_{\alpha\beta\gamma}. \qquad (12)$$

The coordinates of vector x in the canonical basis are called symmetric. The index α in the notation of the symmetric coordinates corresponds to the number of one of the nonequivalent nonreducible representations of which the given reducible representation consists; the index β corresponds to the number of one of the equivalent nonreducible representations of the α-th type; the index γ corresponds to the number of the symmetric coordinates transformed according to one of the representations of the α-th type. The numbers m_α (multiplicity of the nonreducible representation of the α-th type) and s_α (dimensionality of this representation) appearing in expansions (11) and (12) can be found from the tables of nonreducible representations and from the matrices of reducible representation (10):

$$m_1 = m_2 = 3, \quad m_3 = m_4 = 2, \quad m_5 = m_6 = 1,$$
$$s_1 = s_2 = 2, \quad s_3 = s_4 = s_5 = s_6 = 1. \qquad (13)$$

The data presented are sufficient to construct the formulas for converting from symmetric coordinates $q_{\alpha\beta\gamma}$ to the initial coordinates p_k, q_k, and w_k:

$$\left.\begin{aligned}
p_k &= \frac{1}{\sqrt{3}}\left(q_{111}\sin\frac{\pi(k-1)}{3} + q_{112}\cos\frac{\pi(k-1)}{3} + q_{211}\sin\frac{2\pi(k-1)}{3} + \right.\\
&\left. + q_{212}\cos\frac{2\pi(k-1)}{3}\right) + \frac{1}{\sqrt{6}}\left(q_{511}\cos 2\pi(k-1) + q_{611}\cos\pi(k-1)\right),\\
q_k &= \frac{1}{\sqrt{3}}\left(q_{121}\cos\frac{\pi(k-1)}{3} - q_{122}\sin\frac{\pi(k-1)}{3} + q_{221}\cos\frac{2\pi(k-1)}{3} - \right.\\
&\left. - q_{222}\sin\frac{2\pi(k-1)}{3}\right) + \frac{1}{\sqrt{6}}\left(q_{311}\cos 2\pi(k-1) + q_{411}\cos\pi(k-1)\right),\\
w_k &= \frac{1}{\sqrt{3}}\left(q_{131}\cos\frac{\pi(k-1)}{3} - q_{132}\sin\frac{\pi(k-1)}{3} + q_{231}\cos\frac{2\pi(k-1)}{3} - \right.\\
&\left. - q_{232}\sin\frac{2\pi(k-1)}{3}\right) + \frac{1}{\sqrt{6}}\left(q_{321}\cos 2\pi(k-1) + q_{421}\cos\pi(k-1)\right).
\end{aligned}\right\} \qquad (14)$$ /50

Formulas (14) express the functions (6) and (7) in terms of symmetric coordinates. In order for the function (6) thus obtained to be used in describing elastic oscillations relative to the coordinate system xyz (Fig. 3) associated with the structure as a solid, this system must satisfy the conditions:

$$\left.\begin{aligned}
&\sum_{k=1}^{6}\int_{-a/2}^{a/2} m(s)\,w_k(s,t)\,ds = 0,\\
&\sum_{k=1}^{6}\int_{-a/2}^{a/2} m(s)\,w_k(s,t)\left(\frac{\sqrt{3}a}{2}\sin\frac{\pi(k-1)}{3} + s\cos\frac{\pi(k-1)}{3}\right)ds = 0,\\
&\sum_{k=1}^{6}\int_{-a/2}^{a/2} m(s)\,w_k(s,t)\left(-\frac{\sqrt{3}a}{2}\cos\frac{\pi(k-1)}{3} + s\sin\frac{\pi(k-1)}{3}\right)ds = 0.
\end{aligned}\right\} \qquad (15)$$

These conditions lead to three coupling equations between the symmetric coordinates:

$$\left.\begin{aligned}
b_1 q_{111} + b_2 q_{121} + b_3 q_{131} &= 0,\\
b_1 q_{112} + b_2 q_{122} + b_3 q_{132} &= 0,\\
c_1 q_{311} + c_2 q_{321} &= 0,
\end{aligned}\right\} \qquad (16)$$

where the coefficients b_1, b_2, b_3, c_1, and c_2 are expressed in some fashion in terms of the integrals of the functions $A_\ell(s)$ ($\ell = 1, 2, 3, 4$). Thus, if we take the Hermitian polynomials (4) as these functions and assume $m(s) = \text{const}$, then $b_1 = 3a$, $b_2 = -4a$, $b_3 = -5l$, $c_1 = a$, $c_2 = 12$.

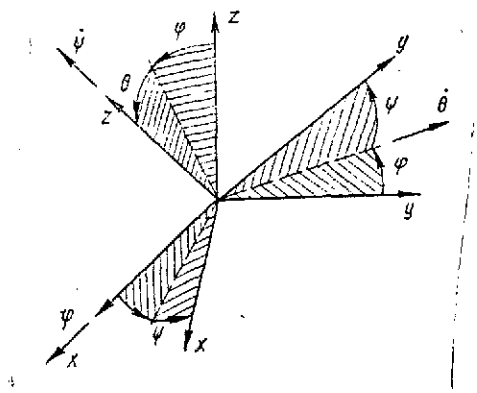

Fig. 3. Planes of symmetry and numbering of rods and assemblies.

Expressing functions (6) and (7) in terms of symmetric coordinates according to formulas (14) and cancelling out the dependent coordinates q_{131}, q_{132}, and q_{321} from the resulting expressions on the basis of Eqs. (16), we get:

$$w_k(s, t) = \sum_{\alpha=1}^{6} \sum_{\beta=1}^{m_\alpha} \sum_{\gamma=1}^{s_\alpha} \varphi^k_{\alpha\beta\gamma}(s)\, q_{\alpha\beta\gamma}, \tag{17}$$

$$\theta_k(s, t) = \sum_{\alpha=1}^{6} \sum_{\beta=1}^{m_\alpha} \sum_{\gamma=1}^{s_\alpha} \theta^k_{\alpha\beta\gamma}(s)\, q_{\alpha\beta\gamma}$$

$$\left(k = 1, \ldots, 6; \quad m_1 = 2, \quad m_2 = 3, \quad m_3 = 1, \quad m_4 = 2, \right. \left. m_5 = m_6 = 1; \quad s_1 = s_2 = 2, \quad s_3 = s_4 = s_5 = s_6 = 1 \right) \tag{18}$$

Nonreducible representations of group C_{6v} are also realized with the functions $\varphi^k_{\alpha\beta\gamma}(s)$, and $\theta^k_{\alpha\beta\gamma}(s)$ ($k = 1, \ldots, 6$). This enables us to classify the functions $\phi^k_{\alpha\beta\gamma}(s)$ and $\theta^k_{\alpha\beta\gamma}(s)$ by types in accordance with the nonreproducible representations of group C_{6v}. Thus, the functions $\phi^k_{311}(s)$ and $\theta^k_{311}(s)$ ($k = 1, \ldots, 6$) are symmetric relative to all symmetry operations of group C_{6v}; the functions $\varphi^k_{411}(s)$, $\varphi^k_{421}(s)$, $\theta^k_{411}(s)$, , and $\theta^k_{421}(s)$ ($k = 1, \ldots, 6$) are symmetric relative to the rotations $\hat{C}^1_6$, $\hat{C}^3_6$, and $\hat{C}^5_6$, and the reflections $\hat{\sigma}_1$, $\hat{\sigma}_3$, and $\hat{\sigma}_5$, and are antisymmetric relative to the remaining operations. The functions $\phi^k_{511}(s)$ and $\theta^k_{511}(s)$ are symmetric relative to all rotations and antisymmetric relative to all reflections of group C_{6v}. The functions $\varphi^k_{1\beta\gamma}(s)$, and $\theta^k_{1\beta\gamma}(s)$ ($k = 1, \ldots, 6$; $\beta = 1, 2$; $\gamma = 1, 2$), when acted on by the symmetry operations are transformed one into the other. This also applies to the functions $\varphi^k_{2\beta\gamma}(s)$ and $\theta^k_{2\beta\gamma}(s)$ ($k = 1, \ldots, 6$; $\beta = 1, 2, 3$; $\gamma = 1, 2$). /51

Let us proceed to the direct setting up of the equations of motion on the Lur'ye form [11] as applied to the object under consideration.

Considering the method of reducing quadratic forms with symmetric matrices given in the work [10], for the kinetic energy of elastic oscillations we have the expression:

$$T = \sum_{\alpha=1}^{6} \sum_{\gamma=1}^{s_\alpha} T_{\alpha\gamma}, \quad T_{\alpha\gamma} = \frac{1}{2} \sum_{\beta,\beta'=1}^{m_\alpha} A^{\alpha}_{\beta\beta'} \dot{q}_{\alpha\beta\gamma} \dot{q}_{\alpha\beta'\gamma}, \tag{19}$$

where

$$A^{\alpha}_{\beta\beta'} = \frac{1}{s_\alpha} \sum_{\gamma=1}^{s_\alpha} \sum_{k=1}^{6} \left(\gamma F \int_{-a/2}^{a/2} \varphi^{k}_{\alpha\beta\gamma}(s)\, \varphi^{k}_{\alpha\beta'\gamma}(s) + \gamma I_\rho \int_{-a/2}^{a/2} \theta^{k}_{\alpha\beta\gamma}(s)\, \theta^{k}_{\alpha\beta'\gamma}(s)\, ds \right), \tag{20}$$

I_p is the polar moment of inertia of the section of the k-th rod; γ is the density of the k-th rod; and F is the cross-sectional area.

The potential energy of the elastic oscillations is:

$$\pi = \sum_{\alpha=1}^{6} \sum_{\gamma=1}^{s_\alpha} \pi_{\alpha\gamma}, \quad \pi_{\alpha\gamma} = \frac{1}{2} \sum_{\beta,\beta'=1}^{m_\alpha} c^{\alpha}_{\beta\beta'} q_{\alpha\beta\gamma} q_{\alpha\beta'\gamma}, \tag{21}$$

where

$$c^{\alpha}_{\beta\beta'} = \frac{1}{s_\alpha} \sum_{\gamma=1}^{s_\alpha} \sum_{k=1}^{6} \left(EI_x \int_{-a/2}^{a/2} \frac{\partial^2 \varphi^{k}_{\alpha\beta\gamma}(s)}{\partial s^2} \cdot \frac{\partial^2 \varphi^{k}_{\alpha\beta'\gamma}(s)}{\partial s^2}\, ds + GI_\rho \int_{-a/2}^{a/2} \frac{\partial \theta^{k}_{\alpha\beta'\gamma}(s)}{\partial s} \cdot \frac{\partial \theta^{k}_{\alpha\beta'\gamma}(s)}{\partial s}\, ds \right), \tag{22}$$

EI_x is the flexural rigidity of the k-th rod, and GI_p is the torsional rigidity of the k-th rod.

The potential energy of centrifugal forces in this case is of the form:

$$\pi^{\Omega} = \sum_{\alpha=1}^{6} \sum_{\gamma=1}^{s_\alpha} \pi^{\Omega}_{\alpha\gamma}, \quad \pi^{\Omega}_{\alpha\gamma} = \frac{1}{2} \Omega^2 \sum_{\beta,\beta'=1}^{m_\alpha} m^{\alpha}_{\beta\beta'} q_{\alpha\beta\gamma} q_{\alpha\beta'\gamma}, \tag{23}$$

where

$$m^{\alpha}_{\beta\beta'} = \frac{1}{s_\alpha} \sum_{\gamma=1}^{s_\alpha} \sum_{k=1}^{6} \left(\gamma F \int_{-a/2}^{a/2} s \int_{0}^{s} \frac{\partial \varphi^{k}_{\alpha\beta\gamma}(\sigma)}{\partial \sigma} \cdot \frac{\partial \varphi^{k}_{\alpha\beta'\gamma}(\sigma)}{\partial \sigma}\, d\sigma - \gamma I_x \int_{-a/2}^{a/2} \theta^{k}_{\alpha\beta\gamma}(s)\, \theta^{k}_{\alpha\beta'\gamma}(s)\, ds \right), \tag{24}$$

Ω is the angular rate of rotation of the station relative to the z axis, and I_x is the equatorial moment of inertia of the section of the k-th rod.

With reference to (19), (21), and (23), we obtain the equations of the elastic oscillations of this control object in the form:

$$\sum_{\beta'=1}^{m_\alpha} [A^\alpha_{\beta\beta'}\ddot{q}_{\alpha\beta'\gamma} + (c^\alpha_{\beta\beta'} + \Omega^2 m^\alpha_{\beta\beta'}) q_{\alpha\beta'\gamma}] = Q_{\alpha\beta\gamma}$$
$$\begin{pmatrix} \alpha = 1, \ldots, 6; \quad \gamma = 1, \ldots, s_\alpha; \quad m_1 = 2, \\ m_2 = 3, \quad m_3 = 1, \quad m_4 = 2, \\ m_5 = m_6 = 1 \end{pmatrix}. \tag{25}$$

Here $Q_{\alpha\beta\gamma}$ are the generalized applied forces.

In setting up this equation, we did not make allowance for the effects associated with rotation of the rod sections relative to the radial directions. /52

From (25) we see that the system of the corresponding homogeneous equations can be decomposed into eight subsystems in accordance with the splitting of the space L (11). The systems of equations for coordinates from the subspaces E_{11} and E_{12} have identical coefficients and each contain two equations; the systems of equations for coordinates from the subspaces E_{21} and E_{22} also have identical coordinates and each contain three equations; for the coordinates from the subspaces E_{31}, E_{51}, and E_{61}, each system of equations has one equation, and for the coordinates from the subspace E_{41} -- a system of two equations.

The structure of the characteristic equation corresponding to Eq. (25) can be represented as:

$$\begin{aligned} \det \| c^\alpha_{\beta\beta'} + \Omega^2 m^\alpha_{\beta\beta'} - \omega^2 A^\alpha_{\beta\beta'} \| = \{\det \| c^{(1)}_{\beta\beta'} + \Omega^2 m^{(1)}_{\beta\beta'} - \omega^2 A^{(1)}_{\beta\beta'} \|^2_1\}^2 \times \\ \times \{\det \| c^{(2)}_{\beta\beta'} + \Omega^2 m^{(2)}_{\beta\beta'} - \omega^2 A^{(2)}_{\beta\beta'} \|^3_1\}^2 (c^{(3)}_{11} + \Omega^2 m^{(3)}_{11} - \omega^2 A^{(3)}_{11}) \times \\ \times \det \| c^{(4)}_{\beta\beta'} + \Omega^2 m^{(4)}_{\beta\beta'} - \omega^2 A^{(4)}_{\beta\beta'} \|^2_1 (c^{(5)}_{11} + \Omega^2 m^{(5)}_{11} - \omega^2 A^{(5)}_{11}) \times \\ \times (c^{(6)}_{11} + \Omega^2 m^{(6)}_{11} - \omega^2 A^{(6)}_{11}) = 0. \end{aligned} \tag{26}$$

From Eq. (26) it follows that the control object has two series of frequencies of free oscillations; symmetric coordinates q_{311}, q_{511}, and q_{611} coincide with the normal coordinates; and the forms corresponding to them coincide with the normal forms of the free oscillations of the structure. From Eqs. (26) we can readily determine the frequencies of the oscillations for

these forms. To find other frequencies, we must solve two characteristic equations of the second order, and one of the third order in ω^2.

Certain simplifications owing to the symmetry of the control object emerge also in the analysis of the closed stabilization system. Thus, in the control of balanced forces that are applied as shown in Fig. 2, and in the placement of transducers in accordance with the symmetry group of the object, only the tone of elastic oscillations of the degenerate type (E_{11}, E_{12}) will be excited. This fact simplifies the solution of the stability problem, since the characteristic determinant of the corresponding system of equations can be reduced to the block-diagonal form. Given another structure of the system of equations (for example, each control moment is applied along each axis and an asymmetric transducer arrangement is used) all tones of the oscillations can be excited. However, employing the symmetry properties of the object even in this case facilitates the solution of different problems of object control. Thus, the problem of stability of motion can be solved by decomposing the characteristic determinant into blocks on the basis of the object symmetry (cf. the structure of determinant (26) with subsequent expansion in the neighborhood of the poles of these blocks as has been done in the study [2]). Some simplification arises also in solving problems of optimizing objects described by symmetric matrices. To solve these problems, often the procedure called the method of decomposition is used. If the control object is symmetric, subdivision into subsystems is carried out in a natural way by converting to symmetric coordinates, which considerably reduces the volume of computations required for taking account of the remaining interconnections.

An algorithm for solving the problem of stabilizing multidimensional elastic flight craft with liquid contents. Let us examine the perturbed motion of an elastic flight craft (FC) with liquid contents in the yawing plane, characterized by lateral displacement [sideslip] $z(t)$ and yawing angle $\psi(t)$ of an object as a solid body, generalized coordinates $q_i(t)$ ($i = 1, 2, \ldots, k$) of elastic oscillations of the FC body, and generalized coordinates r_s ($s = 1, 2, \ldots, p$) of oscillations of the overall surface of the liquid in the s-th tank given the condition that only the first (fundamental) tone is excited in each tank. The system of equations of motion in this case is of the form [3, 12-14]: /53

$$
\begin{aligned}
&\ddot{z} = a_{zz}\dot{z} + a'_{z\psi}\dot{\psi} + a_{z\psi}\psi + \sum_{i=1}^{k}(a_{zq_i}q_i + a'_{zq_i}\dot{q}_i) + \sum_{s=1}^{p} a_{zr_s}\ddot{r}_s + a_{z\delta}\delta,\\
&\ddot{\psi} = a_{\psi z}\dot{z} + a'_{\psi\psi}\dot{\psi} + a_{\psi\psi}\psi + \sum_{i=1}^{k}(a_{\psi q_i}q_i + a'_{\psi q_i}\dot{q}_i) + \sum_{s=1}^{p} a_{\psi r_s}\ddot{r}_s + a_{\psi\delta}\delta,\\
&\ddot{q}_i + \varepsilon_{q_i}\dot{q}_i + \omega^2_{q_i}q_i = a_{q_iz}\dot{z} + a'_{q_i\psi}\dot{\psi} + a_{q_i\psi}\psi + \sum_{s=1}^{p} a_{q_ir_s}\ddot{r}_s + a_{q_i\delta}\delta,\\
&\ddot{r}_s + \varepsilon_{r_s}\dot{r}_s + \omega^2_{r_s}r_s = a_{r_sz}\ddot{z} + a_{r_s\psi}\ddot{\psi} + \sum_{i=1}^{k} a_{r_sq_i}\ddot{q}_i\\
&\qquad (i = 1, 2, \ldots, k;\quad s = 1, 2, \ldots, p).
\end{aligned}
\tag{27}
$$

For heavy ballistic type flight craft with large aspect ratio and a large number of fuel tanks, allowing for the elasticity of the body and the oscillations of fuel in the tanks leads to the system of differential equations (27) being of fairly high order. Thus, allowing only for one form of elastic oscillations of the body and one tone of oscillations of the liquid in one tank of the FC increases the order of the system of differential equations by four. Accordingly, developing methods of analyzing the dynamics of controlled elastic flight craft with liquid contents as an essentially multidimensional system of automatic control is an urgent problem.

Let us introduce into consideration the 2(k + p + 2)-dimensional vector x with components

$$x_1 = z, \quad x_2 = \dot{z}, \quad x_3 = \psi, \quad x_4 = \dot{\psi}, \quad x_{2i+3} = q_i,$$

$$x_{2(i+2)} = \dot{q}_i, \quad x_{2(i+s)+3} = r_s, \quad x_{2(i+s+2)} = \dot{r}_s$$

$$(i = 1, 2, \ldots, k; \; s = 1, 2, \ldots, p).$$

Then, system of equations (27) can be reduced to the form:

$$\dot{x} = Ax + b\delta \tag{28}$$

where A is a square matrix of order 2(k + p + 2), with the following structure: the elements of the (2μ - 1)-th row are equal to zero, with the exception of the (2μ - 1,2μ)-th element, which is equal to unity, and the (2μ, 2ν - 1)-th and (2μ, 2ν)-th elements of matrix A are equal to the (μ, ν)-th elements of the matrices $M^{-1}P$ and $M^{-1}N$, correspondingly (μ, ν = 1, 2, ..., k + p + 2); b - 2(k + p + 2)-dimensional vector, whose components with uneven numbers are equal to zero, and those with even numbers are calculated by the formulas:

$$b_{2\mu} = m^{-1}_{\mu,1} a_{z\delta} + m^{(-1)}_{\mu,2} a_{\psi\delta} + \sum_{i=1}^{k} m^{(-1)}_{\mu,i+2} a_{q_i\delta}.$$

Here $m^{(-1)}_{\mu,\nu}$ are the elements of matrix M^{-1},

$$M^{-1} = \begin{bmatrix} E_{k+2} + M_{12}(E_p - M_{21}M_{12})^{-1}M_{21} & -M_{12}(E_p - M_{21}M_{12})^{-1} \\ -(E_p - M_{21}M_{12})^{-1}H_{21} & (E_p - M_{21}M_{12})^{-1} \end{bmatrix},$$

$$P = \begin{bmatrix} P_{11} & 0 \\ 0 & P_{22} \end{bmatrix}, \qquad N = \begin{bmatrix} N_{11} & 0 \\ 0 & N_{22} \end{bmatrix},$$

$$M_{12} = \begin{bmatrix} -a_{zr_1} & \ldots & -a_{zr_p} \\ -a_{\psi r_1} & \ldots & -a_{\psi r_p} \\ -a_{q_1\rho_1} & \ldots & -a_{q_1 r_p} \\ \vdots & & \vdots \\ -a_{q_k r_1} & \ldots & -a_{q_k r_p} \end{bmatrix},$$

$$M_{21} = \begin{bmatrix} -a_{r_1 z} & -a_{r_1 \psi} & -a_{r_1 q_1} & \dots & -a_{r_1 q_k} \\ \vdots & \vdots & \vdots & & \vdots \\ -a_{r_p z} & -a_{r_p \psi} & -a_{r_p q_1} & \dots & -a_{r_p q_k} \end{bmatrix},$$

$$N_{11} = \begin{bmatrix} a_{zz} & a'_{z\psi} & a'_{zq_1} & \dots & a'_{zq_k} \\ a_{\psi z} & a'_{\psi\psi} & a'_{\psi q_1} & \dots & a'_{\psi q_k} \\ a_{q_1 z} & a'_{q_1 \psi} & -\varepsilon_{q_1} & \dots & 0 \\ \vdots & \vdots & \vdots & & \vdots \\ a_{q_k z} & a'_{q_k \psi} & 0 & \dots & -\varepsilon_{q_k} \end{bmatrix},$$

$$P_{11} = \begin{bmatrix} 0 & a_{z\psi} & a_{zq_1} & \dots & a_{zq_k} \\ 0 & a_{\psi\psi} & a_{\psi q_1} & \dots & a_{\psi q_k} \\ 0 & a_{q_1 \psi} & -\omega^2_{q_1} & \dots & 0 \\ \vdots & \vdots & \vdots & & \vdots \\ 0 & a_{q_k \psi} & 0 & \dots & \omega^2_{q_k} \end{bmatrix},$$

$$N_{22} = \operatorname{diag}\{-\varepsilon_{r_s}\}_1^p; \quad p_{22} = \operatorname{diag}\{-\omega^2_{r_s}\}_1^p;$$

E_{k+2} and E_p are unit matrices of (k + 2)-th and p-th orders, respectively.

The problem of the stabilization of the unperturbed motion of an elastic flight craft with liquid contents consists of finding the control action $\delta = \delta(x_1, \dots, x_{2(k+p+2)})$ as a function of the components of the vector of state x, which would ensure the asymptotic stability of the unperturbed motion $x = 0$ by virtue of the equations of perturbed motion (28).

The following algorithm for solving the problem of stabilizing multidimensional elastic FC with liquid contents is proposed.

1. Let us isolate three subsystems in the multidimensional system "elastic FC with liquid contents" under consideration: 1 -- "solid," 2 -- "elastic body," and 3 -- "liquid contents." To this representation of the dynamic system will correspond the following block form of the notation of the equations of perturbed motion (28):

$$\begin{bmatrix} \dot{x}^{(1)} \\ \dots \\ \dot{x}^{(2)} \\ \dots \\ \dot{x}^{(3)} \end{bmatrix} = \left[\begin{array}{c:c:c} A_{11} & A_{12} & A_{13} \\ \hdashline A_{21} & A_{22} & A_{23} \\ \hdashline A_{31} & A_{32} & A_{33} \end{array}\right] \begin{bmatrix} x^{(1)} \\ \dots \\ x^{(2)} \\ \dots \\ x^{(3)} \end{bmatrix} + \begin{bmatrix} b^{(1)} \\ \dots \\ b^{(2)} \\ \dots \\ b^{(3)} \end{bmatrix} \delta, \qquad (29)$$

where

$$x^{(1)} = \text{colon}\,\{z, \dot{z}, \psi, \dot{\psi}\},$$

$$x^{(2)} = \text{colon}\,\{q_1, \dot{q}_1, \ldots, q_k, \dot{q}_k\},$$

$$x^{(3)} = \text{colon}\,\{r_1, \dot{r}_1, \ldots, r_p, \dot{r}_p\}.$$

2. For each individual subsystem:

$$\dot{x}^{(i)} = A_{ii}x^{(i)} + b^{(i)}\delta^{(i)} \qquad (i = 1, 2, 3) \tag{30}$$

the problem of stabilization is solved by one of the known methods, as a result of which the control actions $\delta^{(i)}$ are determined as functions of the components of each of the vectors $x^{(i)}$: /55

$$\delta^{(i)} = K^{(i)}x^{(i)} \qquad (i = 1, 2, 3) \tag{31}$$

such that the zero solution of each of the subsystems

$$\dot{x}^{(i)} = (A_{ii} + b^{(i)}K^{(i)})\,x^{(i)} \tag{32}$$

will be asymptotically Lyapunov-stable.

3. The control action for the system as a whole is selected in the form:

$$\delta = \sum_{i=1}^{3} \delta^{(i)}(x_1^{(i)}, \ldots, x_{n_i}^{(i)}) = Kx, \tag{33}$$

where the matrix-row K, as follows from (31) and (33), has the following structure:

$$K = [K^{(1)} \vdots K^{(2)} \vdots K^{(3)}]. \tag{34}$$

4. The stability of the closed system of the object (28) + controller (33) is verified by one of the existing methods.

It must be noted that the structure of the gain matrix K depends essentially on the nature of the information used in forming the control actions. Let us examine several typical variants of the specifying of information concerning parameters characterizing the motion of an elastic FC with liquid contents.

Variant 1. Let us assume that we are able to directly measure or determine by indirect means all the components of the state vector of the control object. In this case, the submatrices $K^{(i)}$ of the matrix K (34) will be of the form:

$$K^{(i)} = \{k_j^{(i)}\}_{j=1}^{n_i} \qquad (i = 1, 2, 3; \quad n_1 = 4, \quad n_2 = 2k, \quad n_3 = 2p).$$

Variant 2. If the components of vector $x^{(3)}$, which are the parameters $r_s(t)$ and $\dot{r}_s(t)$ (s = 1, 2, ..., p) characterizing the oscillations of the free surface of the liquid in the FC tanks, are inaccessible to direct measurement and if the control action $\delta^{(3)}(x_1^{(3)}, \ldots, x_{2p}^{(3)})$ cannot be constructed on the feedback principle, the submatrix $K^{(3)}$ must be of the zero order, and the matrix K will be of the form:

$$K = [K^{(1)} \vdots K^{(2)} \vdots 0]. \tag{35}$$

Variant 3. Let us assume that by using (k + 1) rate transducers and one linear displacement transducer, we obtain segregated data on the rate of lateral displacement [sideslip] $\dot{z}(t)$ and the angular rate $\dot{\psi}(t)$ of the object as a solid, and also data on the generalized rates $\dot{q}_i(t)$ (i = 1, 2, ..., k) characterizing the elastic oscillations of the FC body [15, 16]. Moreover, by integrating the signal from the linear rate transducer we determine the instantaneous values of the lateral displacement $z(t, \xi_1)$ at the point of transducer placement ξ_1, and also by using the rate transducer we directly measure the values of the yaw angle $\psi(t, \xi_2)$ at the point ξ_2. By using this data on the state of the control object, let us formulate the control action in the form:

$$\delta = k_z z(t, \xi_1) + k_{\dot{z}} \dot{z}(t) + k_\psi \psi(t, \xi_2) + k_{\dot{\psi}} \dot{\psi}(t) + \sum_{i=1}^{k} k_{\dot{q}_i} \dot{q}_i(t). \tag{36}$$

The summed signals $z(t, \xi_1)$ and $\psi(t, \xi_2)$ can be represented as:

$$z(t, \xi_1) = z(t) - (\xi_1 - \xi_G)\psi(t) + \sum_{i=1}^{k} q_i(t) f_i(\xi_1),$$

$$\psi(t, \xi_2) = \psi(t) - \sum_{i=1}^{k} q_i(t) f_i(\xi_2),$$

where ξ_G is the coordinate of the metacenter of the object [12]; /56
$f_i(\xi)$ and $f_i'(\xi)$ are the intrinsic forms and the derivatives thereof of the elastic oscillations of the FC body.

In this case, the matrix K (34) has the form (35), and the submatrices $K^{(1)}$ and $K^{(2)}$ are defined by the expressions:

$$K^{(1)} = [k_z\, k_{\dot{z}}\, k_\psi - (\xi_1 - \xi_G) k_z\, k_{\dot{\psi}}], \tag{37}$$

$$K^{(2)} = [k_z f_1(\xi_1) - k_\psi f_1'(\xi_2)\ k_{q_1} \ \ldots\ k_z f_k(\xi_1) - k_\psi f_k'(\xi_2)\ k_{q_k}]. \tag{38}$$

Variant 4. If we use the summed signals $z(t, \xi_1)$, $\dot{z}(t, \xi_1)$, $\psi(t, \xi_2)$ and $\dot{\psi}(t, \xi_2)$ to form the control actions, the control law is of the form:

$$\delta = k_z^* z(t, \xi_1) + k_{\dot{z}}^* \dot{z}(t, \xi_1) + k_\psi^* \psi(t, \xi_2) + k_{\dot{\psi}}^* \dot{\psi}(t, \xi_2), \tag{39}$$

which can also be represented in the form (33) with the matrix K by the assigned formula (35), and the submatrices $K^{(1)}$ and $K^{(2)}$ in this case will be defined by the expressions:

$$K^{(1)} = [k_z^*\, k_{\dot{z}}^*\, k_\psi^* - (\xi_1 - \xi_G) k_z^*\, k_{\dot{\psi}}^* - (\xi_1 - \xi_G) k_{\dot{z}}^*], \tag{40}$$

$$K^{(2)} = [k_z^* f_1(\xi_1) - k_\psi^* f_1'(\xi_2)\, k_{\dot{z}}^* f_1(\xi_1) - k_{\dot{\psi}}^* f_1'(\xi_2) \ \ldots\ k_{\dot{z}}^* f_k(\xi_1) - k_\psi^* f_k'(\xi_2)\ \ k_{\dot{z}}^* f_k(\xi_1) - k_{\dot{\psi}}^* f_k'(\xi_2)]. \tag{41}$$

Analysis of the stability of the closed multidimensional control system in several cases can be made by the method of the Lyapunov vector function [17-19]. However, this method, based on overstated estimates of the Lyapunov functions $V^{(i)}(x^{(i)})$ constructed for each of the subsystems, leads to intensified sufficient conditions for the stability of the closed multidimensional system and in practical use cannot yield the desired results. In practice, when synthesizing a stabilization system we must have certain confidence of the stability or instability of the closed control system, which can be achieved by using a reliable (within the frame of necessary and sufficient conditions) stability criterion. A key feature of this criterion must be its simplicity from the standpoint of feasibility in a digital computer.

One such criterion, in our view, is the Zubov criterion [20], which is based on setting up the matrix:

$$R = E + 2(A + bK - E)^{-1} \tag{42}$$

and raising it to the power $\sigma = 2^\nu$ ($\nu = 0, 1, 2, \ldots,$). According to the Zubov criterion, the unperturbed motion of the closed system

under analysis will be asymptotically Lyapunov-stable if and only if in the raising of the matrix R to the power σ the elements of the matrix $R^{\sigma} = \|r_{ij}^{(\sigma)}\|_1^{2(k+p+2)}$ will tend to zero as $\sigma \to \infty$. This will occur each time when the inequalities

$$\sum_{i=1}^{2(k+p+2)} |r_{ii}^{(\sigma)}| < 2(k+p+2), \quad L^{(\sigma)} = \sum_{i,j=1}^{2(k+p+2)} (r_{ij}^{(\sigma)})^2 < 1. \tag{43}$$

will be satisfied for a sufficiently large σ. But if the selected controller parameters do not belong to the domain of system stability in the space of admissible values, the sums in relations (43) will rise sharply with increase in σ.

The above-described approach was used in the practical solution of the problem of stabilizing the unperturbed motion of an elastic object with liquid contents, whose perturbed motion is described by a 30th-order system of differential equations. For all the above-indicated variants of specifying information used in forming control actions, values of the controller parameter were found for which the closed multidimensional control system exhibits the property of asymptotic Lyapunov stability. /57

REFERENCES

1. Lyubarskiy, G.Ya., Teoriya grupp i yeye primeneniye v fizike [Theory of groups and its application in physics], Fizmatgiz, Moscow, 1958.

2. Gewarter, W.B., J. Spacecraft and Rockets 4, 70 (1967).

3. Gladkiy, V.F., Dinamika konstruktsii letatel'nogo apparata [Dynamics of flight craft structures], "Nauka" Press, Moscow, 1969.

4. Fomii, V.M., in the book: Raspredelennoye upravleniye protsessami v sploshnykh sredakh [Distributed control of processes in continuous media], Institute of Cybernetics of the Ukrainian SSR Academy of Sciences, Kiev, 1969.

5. Samoylenko, Yu.I., in the book: Kibernetika i vychislitel'naya tekhnika [Cybernetics and computers], Vol. 5, "Naukova Dumka," Kiev, 1970.

6. Kukhtenko, A.I. and V.V. Udilov, "A group representation theory application for solving flexible cosmic controlled stabilization problems," Eighth International Symposium on Space Technology and Science, Tokyo, 1969.

7. Kukhtenko, A.I., V.V. Udilov, "A group theory application while designing symmetrical dynamic systems," IFAC Symposium, 7-8 October 1968, Düsseldorf.

8. Udilov, V.V. and G.T. Kovbasa, in the book: Kibernetika i vychislitel'naya tekhnika, Vol. 1, "Naukova Dumka," Kiev, 1969.

9. Udilov, V.V., in the book: Kibernetika i vychislitel'naya tekhnika, Vol. 1, "Naukova Dumka," Kiev, 1970.

10. Udilov, V.V., in the book: Kibernetika i vychislitel'naya tekhnika, Vol. 5, "Naukova Dumka," Kiev, 1968.

11. Lur'ye, A.I., Analiticheskaya mekhanika [Analytic mechanics], Fizmatgiz, Moscow, 1961.

12. Mikishev, G.N. and B.I. Rabinovich, Dinamika tverdogo tela s polostyami, chastichno zapolnennymi zhidkost'yu [Dynamics of a solid with cavities partially filled with liquid], Mashinostroyeniye, Moscow, 1968.

13. Kolesnikov, K.S., Zhidkostnaya raketa kak ob'yekt regulirovaniya [Liquid-fuel rocket as a control object], Mashinostroyeniye, Moscow, 1969.

14. Rabinovich, B.I., Izv. AN SSSR, OTN, Mekhanika i mashinostroyeniye, No. 4 (1959).

15. Selezov, I.T., B.A. Gudymenko, Prikladnaya mekhanika 2(11) (1959).

16. Gudymenko, B.A., in the book: Slozhnyye sistemy upravleniya [Complex control systems], "Naukova dumka," Kiev, 1966.

17. Gudymenko, B.A. and V.V. Udilov, in the book: Slozhnyye sistemy upravleniya, Vol. 1, Institute of Cybernetics of the Ukrainian SSR Academy of Sciences, Kiev, 1968.

18. Gudymenko, B.A. and V.V. Udilov, in the book: Kibernetika i vychislitel'naya tekhnika, Vol. 1, "Naukova dumka," Kiev, 1969.

19. Zadorozhnyy, V.F., in the book: Kibernetika i vychislitel'naya tekhnika, Vol. 1,"Naukova dumka," Kiev, 1969.

20. Zubov, V.I., Matematicheskiye metody issledovaniya sistem avtomaticheskogo regulirovaniya [Mathematical methods of analyzing automatic control systems], Sudpromgiz, Leningrad, 1959.

ANALYSIS OF NATURAL OSCILLATIONS OF A SPACECRAFT

N.F. Gerasyuta, Yu.D. Sheptun, and S.V. Yaroshevich

Let us consider the oscillations of a spacecraft with a relay jet orientation system traveling in the atmosphere at the altitude h = 100 - 120 km and acted on by a constant perturbing moment; let us investigate the dependence of the form of the spacecraft oscillatory motions on the actuator efficiency.

The equations of spacecraft oscillatory motion are of the form:

$$\ddot{\vartheta} + a_{\vartheta\vartheta}\vartheta = a_{\vartheta\delta}\varkappa + M. \tag{1}$$

$$\varkappa = \begin{cases} -\delta_1 \text{ for } j \geqslant \Delta;\ j > m\Delta \text{ and } \frac{dj}{d\tau} < 0, \\ 0 \text{ for } |j| \leqslant m\Delta;\ \Delta > |j| > m\Delta \text{ and } \frac{dj}{d\tau} > 0, \\ +\delta_2 \text{ for } j \leqslant -\Delta;\ j \leqslant -m\Delta \text{ and } \frac{dj}{d\tau} > 0; \end{cases}$$

$$j = T_d\dot{\vartheta} + \vartheta, \quad \delta_1 \neq \delta_2;$$

θ and δ are coordinates characterizing the attitude of the spacecraft in motion about its center of mass and the state of the stabilization system actuators, respectively; Δ is the zone of insensitivity of the stabilization system relays; m is the characteristic of relay ambiguity; T_d is the time constant of the differentiating loop; M is the reduced perturbing moment; $a_{\theta\theta}$ and $a_{\theta\delta}$ are coefficients characterizing aerodynamic and control moments, respectively. Let us reduce these equations to the dimensionless form [1]. We introduce the new variables τ and φ: /58

$$t = \tau\sqrt{\frac{\Delta}{a_{\vartheta\delta}}}, \quad \vartheta = \Delta\varphi.$$

we obtain:

$$\ddot{\varphi} = \varkappa + \lambda\varphi + L,$$

$$\varkappa(\varphi, \dot{\varphi}) = \begin{cases} -\delta_1 \text{ for } j \geqslant 1,\ j > m \text{ and } \frac{dj}{d\tau} < 0, \\ 0 \text{ for } |j| \leqslant m \text{ and } \frac{dj}{d\tau} > 0, \\ 1 > |j| > m \\ +\delta_2 \text{ for } j \leqslant -1,\ j < -m \text{ and } \frac{dj}{d\tau} > 0. \end{cases} \tag{2}$$

Here:

$$j = T\dot{\varphi} + \varphi, \quad \lambda = -\frac{a_{\vartheta\vartheta}}{a_{\vartheta\delta}}\Delta, \quad T = T_d\sqrt{\frac{a_{\vartheta\delta}}{\Delta}}, \quad L = \frac{M}{a_{\vartheta\delta}}.$$

The equation of the phase trajectory of a spacecraft in dimensionless quantities is written as follows:

$$\dot{\varphi}^2 - \dot{\varphi}_0^2 = 2(\varkappa - L)(\varphi - \varphi_0) + \lambda(\varphi^2 - \varphi_0^2). \tag{3}$$

Changing the variables $\varphi = \psi - \frac{L}{\lambda}$, and $\dot{\varphi} = \dot{\psi}$, let us simplify the phase trajectory equation:

$$\dot{\psi}^2 + \dot{\psi}_0^2 = 2\varkappa(\psi - \psi_0) + \lambda(\psi^2 - \psi_0^2).$$

The form of the possible phase trajectories in the plane $(\psi, \dot{\psi})$ is shown in Fig. 1. The sections i to i + 1, i + 2 to i + 3 (i = 0, 1, 2, ...) correspond to motion with actuators engaged ($\kappa \neq 0$), the sections i + 1 to i + 2, and i + 3 to i + 4 correspond to passive motion ($\kappa = 0$) acted on by aerodynamic and perturbing moments. The change in the angular rate $\dot{\psi}$ of the spacecraft when diametrally opposite jet nozzles of the orientation system are switched on, which occurs when the imaging point leaves the zone $|T\dot{\psi} + \psi| < 1$, are characterized by the quantities $\omega_1, \omega_2 : \omega_1 = \dot{\psi}_{i+1} - \dot{\psi}_i$ and $\omega_2 = \psi_{i+3} - \psi_{i+2}$.

The lines of the switching on and off of the control nozzles in the plane $\psi, \dot{\psi}$ are inclined straight lines, whose equations are as follows:

$$\left.\begin{aligned} T\dot{\psi} + \psi &= 1 + \frac{L}{\lambda} \\ T\dot{\psi} + \psi &= -1 + \frac{L}{\lambda} \end{aligned}\right\} \text{— forward actuation,}$$

$$\left.\begin{aligned} T\dot{\psi} + \psi &= m + \frac{L}{\lambda} \\ T\dot{\psi} + \psi &= -m + \frac{L}{\lambda} \end{aligned}\right\} \text{— forward disengagement (not shown in Fig. 1).}$$

Let us select as segments without contact [2] the segments of the straight lines of inclusion: /59

$$T\dot{\psi} + \psi = 1 + \frac{L}{\lambda}, \quad -1 + \frac{L}{\lambda} \leqslant \psi \leqslant 1 + \frac{L}{\lambda}, \tag{4}$$

$$T\dot{\psi} + \psi = -1 + \frac{L}{\lambda}, \quad -1 + \frac{L}{\lambda} \leqslant \psi \leqslant 1 + \frac{L}{\lambda}. \tag{5}$$

Let us set up the point transformations of the segments (4) and (5) into themselves. Two kinds of simple phase trajectories

are possible, determining these transformations: trajectories intersecting the ordinate axis -- double-impulse cycles (shown with a solid line in Fig. 1), and trajectories not intersecting the ordinate axis -- single-impulse cycles (shown with a dashed line). The lines FF' and KK', whose equations are $\psi = \pm\sqrt{\lambda}$, are the asymptotes of the single-impulse cycle of maximum duration. These lines indicate on the phase plane the largest change in the angular rate

$$\omega_{1\Gamma} = \frac{2(\lambda + L)}{(1 + T\sqrt{\lambda})\sqrt{\lambda}},$$

$$\omega_{2\Gamma} = \frac{2(\lambda - L)}{(1 + T\sqrt{\lambda})\sqrt{\lambda}},$$

for which a single-impulse cycle is still provided. If $\omega_1 > \omega_{1\Gamma}$, , then double-impulse cycles are possible.

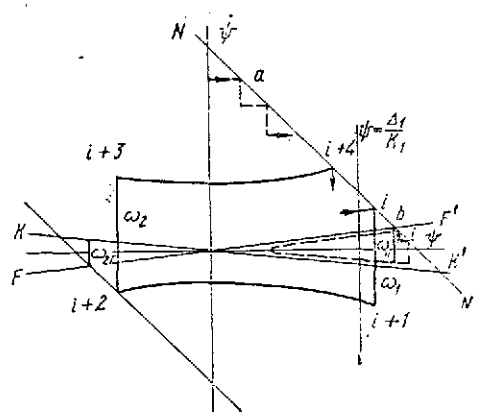

Fig. 1. Possible phase trajectories.

Point transformations are determined by the following recursion functions:

for the segment (4) into itself, if $\omega_1 < \omega_{1\Gamma}$, then:

$$\varepsilon(\psi) = \frac{\alpha_1}{K} - \sqrt{A + \left(\omega - \frac{\Delta_1}{K}\right)^2}; \qquad (6)$$

If $\omega_1 > \omega_{1\Gamma}$, $\omega_2 > \omega_{2\Gamma}$, then:

$$F(\psi) = \begin{cases} \varepsilon(\psi) = \dfrac{\alpha_1}{K} - \sqrt{A + \left(\psi - \dfrac{\Delta_1}{K}\right)^2} \text{ for } \psi < \dfrac{\Delta_1}{K}, \\ \eta(\psi) = \dfrac{\alpha_1}{K} - \sqrt{C + \left(\sqrt{B + \left(\psi - \dfrac{\Delta_1}{K}\right)^2} - \dfrac{\alpha_1 - \Delta_2}{K}\right)^2} \\ \qquad\qquad \text{for } \psi > \dfrac{\Delta_1}{K}; \end{cases} \qquad (7)$$

for the segment (5) into itself, if $\omega_2 < \omega_{2\Gamma}$, then:

$$\beta(\psi) = -\frac{\alpha_2}{K} + \sqrt{C + \left(\psi - \frac{\Delta_2}{K}\right)^2}; \qquad (8)$$

If $\omega_2 > \omega_{2\Gamma}$, $\omega_1 > \omega_{1\Gamma}$, then:

$$f(\psi) = \begin{cases} \beta(\psi) = \dfrac{\alpha_2}{K} + \sqrt{C + \left(\psi - \dfrac{\Delta_2}{K}\right)^2} \text{ for } \psi > -\dfrac{\Delta_2}{K_2}, \\ \gamma(\psi) = -\dfrac{\alpha_2}{K} + \sqrt{B + \left(\sqrt{C + \left(\psi - \dfrac{\Delta_2}{K}\right)^2} - \dfrac{\alpha_1 - \Delta_1}{K}\right)^2} \\ \qquad\qquad \text{for } \psi < -\dfrac{\Delta_1}{K_2}. \end{cases} \qquad (9)$$

Here

$$\alpha_1 = 1 + \frac{L}{\lambda}; \quad \alpha_2 = 1 - \frac{L}{\lambda}; \quad K = 1 - \lambda T^2,$$

$$K_1 = 1 + T\sqrt{\lambda}, \quad K_2 = 1 - T\sqrt{\lambda}, \quad \Delta_1 = \alpha_1 - \omega_1 T, \quad \Delta_2 = \alpha_2 - \omega_2 T,$$

$$A = \frac{1}{K^2}(\alpha_1^2 - \Delta_1^2)(1 - K), \quad B = \frac{1}{K^2}(1 - K)(\alpha_2^2 - \Delta_1^2),$$

$$C = \frac{1}{K^2}(1 - K)(\alpha_1^2 - \Delta_2^2).$$

The form of the recursion functions (the Koenigs-Lamereaux plot) is shown in Fig. 2.

If the perturbing moment acting on the flight craft is equal to zero (L = 0), Eqs. (3) - (9) are simplified.

It is of interest to analyze the effect of the difference in control impulses on the nature of oscillations. The problem is solved by analyzing the oscillations as ω_2 is varied from the largest possible value to zero. The quantity ω_1 is assumed to be constant, satisfying the condition $\omega_1 \geq \omega_{1\Gamma}$.

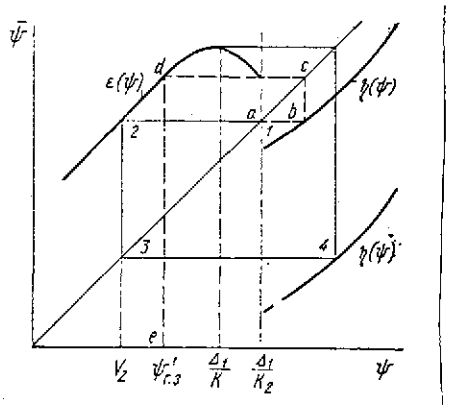

Fig. 2. Koenigs-Lamereaux plot.

The phase trajectory of a spacecraft is a piecewise-continuous function, consisting of elements of hyperbola branches. The conjugate points of the elements of the hyperbolas lie on the engagement-disengagment lines (Fig. 3). The hyperbolas issuing at the points whose coordinates satisfy the conditions $\psi_M < \psi_7$, $\psi_N > \psi_3$ are symmetric relative to the ordinate axis. The endpoints have the coordinates $\psi_N < \psi_4$ and $\psi_M > \psi_8$.

The sections of the trajectories issuing at the points $\psi_1 < \psi_{N'} < \psi_3$, $\psi_7 < \psi_{M'} < \psi_5$, $\psi_3 < \psi_{N'} < \psi_1$ and $\psi_5 < \psi_{M'} < \psi_7$, are elements of the branches of hyperbolas symmetric relative to the abscissa axis. The trajectories terminate at the points of the segments of the inclusion lines NN, MM, $\psi_4 \leqslant \psi_N \leqslant \psi_{10}$ and $\psi_9 \leqslant \psi_M \leqslant \psi_8$.

The trajectories issuing at the points with coordinates $\psi_1 < \psi_{N'} < \psi_2$ or $\psi_5 > \psi_{M'} > \psi_6$ lie only in the upper or lower half-planes, respectively.

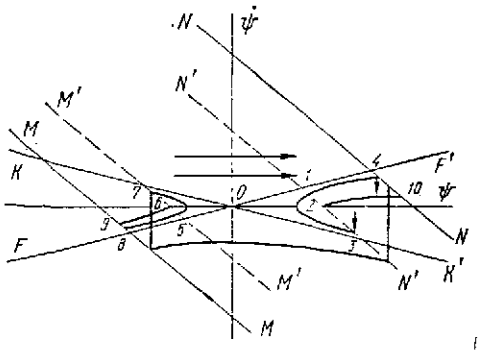

Fig. 3. Characteristic elements and points of phase trajectories.

The possible motions of a spacecraft are wholly defined by the phase trajectories consisting of the above-indicated hyperbola sections.

Let us indicate the abscissae of the charateristic points 1 to 10 (see Fig. 3) of the phase plane ψ, $\dot{\psi}$:

$$\psi_1 = \frac{\Delta_1}{K_1}, \quad \psi_2 = \Delta_1, \quad \psi_3 = \frac{\Delta_1}{K_2}, \quad \psi_4 = \frac{\alpha_1}{K_1}, \quad \psi_5 = -\frac{\Delta_2}{K_1},$$

$$\psi_6 = -\Delta_2, \quad \psi_7 = -\frac{\Delta_2}{K_2}, \quad \psi_8 = -\frac{\alpha_2}{K_1},$$

$$\psi_9 = -\frac{\alpha_2}{K} + \sqrt{C + \Delta_2^2\left(1 - \frac{1}{K}\right)^2}, \quad \psi_{10} = \frac{\alpha_1}{K} - \sqrt{A + \Delta_1^2\left(1 - \frac{1}{K}\right)^2}.$$

/61

Let us limit ourselves to studying the oscillations characterized by the transformations of the form

With decrease in ω_2, the form of part of the phase trajectory lying to the right of the straight line $\psi = \Delta_1/K_1$ changes, and the number of steps of the sliding regime between the points a and b becomes smaller (cf. Fig. 1). A conversion occurs from the transformation $\Pi_l^e = T_\varepsilon^{l-2} T_\eta T_\varepsilon$ to the transformation

$\Pi_{l-1}^e = T_\varepsilon^{l-3} T_\eta T_\varepsilon$, $\Pi_{l-2}^e = T_\varepsilon^{l-4} T_\eta T_\varepsilon$, ..., $\Pi_2 = T_\eta T_\varepsilon$ with the recursion functions

$F_l^e(\psi) = \varepsilon_{l-2}\{\eta[\varepsilon(\psi)]\}$, $F_{l-1}^e = \varepsilon_{l-3}\{\eta[\varepsilon(\psi)]\}$, $F_{l-2}^e(\psi) = \varepsilon_{l-4}\{\eta[\varepsilon(\psi)]\}$, ... and $F(\psi) = \eta[\varepsilon(\psi)]$.

A further decrease in the parameter ω_2 causes the successive appearance of the transformations $\Pi_3^\eta = T_\eta^2 T_\varepsilon$, $\Pi_4^\eta = T_\eta^3 T_\varepsilon$, ..., $\Pi_n^\eta = T_\eta^{n-1} T_\varepsilon$, $|T_\eta|$ and then oscillations characterized by complex transformations of the form $P_n^\delta = T_\gamma^{n-1} T_\beta$ are produced.

The transformation multiplicity n is reduced; when $\omega_2 < \omega_{2\Pi}$, the simple transformation T_β appears.

TABLE 1.

Designation of Bifurcation Instant	Nature of Bifurcation Instant	Equality Corresponding to Bifurcation Instant	ω_2
A_2	Inception of the transformation Π_2	$\varepsilon\left\{\eta\left[\varepsilon\left(\frac{\Delta_1}{K}\right)\right]\right\}=\frac{\Delta_1}{K_2}$	3.82
B_2	Disappearance of the fixed point of the preceding transformation	$\varepsilon\left\{\eta\left[\varepsilon\left(\frac{\Delta_1}{K_2}\right)\right]\right\}=\frac{\Delta_1}{K_2}$	3.78
C_2	Inception of the fixed point of transformation Π_2	$\varepsilon\left[\eta\left(\frac{\Delta_1}{K_2}\right)\right]=\frac{\Delta_1}{K_2}$	3.17
E_2	Change in the form of the hyperbola of transformation T_ε	$\eta\left[\varepsilon\left(\frac{\Delta_1}{K_1}\right)\right]=\frac{\Delta_1}{K_1}$	2.72
F_2	Appearance of the hyperbola of transformation T_ε in the domain $\psi < 0$	$\eta[\varepsilon(\Delta_1)]=\Delta_1$	2.59
G_2	Inception of the transformation $\Pi_3=T\eta^2T\varepsilon$	$\eta\left[\varepsilon\left(\frac{\Delta_1}{K}\right)\right]=\frac{\Delta_1}{K_2}$	2.34
H_2	Disappearance of the fixed point of transformation Π_2	$\eta\left[\varepsilon\left(\frac{\Delta_1}{K_2}\right)\right]=\frac{\Delta_1}{K_2}$	2.3

Let us examine the sequence of conversion from some forms of oscillations to others, with the example of the motions characterized by the transformation Π_2. Following the work [2], we note the principal bifurcation instants of the transformation $\Pi_2 = T_\eta T_\varepsilon$. The nature of the bifurcation instants, the equations of the recursion functions (in symbolic form) and the system parameters are given in Table 1 ($\omega_1 = 1.5$).

The generalized form of notation for the equalities corresponding to the bifurcation moments is

$$\eta[\varepsilon(r)]=R. \tag{10}$$

In equality (1) r and R take on the values Δ_1/K and $\bar{\varepsilon}(\Delta_1/K)$ for the equation of moment A_2; the values Δ_1/K and $\varepsilon(\Delta_1/K_2)$ for the equation of moment B_2, and so on. Here $\bar{\varepsilon}(\psi)$ is the transformation that is the inverse of $\varepsilon(\psi)$ [2]. To obtain the generalized equation of the bifurcation curves $\omega_2 = \omega_1(\lambda)$, let us rewrite equality (10) in the expanded form: /62

$$\frac{\alpha_1}{K} - \sqrt{C + \left(\sqrt{\left(\varepsilon(r) - \frac{\Delta_1}{K}\right)^2 + B} - \frac{\alpha_2 - \Delta_2}{K}\right)^2} = R. \qquad (11)$$

Solving (11) for ω_2, we get

$$\omega_2 = \frac{1}{T}(\alpha_2 - D \pm \sqrt{\Phi^2 + D}),$$

where

$$\Phi = \sqrt{\left[\varepsilon(r) - \frac{\Delta_1}{K}\right]^2 \pm B} - \frac{\alpha_2}{K}; \quad D = (\alpha_1 - RK)^2 \frac{1}{K} + \left(1 - \frac{1}{K}\right)\alpha_1^2 - K\Phi^2.$$

Here $K = K(\lambda)$.

The Koenigs-Lamereaux plot corresponding to the moment of inception of transformation Π_2 is illustrated in Fig. 2. Analysis of the plot establishes the range of the determination of function F_2. One limit of the range is the value $\psi_3 = \Delta_1/K_2$. To find the second limit, let us write the equality that is satisfied at the moment of inception of the transformation:

$$\varepsilon\left\{\eta\left[\varepsilon\left(\frac{\Delta_1}{K}\right)\right]\right\} = \frac{\Delta_1}{K_2}$$

and let us denote the value of function F_2 at the moment of inception by:

$$V_2 = \eta\left[\varepsilon\left(\frac{\Delta_1}{K}\right)\right].$$

Then $\varepsilon(V_2) = \Delta_1/K$ or $V_2 = \bar{\varepsilon}(\Delta_1/K_2)$. In Fig. 2, the dashed line 123 indicates the transformation $\bar{\varepsilon}(\Delta_1/K_2)$ and the left boundary $\psi = V_2$ of the range of determination of function F_2 is noted. The function F_2 is defined for the values $\psi \in (V_2, \psi_3)$.

Let us indicate the bounds to the determination of transformation $\Pi_3 = T_\eta^2 T_\varepsilon$. The recursion function of the transformation is:

$$F_3 = \eta\{\eta[\varepsilon(\psi)]\}.$$

The left bound of the range of the determination of Π_3 is the coordinate of the point of intersection of the abscissa axis and the dashed line abcde (see Fig. 2):

$$\psi'_{r3} = \bar{\varepsilon}\left[\bar{\eta}\left(\frac{\Delta_1}{K_2}\right)\right].$$

The left bound is $\inf\left(\psi^*_{r3}, \frac{\Delta_1}{K_2}\right)$, where $\psi^*_{r3} = 2\frac{\Delta_1}{K} - \psi'_{r3}$.

A further decrease in the parameter ω_2 causes the successive appearance of the transformations $\Pi_4, \Pi_5, \Pi_6, \ldots, \Pi_n$. The nature of the onset of the bifurcation moments of transformations Π_n is similar to the nature of the onset of the corresponding moments in the transformation Π_2. The ranges in which the transformations exist are determined by graphical methods used above for the transformations Π_2 and Π_3. Analysis of the Koenigs-Lamereaux plot (Fig. 4) shows that as ω_2 decreases, the function $\eta(\psi, \omega_2)$ approaches the bisector of the right angle and therefore the bifurcation moments E_n and F_n in the transformation Π_n can be absent. The conditions of the existence of the bifurcation instants E_n and F_n are, respectively, the inequalities: /63

$$\eta\left(\frac{\Delta_1}{K_2}\right) \leqslant \psi_1, \tag{12}$$

$$\eta\left(\frac{\Delta_1}{K_2}\right) \leqslant \psi_2. \tag{13}$$

Both conditions must be determined when $\omega_2 = \omega_2^{A_n}$. Using inequalities (12) and (13), we can indicate the transformations Π_k and Π_ℓ such that after these the bifurcation moments E_{k+1} and $F_{\ell+1}$ are absent.

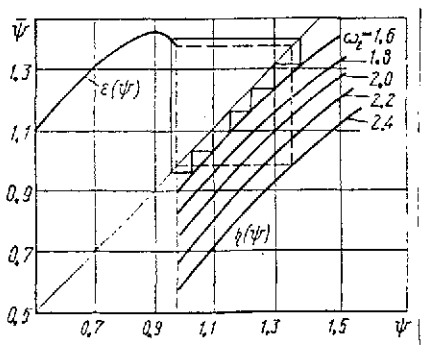

Fig. 4. Koenigs-Lamereaux plot for various ω_2.

The value $\omega_2 = \omega_2^1$ for which the condition:

$$\eta\left(\frac{\Delta_1}{K_2}\right) = \frac{\Delta_1}{K_2}, \tag{14}$$

is satisfied is the bifurcation value of the appearance of the fixed point of the simple space T_η. From equality (14) we find:

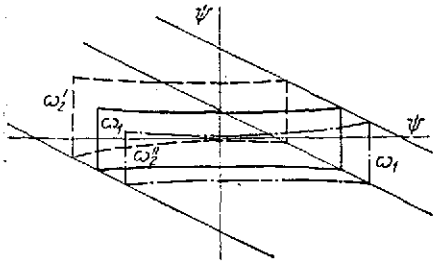

Fig. 5. Double-impulse cycles at the moments of the inception, disappearance, and transformation T_η, and also the symmetric double-impulse cycle.

$$\omega_2^1 = \frac{1}{T}\left[\alpha_2\left(1-\frac{1}{K_1}\right)+\sqrt{\frac{\alpha_2^2}{K_1}-\frac{\Phi}{K}}\right] > \omega_1,$$

where

$$\Phi_1 = \lambda T^2\alpha_1^2 + K_2^2\alpha_2^2 - (\alpha_1 - K_1\Delta_1)^2.$$

The phase trajectory corresponding to ω_2^1 is of the form of a closed double-impulse cycle displaced along the ordinate axis toward the positive values. With decrease in ω_2, the trajectory is displaced toward the side of negative $\dot{\psi}$ values (Fig. 5); when the equality

$$\eta\left[\frac{1}{K_1}\right] = \frac{1}{K_1},$$

is satisfied, to which the value

$$\omega_2^{II} = \frac{1}{T}(\alpha_2 + K_2\Phi_2) < \omega_1,$$

corresponds, where $\Phi_2 = -\frac{\alpha_2}{K_2} + \sqrt{B + \left(\frac{\alpha_1}{K_1} - \frac{\Delta_1}{K}\right)^2}$,

the fixed point of transformation T_η disappears.

The coordinate of the fixed point of the transformation is defined by the equality /64

$$\psi^* = \frac{2\Delta_1\omega_2^2 T + \omega_1 R_1 - \sqrt{(2\Delta_1\omega_2^2 T + \omega_1 R_1)^2 - S(\omega_2^2 - \omega_1^2)}}{2Tk(\omega_2^2 - \omega_1^2)},$$

where

$$R_1 = K^2(B + C) + \Delta_1^2 - \alpha_1^2 + \omega_2^2 T^2; \quad S = 4T^2\omega_2^2(K^2 B + \Delta_1^2) - R_1^2.$$

Here and above roots satisfying the physical meaning of the problem

$$\psi_i^* \in \left(\frac{\Delta_1}{1 - T\sqrt{\lambda}}, \quad \frac{\alpha_1}{1 + T\sqrt{\lambda}}\right).$$

were indicated. If $\omega_1 = \omega_2$ and $L = 0$, then $\psi_0^* = 1 - \frac{\omega_1}{2}T$

(the phase trajectory is symmetric relative to the coordinate axes). We note that when the perturbing moment is present (L = = const = 0), it is impossible to establish the double-impulse closed cycle when $\omega_1 = \omega_2$.

When $\omega_2 < \omega_2^{II}$, the nonsymmetric closed double-impulse cycle converts into an m-impulse closed cycle, consisting of m - 1 double-impulse and one single-impulse closed cycles. The single-impulse cycle begins and terminates at the line MM (cf. Fig. 3). We will analyze possible motions by using the recursion function (9). The Koenigs-Lamereaux plots for $\omega_2 < \omega_2^{II}$ are shown in Fig. 6. With decrease in ω_2, the abscissa of the bound to the discontinuity of the recursion function of the point transformation increases modulus-wise and the curves $\beta(\psi)$ and $\gamma(\psi)$ are shifted parallel to the abscissa axis. Here there is a successive conversion from the m-impulse cycle to the cycles m - 1, m - 2, ..., m - ℓ = 1. We illustrate the inception and disappearance of these cycles with the example of a three-impulse cycle, which corresponds to the point transformation $P_2 = T_\beta T_\gamma$, with the recursion function $f_2(\psi) = \gamma|\beta(\psi)|$. The bifurcation instants, which can occur in the transformation P_2, are shown in Table 2.

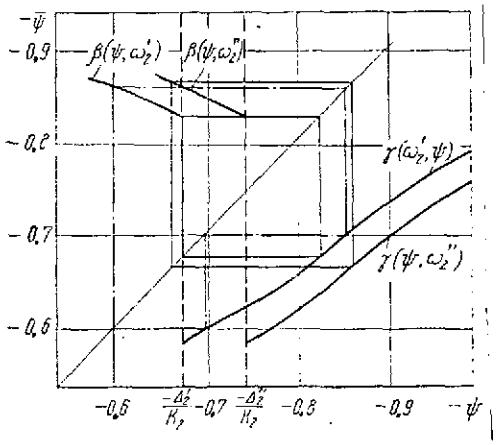

Fig. 6. Examples of the Koenigs-Lamereaux plots for the transformation P_n $(\omega_2' > \omega_2'')$.

A feature of P_n type transformations is the possibility that for the same ω_2 values fixed points of two neighboring transformations P_n and P_{n-1} exist. Figure 6 shows the plots corresponding to the limiting transformation cycles plotted for the same ω_2. The form of the limiting cycle depends on the initial coordinates of motion. The set of possible motions observed with change in ω_2 depends on the selected ω_1. Thus, the transformation $P_2 = T_\beta T_\gamma$, with decrease in ω_2, can convert either to the transformation $P_n^\beta = T_\gamma T_\beta^{n-1}$, or to the simple transformation T_β. The condition of the existence of transformation P_n^β is that the inequality:

$$\beta_{n-2}\left[\gamma\left(-\frac{\Delta_2}{K_2}\right)\right] > -\frac{\Delta_2}{K_2}.$$

be satisfied. Here

$$\gamma\left(-\frac{\Delta_2}{K_2}\right)=-\frac{1}{K}[1-\sqrt{T^2\lambda(1-\Delta_1^2)+(\Delta_1-K_2)^2}];\ \Delta_1=\Delta_1(\omega_1).$$

The disappearance of the transformation P_n^β occurs when

$$\beta\left(-\frac{\Delta_2}{K_2}\right)=-\frac{\Delta_2}{K_2}.$$

After this equality has been satisfied, the existence of only the simple transformation T_β is possible. /65

The possibility that the bifurcation instants C_n^* and E_n^* exist is also determined by the value of parameter ω_1. The conditions for the existence of these instants are, respectively, the inequalities $\gamma\left(-\frac{\Delta_2}{K_2}\right)\geqslant-\Delta_{2r}$ and $\gamma\left(-\frac{\Delta_2}{K_2}\right)\geqslant-\frac{\Delta_{2r}}{K_1}$, where $\Delta_{2r}=-(\Delta-\omega_{2r}T)$.

The principal phases of change in the point transformations are illustrated by Fig. 7, where the bifurcation curves in the coordinates ω_2 and λ are represented. All curves are plotted for the values $\omega_1 = 1.5$ and $L = 0$. The first (L) group of curves corresponds to the transformation Π_2, the second (II) -- to the transformation T_η, and the third (III) -- to the transformation P_2. The notations of the curves coincide with the notations of the bifurcation instants. The functions C_η, H_η, and C_β^* correspond to the bifurcation instants of the inception (C_η, C_β^*) and disappearance (H_η) of the simple transformations T_η and T_β. The line Q_η (ω_2 = const) characterizes the function $\omega_2 = \omega_2(\lambda)$ for the case of the symmetric cycle ($\omega_2 = \omega_1$). Analysis of the bifurcation curves allows us to conclude the following:

-- with increase in the effect of the atmosphere (with decrease in the flight altitude), the multiplicity of the complex point transformations (the number of impulses in the closed cycles) becomes smaller. This follows from the drawing together of the bifurcation curves of groups I, II, and III, with increase in λ;

-- the value of λ affects the sequence of the onset of bifurcation instants, which is illustrated by the nature of the curves C_β^* and G_5^*. If $\lambda < \lambda_1$, then the fixed point of transformation T_β appears for ω_2 values that are smaller than those for which the fixed point of transformation P_2 disappears. If $\lambda > \lambda_1$, the moment of the disappearance of

the fixed point P_2 sets in for smaller ω_2 values and the instant of the inception of the simple transformation T_β. In the domain $0 < \lambda < \lambda_1$, the transformations P_n^β are possible; and

-- if $\omega_1 = \omega_2$ ($\Delta\omega = 0$), then regardless of the value of λ (regardless of the flight altitude), only the double-impulse symmetric cycle is established. /66

TABLE 2.

Notation of the Bifurcation Instants	Nature of the Bifurcation Instant	Equality Corresponding to the Bifurcation Instant
A_2^*	Instant of the inception of the fixed point of transformation P_2	$\gamma\left(-\frac{1}{K_1}\right) = -\frac{\Delta_2}{K_2}$
B_2^*	Instant of the disappearance of the fixed point of transformation P_3^γ	$\gamma\left\{\beta\left[\gamma\left(-\frac{\Delta_2}{K_2}\right)\right]\right\} = -\frac{\Delta_2}{K_2}$
C_2^*	Instant of the change in the form of the hyperbola in the transformation T_β	$\gamma[\beta(-\Delta_2)] = -\Delta_2$
E_2^*	Appearance of the hyperbola of transformation T_β in the domain $\dot{\psi} < 0$	$\gamma\left(-\frac{1}{K_1}\right) = -\frac{\Delta_2}{K_1}$
F_2^*	Instant of the inception of the fixed point of transformation $P_3^\beta = T_\beta^2 T_\gamma$ |	$\beta\left[\gamma\left(-\frac{1}{K_1}\right)\right] = -\frac{\Delta_2}{K_2}$
G_2^*	Instant of the disappearance of the fixed point of transformation P_2	$\beta\left[\gamma\left(-\frac{\Delta_2}{K_2}\right)\right] = -\frac{\Delta_2}{K_2}$

Let us examine the stability of the craft oscillations (the stability of the fixed points of transformations Π_n and P_n.

We can find the fixed point of transformations Π_n and P_n by solving the equations:

$$\begin{aligned} F_n(\psi) - \psi = 0, \\ f_n(\psi) - \psi = 0. \end{aligned} \tag{15}$$

As an example, in Fig. 8 are presented the curves of the recursion functions F_2 corresponding to the transformation Π_2 and constructed for different ω_2, with constant ω_1. The abscissae of the points of intersection of the curves with the bisector of the right angle are the solutions of the first of the equations (15). The initial data used in constructing these recursion functions are as follows: $\omega_1 = 1.5$, $T = 0.4$, $\lambda = 4.2 \cdot 10^{-2}$, and $L = 2.1 \cdot 10^{-2}$.

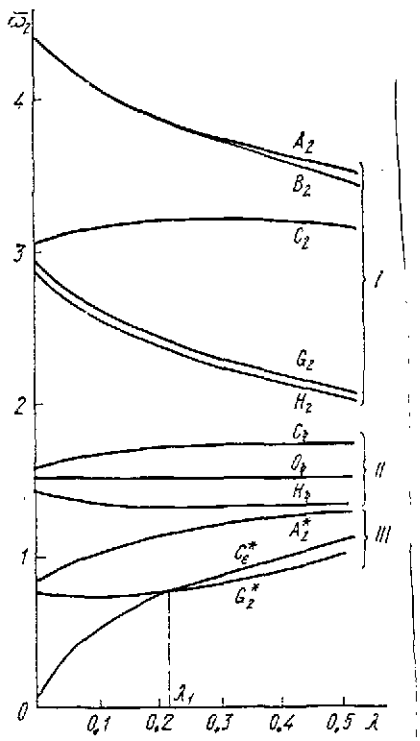

Fig. 7. Bifurcation curves.

The stability of the fixed points, according to the Koenigs theorem, is defined by the value of the derivative recursion function at the fixed point ($\psi = C$). If $\left|\frac{dF_n}{d\psi}\right|_{\psi=C} = 1$, the fixed point is stable, and when $\left|\frac{dF_n}{d\psi}\right|_{\psi=C} > 1$ it is unstable [1, 2].

Let us examine the case when the perturbing moment is equal to zero ($L = 0$). The simple fixed points of transformation T_ε are defined from the equation $\varepsilon(\psi) - \psi = 0$, or, which amounts to the same thing:

$$\frac{1}{K} - \sqrt{\tilde{A} + \left(\psi - \frac{\tilde{\Delta}_1}{K}\right)^2} - \psi = 0,$$
$$\tilde{A} = \frac{1}{K^2}(1 - \tilde{\Delta}_1^2)(1 - K), \quad \tilde{\Delta}_1 = 1 - \omega_1 T.$$

The equation has the single root $\psi^* = \frac{1 + \tilde{\Delta}_1}{2}$, and therefore the transformation T_ε corresponding to the single-impulse oscillations of the spacecraft, when $\omega_j = \inf(\omega_1, \omega_2) < \omega_\Gamma$, has the single /67

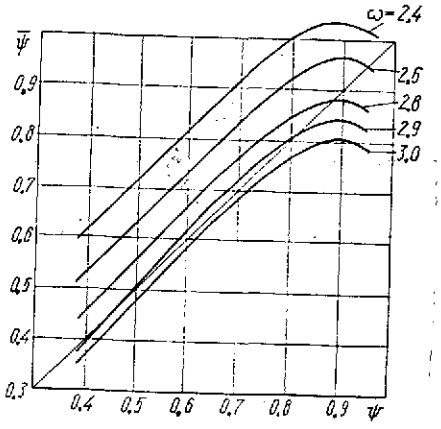

Fig. 8. Recursion functions of the point transformation $\Pi_2 = T_\eta T_\varepsilon \left(\omega_2 < \frac{2L}{\lambda T}\right)$. $\omega_2 > \omega_{2r}$,

simple fixed point

$$\psi^* \in \left(\frac{1}{1+T\sqrt{\lambda}}, 1\right).$$

The derivative recursion function $\varepsilon(\psi)$ is of the form:

$$\frac{d\varepsilon}{d\psi} = -\frac{\psi - \frac{\tilde{\Delta}_1}{K}}{\sqrt{\tilde{A} + \left(\psi - \frac{\tilde{\Delta}_1}{K}\right)^2}};$$

its value at the fixed point is:

$$\left.\frac{d\varepsilon}{d\psi}\right|_{\psi=\psi^*} = -\frac{\frac{1+\tilde{\Delta}_1}{2} - \frac{\tilde{\Delta}_1}{K}}{\sqrt{\tilde{A} + \left(\frac{1+\tilde{\Delta}_1}{2} - \frac{\tilde{\Delta}_1}{K}\right)^2}}.$$

Since $\lambda \geqslant 0$, for any values $\tilde{\Delta}_1$ we have:

$$\left|\left.\frac{d\varepsilon}{d\psi}\right|_{\psi=\psi^*}\right| < 1. \tag{16}$$

Therefore, the fixed point of transformation T_ε is always stable, regardless of the values of the system parameters. The fixed points of transformation T_η are always stable; for any $\lambda > 0$ and $\varphi \in \left(0, \frac{1}{1+T\sqrt{\lambda}}\right)$, the equation

$$\left|\left.\frac{d\eta}{d\psi}\right|_{\psi=C}\right| < 1. \tag{17}$$

is satisfied.

Since the inequalities (16) and (17) are valid, the fixed points of the complex transformations Π_n and P_n are stable, which follows from an analysis of the expressions for $\frac{dF_n}{d\psi}$ and $\frac{df_n}{d\psi}$. For example, the derivative

$$\frac{dF_n^\eta(\psi)}{d\psi} = \frac{d\varepsilon(\psi)}{d\psi}\prod_{i=1}^{n-1}\frac{d\eta[f_i(\psi)]}{d\psi}$$

for all ψ values does not exceed unity modulus-wise, since

$$\left|\frac{d\varepsilon}{d\psi}\right| < 1, \quad \left|\frac{d\eta}{d\psi}\right| < 1, \text{ and } \quad f_i(\psi) = \eta_{i-1}[\varepsilon(\psi)].$$

If the perturbing moment is not equal to zero ($L \neq 0$), the derivatives of the simple recursion functions are of the form:

$$\frac{d\varepsilon}{d\psi} = -\frac{\psi - \frac{\Delta_1}{K}}{\sqrt{A + \left(\psi - \frac{\Delta_1}{K}\right)^2}},$$

$$\frac{d\eta}{d\psi} = \frac{\left(\sqrt{B + \left(\psi - \frac{\Delta_1}{K}\right)^2} - \frac{\alpha_2 - \Delta_2}{K}\right)\left(\psi - \frac{\Delta_1}{K}\right)}{\sqrt{C + \left(\sqrt{B + \left(\psi - \frac{\Delta_1}{K}\right)^2} - \frac{\alpha_2 - \Delta_2}{K}\right)^2}\sqrt{B + \left(\psi - \frac{\Delta_1}{K}\right)^2}}.$$

The fixed points of transformation T_ε are stable for any values of ψ, if the condition $A > 0$ is satisfied, or which amounts to the same thing, $2 - \omega_1 T > -\frac{2L}{\lambda}$. The latter is always satisfied, and therefore, the single-impulse cycle is stable.

The fixed points of transformation T_η are stable for any values of ψ, if $C > 0$ and $B > 0$, or which amounts to the same thing: /68

$$(2 - \omega_2 T)(2L + \omega_2 T\lambda) > 0, \quad (18)$$

$$2L(2 - \omega_1 T) < \lambda\omega_1 T(2 - \omega_1 T). \quad (19)$$

Inequality (18) is wholly satisfied, and for inequality (19) to be satisfied, we must have $\omega_1 = 2L/\lambda T$.

In the case $\omega_1 > 2L/\lambda T$, the transformation T_η has a single stable fixed point. If $\omega_1 < 2L/\lambda T$, transformation T_η has two fixed points (see Fig. 8), one of which is always unstable.

The proof of the stability of the second fixed point is analogous to the proof of the stability of the fixed point of the simple transformation corresponding to the double-impulse cycle, for the motion of the craft outside the atmosphere when acted on by a constant perturbing moment [5].

The fixed points of complex transformations Π_n and P_n corresponding to complex periodic motions in the atmosphere when acted on by a constant moment are stable. The proof of the stability in the case $\omega_1 > 2L/\lambda T$ is analogous to the proof of the stability of the fixed points of the complex transformations for motion in the atmosphere in the absence of a perturbing moment, and is also analogous to the proof of the stability of the fixed points of complex transformations for motion outside the atmosphere when acted on by a constant moment.

Let us compare the amount of energy expended in providing oscillations in the atmosphere when $\Delta\omega \neq 0$, with the amount of energy required to produce the symmetric oscillations ($\Delta\omega = 0$) under the same conditions. By integrating the equation of motion (2) and transforming it, we get a formula for determining the period of the closed double-impulse cycle (cf. Fig. 1):

$$T_a = \frac{1}{\sqrt{\lambda}} \ln \frac{(1 - K_2 |\psi_{i+2}|)(1 - K_2\psi_i)}{(K_2 |\psi_{i+2}| - \Delta_2)(K_2\psi_i - \Delta_1)}.$$

Analysis of the dependence $T_a = T_a(\Delta\omega)$ (Fig. 9) shows that in the case of the double-impulse cycle, the symmetric oscillations ($\Delta\omega = 0$, $L = 0$)

$$T_{aC} = \frac{2}{\sqrt{\lambda}} \ln \frac{1 - K_2\psi_i}{K_2\psi_i - \Delta_1}.$$

have the shortest period.

For the complex n-impulse cycle consisting of m_1 single-impulse and m_2 double-impulse cycles ($n = m_1 + m_2$), the period of oscillations can be determined from the formula:

$$T_a = \sum_{i=1}^{m_1} \tau_i^{(1)} + \sum \tau_i^{(2)},$$

where

$$\tau_i^{(1)} = \frac{1}{\sqrt{\lambda}} \ln \frac{1 - K_2\psi_{i+2}}{\Delta_1 - K_2\psi_{i+1}},$$

$$\tau_i^{(2)} = \frac{1}{\sqrt{\lambda}} \ln \frac{(1 + K_2\psi_{i+2})(1 - K_2\psi_{i+4})}{(\Delta_1 - K_2\psi_{i+1})(\Delta_2 + K_2\psi_{i+3})}.$$

Here $\tau_i^{(1)}$ and $\tau_i^{(2)}$ are the durations of the single-impulse and double-impulse cycles, respectively.

If the energy consumption in a single nozzle engagement is denoted by q_j ($j = 1, 2$ -- the nozzle number) and if we assume $q_1 = r\omega_1$, $q_2 = r\omega_2$, where r is the coefficient of proportionality, the consumption of energy in the time t ($t \gg T_a$) for complex cycles of transformations of the form Π_n^η and P_n^γ will be $Q = \frac{rt}{T_a}[(m_2 + 1)\omega_1 + m_2\omega_2]$.

For the symmetric cycle $Q_C = \frac{2rt}{T_{aC}}\omega_i$. In order to compare /69 the energy expenditure, let us examine the ratio $\bar{Q} = Q/Q_C$. Figure 10 shows the dependence of the relative energy expenditure on the

parameter ω_2. It is assumed that L = 0. A plot of the function $\bar{Q}(\omega_2)$ can be considered as consisting of individual sections corresponding to periodic motions of different types. Thus, for this example, the section of the functions $\bar{Q}(0 \leq \omega_2 \leq 0.83)$ illustrates the energy consumption in the case of single-impulse periodic motions. Double-impulse cycles are established in the range of values $1.34 \leq \omega_2 \leq 1.7$. This range of values divides the plot of $\bar{Q}(\omega_2)$ into two parts. The set of parts lying to the left of the point $A(\omega_2 = 1.34, \bar{Q} = 0)$ corresponds to periodic motions, whose phase trajectories contain single-impulse cycles lying in the left phase half-plane; the set of sections to the right of the point $B(\omega_2 = 1.7, \bar{Q} = 0)$ correspond to the motions whose phase trajectories have single-impulse cycles in the right phase half-plane. Thus, the sections $\bar{Q}(0.8 \leq \omega_2 \leq 1.74)$, and $\bar{Q}(2.3 \leq \omega_2 \leq 3.2)$ illustrate the energy consumption in establishing the three-impulse cycles, and the sections $\bar{Q}(1.1 \leq \omega_2 \leq 1.26)$, $\bar{Q}(2 \leq \omega_2 \leq 2.3)$ -- the five-impulse cycles, and so on. The cycle multiplicity increases with increase in ω_2 ($\omega_2 \to 1.7$) and with decrease in ω_2 ($\omega_2 \to 1.34$). The sections of the functions $\bar{Q}$ for the values $1.26 \leq \omega_2 \leq 1.34$, and $1.7 \leq \omega_2 \leq 1.8$ are not shown in Fig. 10.

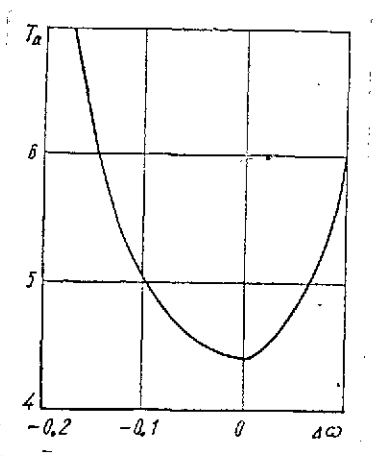

Fig. 9. Plot of the dependence of the duration of the double-impulse cycle on $\Delta\omega$.

The function of the relative expenditure $\bar{Q}(\omega_2)$ has extremal values. The minimum values equal to zero occur at the initial and endpoints isolated above individual sections; the maximum values occur within the sections. At the initial and endpoints of the sections, the first derivative $d\bar{Q}^*/d\omega_2$ is discontinuous. The value of the function $\bar{Q} \to 0$ corresponds to the closed phase trajectories, which include a hyperbola passing near the origin of coordinates ($T_a \to \infty$).

By analyzing the dependence of the relative expenditure on the values of ω_2 when ω_1 = const, we note the following: the energy consumption depends essentially on $\Delta\omega$; the smallest energy consumption to ensure the oscillatory motion is needed when establishing single-impulse cycles; it is difficult to realize periodic motion with energy expenditure close to zero, since at the points of the minimum of function $\bar{Q}$ the derivative $(d\bar{Q}/d\omega_2) \to \infty$; /70 the energy consumption when $\Delta\omega$ = 5 - 10% is much smaller than in the case $\Delta\omega = 0$.

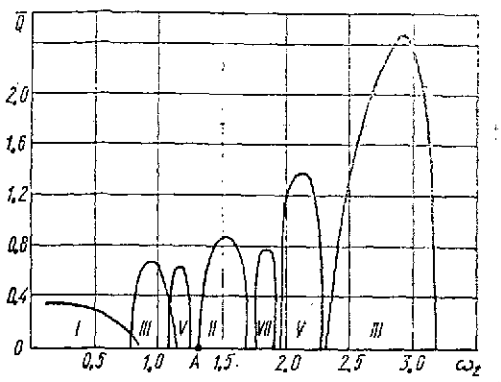

Fig. 10. Functions of the relative energy expenditure.

In conclusion, we can state the following. The form of the oscillatory motions of a spacecraft and the amount of energy expended in orientation depend essentially on the difference of the impulses of the control moments and on the atmospheric density. Simple single-impulse and double-impulse oscillations are possible if the control impulses are identical and the perturbing moment is absent. For uneven impulses and when a perturbing moment is active, complex multi-impulse natural oscillations of different types are possible; with increase in atmospheric density, the oscillation multiplicity becomes smaller and the sequence of bifurcation instants changes. Not all periodic motions of the craft are stable, but in any multi-impulse motion there is a stable cycle. The smallest amount of energy to ensure orientation of the craft is expended when establishing single-impulse cycles; in the realization of multi-impulse cycles, the energy expenditure can be minimized by the appropriate selection of the difference in the impulses of the actuators.

REFERENCES

L. Andronov, A.A., A.A. Vitt, and S.E. Khaykin, Teoriya kolebaniy [Oscillation theory], Fizmatgiz, Moscow, 1959.

2. Gaushus, E.V., Avtomatika i telemekhanika 9(10) (1968).

3. Sheptun, Yu.D. and S.V. Yaroshevich, Kosmicheskiye issledovaniya 6(4) (1968).

4. Gaushus, E.V., Avtomatika i telemekhanika,12 (1966).

5. Gerasyuta, N.F., Yu.D. Sheptun, and S.V. Yaroshevich, "Operating economy of spacecraft stabilization systems," cf. present collection.

INTEGRATION OF EULER'S KINEMATIC EQUATIONS

A.I. Tkachenko

To stabilize the attitude of a spacecraft (SC), in several cases one must know the instantaneous values of the Euler angles characterizing the orientation of the SC in space. One method for the autonomous determination of these angles is the integration of Euler's kinematic equations in an onboard digital computer using data arriving from rate transducers mounted on the spacecraft. Here we must select for the computations a sufficiently simple and exact algorithm that does not impose overly rigorous requirements on the characteristics of the computer.

Let us determine the orientation of the right-handed orthogonal trihedron xyz associated with the SC relative to the same nonrotating trihedron $\xi\eta\zeta$ by means of "aircraft" angles: yaw ψ, pitch θ, and roll γ. Let us introduce the notation:

$$\left.\begin{aligned} X_1 &= \sin\psi, & X_2 &= \cos\psi, \\ Y_1 &= \sin\vartheta, & Y_2 &= \cos\vartheta \neq 0, \\ Z_1 &= \sin\gamma, & Z_2 &= \cos\gamma. \end{aligned}\right\} \tag{1}$$

The kinematic equations that the variables ψ, θ, and γ satisfy can be written as:

$$\left.\begin{aligned} \dot{\psi} &= \frac{1}{Y_2}\left(\omega_y Z_2 - \omega_z Z_1\right), \\ \dot{\vartheta} &= \omega_z Z_2 + \omega_y Z_1, \\ \dot{\gamma} &= \frac{1}{Y_2}\left(\omega_z Z_1 - \omega_y Z_2\right) Y_1 + \omega_x. \end{aligned}\right\} \tag{2}$$

Here ω_x, ω_y, and ω_z are the projections of the angular rate of the SC onto the x, y, and z axes. To determine the orientation of the SC relative to the trihedron $\xi\eta\zeta$, we must integrate Eqs. (2) jointly with the system of equations: /71

$$\left.\begin{aligned} \dot{X}_1 &= \dot{\psi}X_2, & \dot{X}_2 &= -\dot{\psi}X_1, \\ \dot{Y}_1 &= \dot{\vartheta}Y_2, & \dot{Y}_2 &= -\dot{\vartheta}Y_1, \\ \dot{Z}_1 &= \dot{\gamma}Z_2, & \dot{Z}_2 &= -\dot{\gamma}Z_1. \end{aligned}\right\} \tag{3}$$

We can use the quantities $X_1, \ldots, Z_2$ to compute the direction cosines characterizing the relative orientation of the trihedra xyz and $\xi\eta\zeta$.

We will assume that the data on the SC angular rate arrives at the computer in the form of the increments θ_x, θ_y, and θ_z of the integrals of ω_x, ω_y, and ω_z in the time (step) of constant duration h:

$$\theta_{x,n+1} = \int_{t_n}^{t_{n+1}} \omega_x dt, \quad \theta_{y,n+1} = \int_{t_n}^{t_{n+1}} \omega_y dt,$$
$$\theta_{z,n+1} = \int_{t_n}^{t_{n+1}} \omega_z dt, \quad t_{n+1} = t_n + h. \tag{4}$$

By introducing the notation

$$q = \begin{bmatrix} \psi \\ \vartheta \\ \gamma \end{bmatrix}, \quad \omega = \begin{bmatrix} \omega_x \\ \omega_y \\ \omega_z \end{bmatrix}, \quad \theta = \begin{bmatrix} \theta_x \\ \theta_y \\ \theta_z \end{bmatrix},$$
$$X = \begin{bmatrix} X_1 \\ X_2 \\ Y_1 \\ Y_2 \\ Z_1 \\ Z_2 \end{bmatrix}, \quad \Phi = \begin{bmatrix} 0 & \psi & 0 & 0 & 0 & 0 \\ -\psi & 0 & 0 & 0 & 0 & 0 \\ 0 & 0 & 0 & \vartheta & 0 & 0 \\ 0 & 0 & -\vartheta & 0 & 0 & 0 \\ 0 & 0 & 0 & 0 & 0 & \gamma \\ 0 & 0 & 0 & 0 & -\gamma & 0 \end{bmatrix}, \tag{5}$$
$$F(X) = \begin{bmatrix} 0 & \frac{Z_2}{Y_2} & -\frac{Z_1}{Y_2} \\ 0 & Z_1 & Z_2 \\ 1 & -\frac{Y_1 Z_2}{Y_2} & \frac{Y_1 Z_1}{Y_2} \end{bmatrix},$$

we can represent the systems of equations (2) and (3) in the form

$$\varphi = F\omega, \tag{6}$$
$$\dot{X} = \Phi X. \tag{7}$$

To derive the formulas of the numerical integration of Eqs. (6) and (7), using the information (4) let us make the assumption that the functions ω_x, ω_y, and ω_z are analytic in the neighborhood of the points $t = t_n$, which can be written as:

$$\omega(t) = \omega_n + \dot{\omega}_n (t - t_n) + \frac{1}{2} \ddot{\omega}_n (t - t_n)^2 + \ldots \tag{8}$$

Then we can introduce the expansions

$$\begin{gathered} \Phi(t) = \Phi_n + \dot{\Phi}_n (t - t_n) + \frac{1}{2} \ddot{\Phi}_n (t - t_n)^2 + \ldots \\ F[X(t)] = F(X_n) + \dot{F}(X_n)(t - t_n) + \ldots \\ X(t) = X_n + \dot{X}_n (t - t_n) + \frac{1}{2} \ddot{X}_n (t - t_n)^2 + \ldots \\ \varphi(t) = \varphi_n + \dot{\varphi}_n (t - t_n) + \ldots \end{gathered} \tag{9}$$

172

By integrating equalities (8) and (9) in the limits from t_n to t_{n+1} and with reference to formulas (6) and (7), we get the power series:

$$\theta_{n+1} = \omega_n h + \frac{1}{2} \dot{\omega}_n h^2 + \frac{1}{6} \ddot{\omega}_n h^3 + \ldots \tag{10}$$

$$\Delta\Phi_{n+1} = \Phi_{n+1} - \Phi_n = \dot{\Phi}_n h + \frac{1}{2} \ddot{\Phi}_n h^2 + \ldots \tag{11}$$

$$\Delta\varphi_{n+1} = \varphi_{n+1} - \varphi_n = F(X_n)\omega_n h + \frac{1}{2}[\dot{F}(X_n)\omega_n + F(X_n)\dot{\omega}_n] h^2 + \ldots \tag{12}$$

$$\begin{aligned} X_{n+1} = \Big[E + \dot{\Phi}_n h + \frac{1}{2}(\ddot{\Phi}_n + \dot{\Phi}_n^2) h^2 + \\ + \frac{1}{6}(\dddot{\Phi}_n + 3\ddot{\Phi}_n \dot{\Phi}_n + \dot{\Phi}_n^3) h^3 + \ldots \Big] X_n. \end{aligned} \tag{13}$$

The unit matrix E with dimensions 6 x 6 was introduced into formula (13) and the equality $\ddot{\Phi}\dot{\Phi} = \dot{\Phi}\ddot{\Phi}$ was taken into account.

The simplest first-order algorithm for integrating Eqs. (6) and (7) has the following form:

$$\Delta\varphi_{n+1} = F(X_n)\theta_{n+1}, \tag{14}$$

$$X_{n+1} = (E + \Delta\Phi_{n+1}) X_n. \tag{15}$$

in matrical notation.

The increments of the Euler angles in the step are found from the formulas:

$$\begin{aligned} \Delta\vartheta_{n+1} &= \theta_{z,n+1} Z_{2n} + \theta_{y,n+1} Z_{1n}, \\ \Delta\psi_{n+1} &= \frac{1}{Y_{2n}} (\theta_{y,n+1} Z_{2n} - \theta_{z,n+1} Z_{1n}), \\ \Delta\gamma_{n+1} &= \theta_{x,n+1} - \frac{1}{Y_{2n}} (\theta_{y,n+1} Z_{2n} - \theta_{z,n+1} Z_{1n}) Y_{1n}. \end{aligned} \tag{16}$$

The instantaneous values of the angles ψ, θ, and γ are determined by summing the increments of these angles. The components of the vector X are computed by the formulas:

$$\begin{aligned} X_{1,n+1} &= X_{1n} + \Delta\psi_{n+1} X_{2n}, \\ X_{2,n+1} &= X_{2n} - \Delta\psi_{n+1} X_{1n}, \\ &\cdots\cdots\cdots\cdots \\ Z_{2,n+1} &= Z_{2n} - \Delta\gamma_{n+1} Z_{1n}. \end{aligned} \tag{17}$$

Substituting expressions (10) and (11) into formulas (14) and (15), and comparing the results with formulas (12) and (13), we find the estimates of the errors of the algorithm (14) - (15) in the step:

$$\begin{aligned} \delta\varphi_{n+1} &= -\frac{1}{2} h^2 \dot{F}(X_n)\,\omega_n, \\ \delta X_{n+1} &= -\frac{1}{2} h^2 \Phi_n^2 X_n. \end{aligned} \tag{18}$$

If the quantities ω_X, ω_Y, and ω_Z are large enough, to obtain satisfactory precision we must perform computations using formulas (16) and (17) with a very small step, which leads to a heavy load on the computer. Therefore it is preferable to use more exact algorithms capable of increasing the integration step and of reducing the volume of computations without detriment to precision.

Using the expansion /73

$$F(X_{n-1}) = F(X_n) - \dot{F}(X_n)\,h + \frac{1}{2}\ddot{F}(X_n)\,h^2 + \ldots, \tag{19}$$

we obtain a formula of second-order precision for integrating Eq. (6):

$$\Delta\varphi_{n+1} = \frac{1}{2}[3F(X_n) - F(X_{n-1})]\,\theta_{n+1}. \tag{20}$$

The corresponding expressions for the increments of Euler angles differ from the formulas (16) in that instead of X_{1n}, X_{2n}, ..., Z_{2n}, the quantities $\frac{1}{2}(3X_{1n} - X_{1,n-1}), \ldots, \frac{1}{2}(3Z_{2n} - Z_{2,n-1})$ apppear in them. The error formula (20) in the step is a quantity of third-order smallness relative to each:

$$\delta\varphi_{n+1} = -\frac{1}{12} h^3 [\dot{F}(X_n)\,\dot{\omega}_n + 5\ddot{F}(X_n)\,\omega_n]. \tag{21}$$

For the first step ("fitting" of algorithm (20)), when the values $X_{1,n-1}, \ldots, Z_{2,n-1}$ are not known, we can use formula (14). The error introduced here is a second-order quantity in h, that is, it is comparable with the accumulated error of algorithm (20).

Computations based on formula (20) must be combined with the algorithm for integrating Eqs. (7) more exactly than for formula (15), for example, with the second-order algorithm:

$$X_{1,n+1} = \left(E + \Delta\Phi_{n+1} + \frac{1}{2}\Delta\Phi_{n+1}^2\right) X_n. \tag{22}$$

In scalar notation,

$$\begin{aligned} X_{1,n+1} &= \left(1 - \frac{1}{2}\Delta\psi_{n+1}^2\right) X_{1n} + \Delta\psi_{n+1} X_{2n}, \\ &\cdots\cdots\cdots\cdots\cdots\cdots\cdots \\ Z_{2,n+1} &= \left(1 - \frac{1}{2}\Delta\gamma_{n+1}^2\right) Z_{2n} - \Delta\gamma_{n+1} Z_{1n}. \end{aligned} \tag{23}$$

The error of algorithm (2) in the step is estimated by the expression

$$\delta X_{n+1} = -\frac{1}{6} h^3 \Phi_n^3 X_n. \tag{24}$$

The pair of functions X_1 and X_2 satisfies the system of differential equations with the matrix of coefficients, whose principal-diagonal elements are identically equal to zero. For these systems, the so-called reversible first-order method yields a precision of integration that is comparable to the precision of the second-order algorithms. Calculations were made using the following formulas:

$$\begin{aligned} X_{1,n+1} &= X_{1n} + \Delta\psi_{n+1} X_{2n}, \\ X_{2,n+1} &= X_{2n} - \Delta\psi_{n+1} X_{1,n+1}. \end{aligned} \tag{25}$$

for some (for example, odd) step. In the next (even) step, the expressions:

$$\begin{aligned} X_{2,n+1} &= X_{2n} - \Delta\psi_{n+1} X_{1n}, \\ X_{1,n+1} &= X_{1n} + \Delta\psi_{n+1} X_{2,n+1}. \end{aligned} \tag{26}$$

are realized.

In similar fashion, the functions Y_1, Y_2 and Z_1, Z_2 were computed. The sequence of the replacement of the initial values of the variables by their computed values in each subsystem is opposite in the odd and even steps. This system of computation is much more economical than algorithm (22) and imposes less stringent requirements on the computer. A second-order algorithm similar to formula (20) can also be used in integrating Eq. (7):

$$X_{n+1} = X_n + \frac{1}{2}\Delta\Phi_{n+1}(3X_n - X_{n-1}) \tag{27}$$

with a step error of

/74

$$\delta X_{n+1} = -\frac{1}{2}h^2\left(\dot{\Phi}_n\ddot{\Phi}_n + \frac{5}{6}\dot{\Phi}_n^3\right)X_n. \tag{28}$$

Let us examine one more method of computing Euler angles, based on the "mean ordinate" method. Suppose we know the values $X_{1,n+1/2}, \ldots, Z_{2,n+1/2}$ of the components of vector X in the middle of the next step -- at the instant $t = t_n + 1/2h$. Let us represent in the form of a power series the value of matrix F at the instant $t_{n+1/2}$:

$$F(X_{n+1/2}) = F(X_n) + \frac{1}{2}\dot{F}(X_n)h + \frac{1}{8}\ddot{F}(X_n)h^2 + \ldots \tag{29}$$

With reference to expressions (10), (12), and (29), we can easily see that in computing $\Delta\phi$ according to the formula

$$\Delta\varphi_{n+1} = F(X_{n+1/2})\theta_{n+1} \tag{30}$$

in the step an error of third-order smallness in h is introduced:

$$\delta\varphi_{n+1} = -\frac{1}{12}h^3\left[\frac{1}{2}\ddot{F}(X_n)\omega_n + \dot{F}(X_n)\dot{\omega}_n\right]. \tag{31}$$

The expressions for $\Delta\psi_{n+1}$, $\Delta\theta_{n+1}$, and $\Delta\gamma_{n+1}$ corresponding to formula (30) differ from expression (16) in that instead of X_{1n}, ..., Z_{2n} the values $X_{1,n+1/2}, \ldots, Z_{2,n+1/2}$ figure in them.

Let us introduce the notation

$$D_{n+1} = \frac{1}{2}(3\Delta\Phi_{n+1} - \Delta\Phi_n) = \dot{\Phi}_n h + \ddot{\Phi}_n h^2 + \frac{1}{6}\dddot{\Phi}_n h^3 + \ldots \tag{32}$$

Using the expansions

$$X_{n+1/2} = \left[E + \frac{1}{2}\dot{\Phi}_n h + \frac{1}{8}(\ddot{\Phi}_n + \dot{\Phi}_n^2)h^2 + \cdots\right]X_n,$$
$$X_{n+3/2} = \left[E + \frac{3}{2}\Phi_n h + \frac{9}{8}\left(\ddot{\Phi}_n + \dot{\Phi}_n^2\right)h^2 + \cdots\right]X_n, \quad (33)$$

we obtain a formula for computing the vector X in the middle of the next step

$$X_{n+3/2} = \left(E + D_{n+1} + \frac{1}{2}D_{n+1}^2\right)X_{n+1/2} \quad (34)$$

with the step error

$$\delta X_{n+3/2} = -h^3\left(\frac{1}{6}\dot{\Phi}_n^3 + \frac{3}{8}\ddot{\Phi}_n\right)X_n. \quad (35)$$

When the "mean ordinate" method is used, the values X_1, ..., Z_2 are obtained with a shift for half of the step forward with respect to the input data (4). This factor must be taken into account when performing navigation computations using a direction-cosine matrix. Instead of algorithm (34), one can use the more economical first-order reversible method, similar to the method (25) - (26). For "fitting" in the first step, one can assume

$$F(X_{1/2}) = F(X_0), \quad D_1 = {}^3/_2\Delta\Phi_1,$$

without detriment to the precision of the calculations overall.

It must be expected that in most cases of SC motion, the "mean ordinate" method (30) enables us to determine the Euler angles to a higher precision than does algorithm (20). The accumulated error of the integration of Eq. (6) without allowing for the effect of the error of computing the vector X to the first approximation is equal to the sum of the errors in integration in the step. At the limit, as h → 0, we have

$$\delta\varphi(t) = \frac{1}{h}\int_{t_0}^{t}\delta\varphi_{n+1}(t)\,dt, \quad (36)$$

where $\delta\phi_{n+1}(t)$ is the "local" expression for the error at the step.

By inserting into (36) expression (21) for $\delta\phi_{n+1}$ and by carrying out integration by parts, let us find the estimate of the accumulated error of algorithm (20): /75

$$\delta\varphi(t) = \frac{1}{12} h^2 \left[\dot{F}(X_0)\omega_0 - \dot{F}(X)\omega(t) - 4\int_{t_0}^{t} \ddot{F}(X)\omega dt \right]. \quad (37)$$

By performing the same operations for the error (31), we get an estimate of the accumulated error of algorithm (30):

$$\delta\varphi(t) = \frac{1}{12} h^2 \left[\dot{F}(X_0)\omega_0 - \dot{F}(X)\omega + \frac{1}{2}\int_{t_0}^{t} \ddot{F}(X)\omega dt \right]. \quad (38)$$

If in computing the quantity $1/Y_2$, the operation of division is undesirable, we can use recursion formulas of the type

$$\frac{1}{Y_{2,n+1}} = \frac{1}{Y_{2n}}\left(2 - \frac{Y_{2,n+1}}{Y_{2n}}\right). \quad (39)$$

In conclusion, we note that if the solution to Eqs. (7) is not used in setting up the matrix of direction cosines, then computation of the quantities X_1 and X_2 can be omitted. But if the unknown angles ψ, θ, and γ characterize the orientation of the SC relative to some slow-varying coordinate trihedron (for example, the accompanying trihedron of the orbital system of coordinates), then to the right sides of Eqs. (2) are added small terms that must be taken into account by periodic correction of the solution.

AN ALGORITHM FOR COMPUTING THE TRAJECTORY OF THE INJECTION OF A SPACE OBJECT INTO ORBIT

A.A. Krasovskiy and L.T. Gripp

The solution of problems associated with the motion of a space object over the section of its injection into orbit is impossible without complex and cumbersome computations and requires considerable outlays of labor even when a high-speed computer is used. Statistical methods of analysis of the type of Monte-Carlo method and the random search method are widely used. These methods in several cases can markedly improve the flight characteristics of space objects, however to find the optimal solution requires increasing the speed of calculations by one order of magnitude.

Stringent requirements on ensuring high speed of calculations are also imposed by problems of the encounter of space objects in orbit, developing systems of flexible control of space object motion, and many others. Therefore it is very typical of modern methods of analyzing space object motion that a great deal of attention is given to developing universal calculation algorithms that require minimum outlays of labor and machine time.

Improvements in computational methods of calculating space object motion are following two main trends: development of analytic methods for the most general assumptions possible, on the basis of which a mathematical model of the flight is constructed, and the development of universal numerical methods requiring the smallest possible outlays of labor to arrive at a solution with specified precision.

The most successful solution would be developing an algorithm which would approach in universality numerical methods, and in speed -- analytic methods. An attempt to solve this problem is given in the present article.

Let us examine an algorithm for computing the trajectory of /76
a space object over the section of its injection into orbit for assigned designed characteristics of the object and launch vehicle and for selected control programs.

The mathematical basis of the proposed algorithm is the use of interpolational power polynomials for numerical integration following the scheme of successive approximations.

As a numerical illustration of the results obtained in the article, we used data on hypothetical launch vehicles and space objects published in the periodical literature.

Integration of systems of ordinary differential equations by the scheme of successive approximations. The analysis of procedures of numerical integration based on the Picard method of successive approximations is closely associated with the names A.N. Krylov [1] and V.E. Milne [2]. Below is presented a numerical method of successive approximations based on the concepts of these authors and on the interpolational quadrature formula.

Let us first examine expressions for the coefficients of the interpolational power polynomial.

We know [3] that for any assigned function $\phi(t)$ there exists a unique polynomial of degree m

$$Q_m(t) = \sum_{k=0}^{m} \omega_k t^k, \tag{1}$$

which at $(m + 1)$ arbitrarily placed interpolation nodes t_j ($j = 0, 1, \ldots$; where $t_j \neq t_k$ for $j \neq k$) takes on the assigned values

$$Q_m(t_j) = \psi(t_j).$$

The traditional method of determining the coefficients of the polynomial is solving the system of $(m + 1)$ linear algebraic equations

$$\sum_{k=0}^{m} \omega_k t_j^k = \psi_j, \tag{2}$$

where $\psi_j = \psi(t_j)$. Here and in the following it will be assumed that the indexes k and j run through the values 0, 1, ..., m.

Using mathematical induction, we can show that the coefficients of the interpolational polynomial can be obtained directly from the expression

$$\omega_k = \sum_{j=0}^{m} A_{jk}\psi_j, \tag{3}$$

where

$$A_{jk} = \frac{B_{jk}}{\sum_{k=0}^{m} B_{jk} t_j^k};$$

$$B_{jk} = t_j B_{j,k+1} - \frac{1}{m-k} \sum_{j=0}^{m} t_j B_{j,k+1}; \quad B_{jm} = 1.$$

In the case that is convenient for practical purposes, when the interpolation nodes are equidistant points, the coefficients A_{jk} are found from the simpler expression:

$$A_{jk} = jA_{j,k+1} - \frac{A_{jm}}{m-k}\sum_{j=0}^{m}\frac{jA_{j,k+1}}{A_{jm}}, \qquad (4)$$

where

$$A_{jm} = \frac{(-1)^{m-j}}{j!\,(m-j)!}.$$

Then the interpolational polynomial (1) takes on the form: /77

$$Q_m(t) = \sum_{k=0}^{m}\omega_k\tau^k, \qquad (5)$$

where

$$\tau = \frac{t-t_0}{h}; \quad h = \frac{t'-t_н}{m};$$

t_H and t' are the bounds of the finite limit of change of the independent variable.

Data on machine time outlays (Fig. 1) show that when $m \geq 3$, the recursion expression (4) for determining the coefficients of the interpolational polynomial reduce the time of computation compared with the case when the system of algebraic equations (2) is solved by ordinary methods, for example, the gaussian method.

The advantages of the proposed method of determining the coefficients of the interpolational polynomial also include the explicit analytic representation of the coefficients and the reduction in the required size of the operational memory of the digital computer.

Let us use the interpolational polynomial of the form (5) to construct a quadrature formula to find the integral with variable upper limits

$$x(t) = \int_{t_н}^{t}\psi(t)\,dt,$$

where $t_H \leq t \leq t'$.

By replacing the integrand with the interpolational polynomial (5) and neglecting the residual term, let us construct the rule for approximate quadrature:

$$x(t) \approx h\sum_{k=0}^{m}\frac{\omega_k}{k+1}\tau^{k+1}. \qquad (6)$$

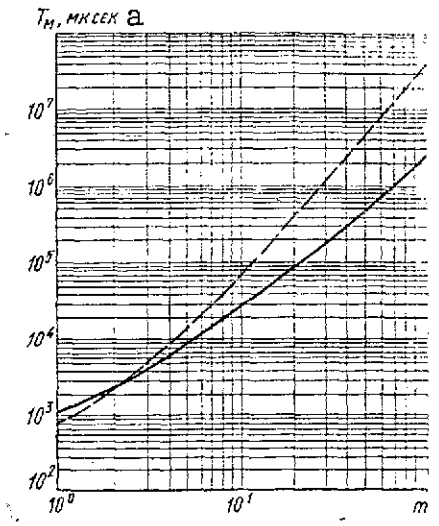

Fig. 1. Machine time required for computing the coefficients of the interpolational polynomial as a function of its order:
—— recursion formula
--- gaussian method

Key: a. μsec

The resulting formula is easily applied to the computation of multiple integrals. Thus, an integral of the form

$$X(t) = \int_{t_н}^{t} \int_{t_н}^{t} \dots \int_{t_н}^{t} \psi(t)\,(dt)^{\chi}$$

can be computed according to the following approximate formula:

$$X(t) \approx h^{\chi} \sum_{k=0}^{m} \frac{k!\omega_k}{(k+\chi)!}\,\tau^{k+\chi}. \qquad (7)$$

When the resulting quadrature formula is used in practical computation of the requirements, the precision of integration can be ensured by varying the order of this formula m and the length of the interval of change of the independent variable $\Delta t = t' - t_н$.

Let us proceed to the problem of integrating ordinary differential equations based on the interpolational quadrature formula of the form (7).

Under the Picard theorem [4], for a first-order differential equation /78

$$\dot{x} = f(t, x), \quad x(t_н) = x_н, \qquad (8)$$

whose right sides satisfy the conditions of the theorem of existence and uniqueness, there is a recursion formula for finding the solution of this equation in the form of these successive approximations:

$$x_ν = x_н + \int_{t_н}^{t} f(t, x_{ν-1})\,dt.$$

Here, it is customary to take the initial condition $x_н$ as the initial approximation x_0.

Using formula (6) to find the quadratures $x_ν$ in the interval $[t_н, t']$, we can represent the approximate solution of differential equation (8) as the power polynomial:

$$x = x_н + h\sum_{k=0}^{m} \frac{\omega_{kr}}{k+1}\tau^{k+1}, \tag{9}$$

whose coefficients ω_{kr} are determined by the recursion relations:

$$\left.\begin{aligned} &\omega_{kv} = \sum_{j=0}^{m} A_{jk} f_{jv}, \\ &f_{jv} = f(t_j, x_{jv}), \\ &x_{jv} = x_н + h\sum_{k=0}^{m} \frac{\alpha_{k,v-1}}{k+1} j^{k+1}, \qquad v = 1, 2, \ldots, r. \end{aligned}\right\} \tag{10}$$

The numbers x_{jv} are values of the v-th approximation of the unknown function at the interpolation nodes.

Computations based on formulas (10) were made up to the value $v = r$, for which the relation $|x_r - x_{r-1}| \leq \varepsilon$ is satisfied, where ε is some assigned small number characterizing the required calculation precision.

This method is generalized to a system of ordinary differential equations of any order that is solvable relative to the major derivatives $x_i^{(\chi)} = f_i(t, x_1, \ldots, x_n, x_1', \ldots, x_n', \ldots, x_1^{(\chi-1)}, \ldots, x_n^{(\chi-1)})$,

$$i = 1, 2, \ldots, n$$

The approximate solution in this case is analogous to (9):

$$x_i \approx x_{iн} + h^{\chi}\sum_{k=0}^{m} \frac{k!\,\omega_{ikr}}{(k+\chi)!}\tau^{k+\chi}. \tag{11}$$

The iterative process (10) for the system of equations is conveniently represented in matrical form

$$[x_v] = [\tilde{x}_н] + h^{\chi}[f_{v-1}][E_m^{\chi}], \qquad v = 1, 2, \ldots, r, \tag{12}$$

where $[E_m^{(\chi)}] = [A_m][D_m^{(\chi)}]$; $[\tilde{x}_н]$, $[f_{v-1}]$ are the rectangular matrices of the type n x m, whose elements $\tilde{x}_{ijн}$ and $f_{i,j,v-1}$ are defined as follows:

$$\tilde{x}_{ijн} = x_{iн} + jhx_{iн}' + \ldots + \frac{(jh)^{\chi-1}x_{iн}^{(\chi-1)}}{(\chi-1)!},$$

$$f_{ij,v-1} = f_i(t_j, x_{1j,v-1}, \ldots, x_{nj,v-1}, x_{1j,v-1}', \ldots$$
$$\ldots, x_{nj,v-1}', \ldots, x_{1j,v-1}^{(\chi-1)}, \ldots, x_{nj,v-1}^{(\chi-1)}),$$

$[A_m]$, $[D_m^{(\chi)}]$ are square matrices of order m; the elements of the matrix $[A_m]$ are found from expression (4); and the elements of the matrix $[D_m^{(\chi)}]$ are calculated by the formula $D_{kl}^{(\chi)} = \frac{k!\, j^{k+\chi}}{(k-\chi)!}$. /79

Iteration (12) is continued until the required integration precision is not attained, after which the coefficients ω_{ikr} are determined:

$$[\omega_r] = [f_r][A_m]. \tag{13}$$

The process of determining the coefficients ω_{ikr} can be accelerated to a large extent if one takes as the initial approximations not the initial values of the unknown functions, but some functions $x_i^*(t)$ that are closer to the exact solution. The closer these functions are taken to the true solution, the more rapidly will the limiting functions $x_i(t)$ be attained, with the degree of precision selected for the computations. In this case, the solution of the system of differential equations and the coefficients of the polynomial are also determined by formulas (11) and (12), where instead of the matrix $[\tilde{x}_H]$ we must take the matrix $[x^*]$, whose elements are $x_{ij}^* = x_i^*(t_j)$.

Integration of equations of motion of the space object. Let us consider the application of the numerical method of successive approximations to integrating the system of differential equations of motion of a space object over the section of its injection into orbit.

The equations of motion of the space object in general form can be represented thusly (in projections onto the axes of the Cartesian system of coordinates with the origin at the launch point):

$$\left.\begin{aligned} \dot{V}_i &= f_i(t, M, x, y, z, V_x, V_y, V_z), \\ \dot{r}_i &= V_i, \qquad i = x, y, z \\ \dot{M} &= g(t), \end{aligned}\right\} \tag{14}$$

where t is the flight time; V is the velocity of the space object; r is the radius-vector ($r_x = x$, $r_y = R_0 + y$, $r_z = z$; R_0 is the radius of the Earth at the launch point); and M is the mass of the launch vehicle bearing the space object.

The algorithm for integrating the equations of motion presented below does not depend on the form of the right sides of the differential equations, therefore the functions f_i are not expanded here. It is only required that these functions satisfy the conditions of the theorem of the existence of uniqueness. The explicit form of the right sides of differential equations (14) is defined by the specific problem and is presented in numerous sources, for example, in [5].

Under the above-presented integration algorithm, the solution of system (14) is best sought by beginning from some initial approximation. In this case, the assignment of the initial approximation reduces the defining the so-called "reference" trajectory for which we take the trajectory of motion of the space object in a vacuum with a constant gravity field. The laws of variation of mass and the pitch angle for the "reference" trajectory are approximated by linear functions. With these assumptions, the differential equations of motion are easily solved in quadratures. The final expressions for computing the "reference" trajectory are not given in this article, since their derivation does not pose fundamental difficulties.

This approach permits, with minimum machine time, computing the values of the kinematic elements of the trajectory, allowing an error of 10-15%, which is wholly acceptable for the initial approximation.

The next problem is to integrate the equations of motion on the basis of the "reference" trajectory adopted.

Suppose that at some time instant t_H the motion of the launch vehicle carrying the space object is characterized by the vectors of velocity $\overline{V}_H$ and position $\overline{r}_H$ and by mass M_H. It is required to determine to the desired precision the velocity, position, and mass at the time interval $[t_H, t']$ satisfying the system of differential equations (14). /80

Let us represent the right sides of the differential equations of motion in the form of a sum of two components, one of which characterizes the motion of the space object along the "reference" trajectory, and the other is a correction corresponding to the difference of the actual and "reference" trajectory; let us integrate them in the limits form t_H to t, and we get

$$V_i = V_i^* + \Delta V_i, \quad r_i = r_i^* + \Delta r_i, \quad M = M^* + \Delta M.$$

The initial conditions here are taken into account in the integrals of the "reference" trajectory V_i^*, r_i^*, and V^*.

Using the above-presented method, we can define the elements of the trajectory in the time interval $[t_H, t']$ by the following functions:

$$\left.\begin{aligned} V_i &= V_i^* + h\sum_{k=0}^{m}\frac{\omega_{ikr}}{k+1}\tau^{k+1},\\ r_i &= r_i^* + h^2\sum_{k=0}^{m}\frac{\omega_{ikr}}{(k+1)(k+2)}\tau^{k+2},\\ M &= M^* + h\sum_{k=0}^{m}\frac{\omega_k}{k+1}\tau^{k+1}. \end{aligned}\right\} \qquad (15)$$

To compute the coefficients of the polynomials, we use the expressions

$$\left.\begin{aligned} \omega_{ikr} &= \sum_{j=0}^{m} A_{jk}\Delta\dot{V}_{ijr},\\ \omega_k &= \sum_{j=0}^{m} A_{jk}\Delta\dot{M}_j. \end{aligned}\right\} \qquad (16)$$

The mass consumption per second M depends only on the flight time; therefore the coefficients ω_K are defined by expression (16), if the corrections $\Delta\dot{M}_j$ to the "reference" value of the per-second consumption $\dot{M}^*$, taken at the interpolation nodes, were computed:

$$\Delta\dot{M}_j = \dot{M}(t_j) - \dot{M}_j^*.$$

The corrections to the acceleration components $\Delta\dot{V}_{ijr}$ are functions of the kinematic trajectory elements and therefore cannot be found directly. The recursion relations

$$\left.\begin{aligned} [V_\nu] &= [V^*] + h[\Delta\dot{V}_{\nu-1}][E_m^{(1)}],\\ [r_\nu] &= [r^*] + h^2[\Delta\dot{V}_{\nu-1}][E_m^{(2)}],\\ [\Delta\dot{V}_{\nu-1}] &= [\dot{V}_{\nu-1}] - [\dot{V}^*], \end{aligned}\right\} \qquad (17)$$

are used to compute these corrections, where [V] and [r] are rectangular matrices of the type 3 x m, with the following form (the indexes * and ν in the notation are omitted for simplicity:

$$[V] = \begin{bmatrix} V_{x0} & V_{x1} & \dots & V_{xm}\\ V_{y0} & V_{y1} & \dots & V_{ym}\\ V_{z0} & V_{z1} & \dots & V_{zm} \end{bmatrix},$$

$$[r] = \begin{bmatrix} x_0 & x_1 & \dots & x_m\\ R_0 + y_0 & R_0 + y_1 & \dots & R_0 + y_m\\ z_0 & z_1 & \dots & z_m \end{bmatrix}.$$

The matrix elements $[V_{\nu-1}]$ are computed by Eqs. (14) for the values of the kinematic elements $[V_{\nu-1}]$ and $[r_{\nu-1}]$ and the corresponding values of flight time and mass. The iterative process described by expression (17) is continued up to an $\nu = r$ such that the condition $|\xi^{max}| \leq \varepsilon$ is satisfied, where ε is the allowable error of the computation of acceleration; $|\xi^{max}|$ is the modulus of the largest of the matrix elements $|\xi|$ characterizing the change in the acceleration components at the interpolation nodes in a single approximation /81

Thus, integration of the system of equations of motion according to the proposed algorithm provides for carrying out the following operations: computing the "reference" (simplified) trajectory from analytic expressions; determining the coefficients of polynomials by successive approximations in accordance with the recursion relations (17); and setting up the time functions of the trajectory parameters according to formulas (15).

Realization of the proposed algorithm of trajectory computation. The main criterion characterizing the suitability of a particular calculation method is providing minimum machine time for the assigned precision of trajectory element computation.

When this algorithm is used, the computation time and the integration precision are determined by three parameters, which depend on the nature of the behavior of the right sides of the differential equations: the order of the interpolation quadrature formula m, the number of successive approximations r, and the integration interval Δt.

Below are presented several general considerations dealing with the assignment of these parameters when computing, on a M-220 high-speed digital computer, the trajectory of the insertion of a space object into orbit.

It is obvious that the methodological error in integration decreases with increase in the order of the quadrature formula m. In addition, for large m errors caused by the inevitable rounding in computing the right sides of the differential equations and the elements of the integration matrices $[E_m^{(1)}]$ and $[E_m^{(2)}]$ begin to have an effect. For this class of trajectories, the seventh-order quadrature formula is preferable. When m = 7, the elements of the integration matrices are of an order not exceeding the computer capacity and, therefore, the rounding errors in computing the elements are absent, while the errors in rounding the right sides are negligibly small.

The number of approximations required for the assigned calculation precision depends to a large extent on the specific problem. In order to avoid possible errors, the selection of the required number of approximations is introduced into the integration algorithm. In this case, the process of successive approximations continues until two neighboring approximations of the trajectory elements are coincident in the limits of the assigned precision. Figure 2 presents the maximum errors of computation as a function of the number of successive approximations for a hypothetical medium-class AES [artificial Earth satellite]. From an examination of these data it follows that in practice three approximations are sufficient for the atmospheric section and two approximations for the extra-atmospheric section; the computation errors here do not exceed 0.001 m/sec in velocity and 0.1 m in position.

With these conditions for selection of the parameters m and r, the required calculation precision is uniquely ensured by the selection of a single parameter -- the integration interval Δt. The parameter Δt is a quantity that is analogous to the integration step in other numerical methods.

The functions given in Fig. 3 show that for a computation error of not more than 0.01 m/sec in velocity and 1 m in position, the step Δt is approximately 20 sec when computing the atmospheric section, and 250 sec when computing motion in the vacuum.

Under the same conditions, the time for computing the trajectory by the numerical method of successive approximations is reduced compared with the time of computation under the Runge-Kutta method by approximately a factor of two for the atmospheric section, and by a factor of 20 for the extra-atmospheric section. /82

The computation time was reduced owing to two factors. First of all, the actual trajectory of the object was computed relative to the "reference" trajectory which considerably reduced the size of the right sides and, therefore, made it possible to increase the integration step. The time outlays for computing the "reference" trajectory, expressed in simple analytic form, are negligibly small compared with the total computation time. Secondly, the interpolational quadrature formula on the basis of which the integration process was constructed has a residual term that is much smaller than the residual term in the Taylor series taken as the basis of the Runge-Kutta method.

Let us point out several features of the realization of the proposed algorithm.

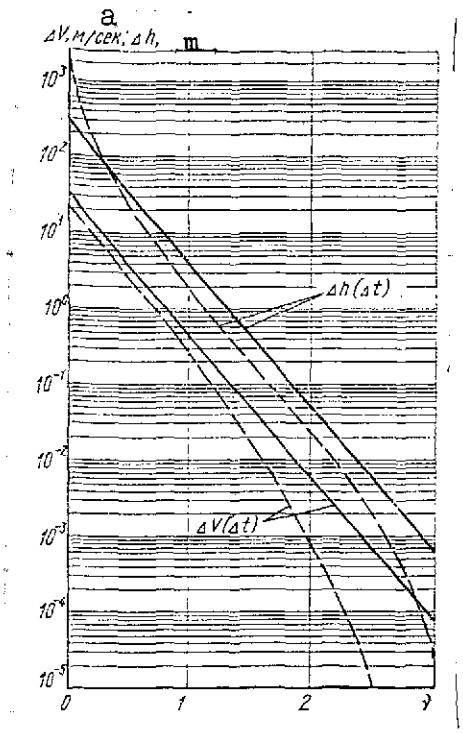

Fig. 2. Errors in computing velocity ΔV and altitude Δh as a function of the number of successive approximations: —— motion in the atmosphere --- motion in vacuum

Key: a. m/sec

The use in this algorithm of a quadrature formula for finding integrals with a variable upper limit makes it possible to arrive at the approximate solution both in numerical and analytic form. Therefore each trajectory parameter must be represented by an analytic expression of two terms. The first term is the expression for the parameter of the "reference" trajectory, and the second is a polynomial of m degree, approximating the difference in the parameters of the true and "reference" trajectories. Thus, as the result of computation, the kinematic parameters of the object trajectory can be obtained in compact form. To do this, it is sufficient to specify the formula for each trajectory element and the table of the parameters of the "reference" trajectory and the polynomial coefficients.

An important feature of the proposed method is the option of simple monitoring of the correctness of the solution on a digital computer. A double solution of the problem followed by a comparison of the results or of control sums is a fairly widespread procedure of monitoring. This procedure involves large outlays of machine time, however it is necessary when solving problems of large scope. When the method of successive approximations is used, the necessity of double computation disappears, since the computation is conducted until two successive approximations coincide within the limits of the assigned precision, as a result of which random digital computer misses can be corrected by the following approximations.

Upon examining this algorithm overall, we can note its following advantages:

-- the method of successive approximations markedly shortens the time needed to compute the injection trajectory;

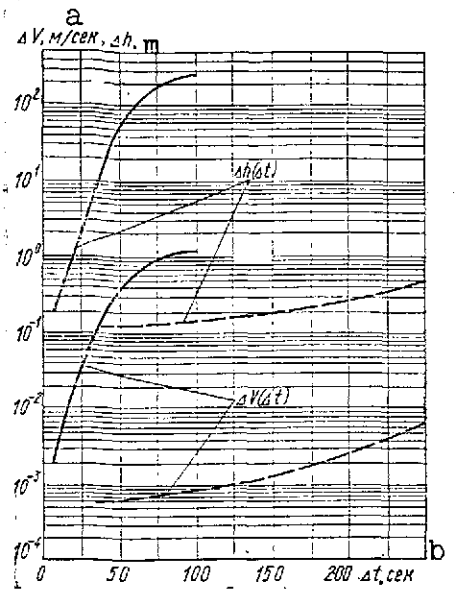

Fig. 3. Errors in computing velocity ΔV and altitude Δh as a function of the integration interval:
—— motion in the atmosphere
--- motion in a vacuum

Key: a. m/sec b. sec

-- the method of successive approximations is convenient for ongoing monitoring of the correctness of the solution when computing the trajectory on a digital computer and makes it possible to avoid double computation; and

-- the results of computing the trajectory by the method of successive approximations can be represented as compact analytic expressions and as a table of coefficients.

The proposed algorithm also proves very effective when used for other problems of space ballistics, for example, for the problem of determining the optimum regime of the injection of a space object into orbit, however this problem is beyond the scope of this article and is a subject for special consideration.

REFERENCES

1. Krylov, A.N., Lektsii o priblizhennykh vychisleniyakh [Lectures on approximate computations], Gostekhizdat, Moscow/Leningrad, 1950.

2. Mili, V.E., Chislennoye resheniye differentsial'nykh uravneniy [Numerical solution of differential equations], IL, Moscow, 1955.

3. Demidovich, B.P., I.A. Maron, and E.Z. Shuvalova, Chislenniye metody analiza [Numerical methods of analysis], "Nauka," Moscow, 1967.

4. Stepanov, V.V., Kurs differentsial'nykh uravneniy [Course on differential equations], Fizmatgiz, 1959.

5. Ostoslavskiy, I.V. and I.V. Strazheva, Dinamika poleta. Trayektorii letatel'nykh apparatov [Flight dynamics, Trajectory of flight craft], Oborongiz, Moscow, 1963.

ANALYTIC-NUMERICAL METHOD OF COMPUTING ATTITUDE CHANGES OF SIMILAR AES

A.A. Krasovskiy, Ye.I. Bushuyev, E.P. Kompaniyets, and A.I. Vasil'yeva

The proposed analytic-numerical method of computing attitude changes of similar AES, with allowance for the noncentrality of the Earth's gravity field and the atmospheric density, when performed with a computer affords a considerable saving in machine time (by a factor of 10-15), with satisfactory precision, which is important when solving problems associated with the long-term prediction of AES attitude changes.

The basis of the method is the familiar procedure [3] of two-cycle integration of the differential equations of motion in osculating elements: integration in the limits of a single revolution (internal cycle) and integration by the number of revolutions (external cycle).

To ensure speed in computations, integration in the internal cycle is replaced by computation using finite formulas with reference to short-periodic fluctuations in flight altitude owing to the noncentrality of the Earth's gravity field and the nonsphericity of the Earth and the dynamic model of atmospheric density that reflects variations in the density of a global nature (11-year cycle, 27-day and semiannual variations, and geomagnetic effects).

These increments in the elements of orbital motion in a revolution are the starting basis for integrating the equations of AES motion in finite differences -- by the number of revolutions. External integration is carried out by one of the methods proposed in [4]. At each step of the external integration, the elements of orbital motion are refined by the value of the long-periodic fluctuations due to the noncentrality of the Earth's gravity field. /84

Short-periodic fluctuations in the flight altitude of an AES in a revolution. For the motion of AES in elliptical and circular orbits, the mechanism of the perturbing action of the atmospheric density differs: in near-circular orbits the satellite is decelerated at virtually all points, but in elliptical orbits -- in the region of the orbital perigee, accordingly, for near-circular orbits with eccentricity $e \leq 0.02$, allowing for the short-periodic fluctuations in altitude was made over the entire revolution, and for elliptical ($e > 0.02$) -- only at the perigee.

In deriving the formulas, allowance was made for the perturbing action only of the second zonal harmonic of the expansion of the Earth gravity potential. In several studies, for example [5], it is shown that higher harmonics lead to negligible short-periodic fluctuations. The perturbing action of the atmospheric density on the flight altitude within the limits of a single revolution was not taken into account.

Near-circular orbits ($e \leq 0.02$). Let us write the instantaneous flight altitude in near-circular orbits in the form

$$h = r - R_e + \Delta h_{per} \tag{1}$$

where r is the radius-vector of the satellite when moving in an unperturbed Keplerian orbit; R_e is the equatorial radius of the Earth; and Δh_{per} are the periodic fluctuations in AES flight altitude in a revolution, caused by the noncentrality of the field and the nonsphericity of the Earth.

Periodic fluctuations of the radius-vector owing to the field noncentrality Δr_{per} are defined by the familiar formula [2]:

$$\Delta r_{per} = -\frac{1}{2p}\frac{\varepsilon}{\mu}\left[\left(2-\frac{3}{4}\sin i\right)(1-\cos u)+\frac{2}{3}\sin^2 i\sin^2 u\right], \tag{2}$$

where ε and μ are constants of the attracting field.

With reference to the instantaneous value of the Earth's radius at the satellite track point:

$$R_з = R_e(1-\alpha\sin^2 i\sin^2 u), \tag{3}$$

where α is the polar contraction of the Earth, we get from (2) and (3):

$$\Delta h_{per} = B\sin^2 u - C(1-\cos u). \tag{4}$$

Here

$$B = \left(R_e\alpha - \frac{1}{3p}\frac{\varepsilon}{\mu}\right)\sin^2 i; \tag{5}$$

$$C = \frac{1}{p}\frac{\varepsilon}{\mu}\left(1-\frac{2}{3}\sin^2 i\right). \tag{6}$$

Formula (4) gives good agreement with an exact computation (about 2%) for $e \leq 0.02$; for larger eccentricities, the error in altitude determination becomes comparable with the value of the correction itself.

Elliptical orbits ($e \geq 0.02$). The altitude at the perigee for a flight in an elliptical orbit is determined by the formula:

$$h_p = (a + a_{per})(1 - e - \Delta e_{per}) - R_\omega \tag{7}$$

where $R_\omega = R_e(1 - \alpha \sin^2 i \sin^2 \omega)$; Δa_{per} and Δe_{per} are the periodic oscillations of the semimajor axis and the eccentricity due to the noncentrality of the Earth gravity field.

Let us represent the rate of change of the parameters a and 1 in the form

$$\frac{de}{du} = \gamma \frac{r^2}{\mu} \left\{ S \sin(u - \omega) + \frac{e + 2\cos(u - \omega) + e\cos^2(u - \omega)}{e\cos(u - \omega) + 1} T \right\}, \tag{8}$$

$$\frac{da}{du} = \gamma \frac{2a^2 r^2}{\mu p} \{ Se \sin(u - \omega) + T[1 + e\cos(u - \omega)] \}, \tag{9}$$

$$\gamma = \frac{1}{1 - \frac{r^2}{\mu} \operatorname{ctg} i \frac{\sin u}{1 + e\cos(u - \omega)} W} \approx 1; \tag{10}$$

/85

$$S = -\frac{3}{2} \frac{C_{20} \mu R_e^2}{r^4} (3 \sin^2 u \sin^2 i - 1); \tag{11}$$

$$T = \frac{3}{2} \frac{C_{20} \mu R_e^2}{r^4} \sin^2 i \sin 2u; \tag{12}$$

$$W = \frac{3}{2} \frac{C_{20} \mu R_e^2}{r^4} \sin u \sin 2i. \tag{13}$$

Using expressions (8) - (13), after transformations we get:

$$\frac{de}{du} = \frac{3}{2} \frac{C_{20} R_e^2}{a^2 (1 - e^2)^2} \sum_{k=1}^{5} [\varepsilon_k \sin k(u - \omega) + \zeta_k \cos k(u - \omega)], \tag{14}$$

$$\frac{da}{du} = 3 \frac{C_{20} R_e^2}{a(1 - e^2)^3} \sum_{k=1}^{5} [\eta_k \sin k(u - \omega) + \xi_k \cos k(u - \omega)], \tag{15}$$

where

$$\begin{aligned}
\eta_1 &= se\left(1 + \frac{1}{4} e^2\right) + \frac{1}{4} e(3 + e^2) c_1, \\
\eta_2 &= se^2 + \left(1 + \frac{3}{2} e^2\right) c_1, \\
\eta_3 &= \frac{1}{4} se^3 + \frac{9}{4} e\left(1 + \frac{1}{4} e^2\right) c_1, \\
\eta_4 &= \frac{3}{2} e^2 c_1, \\
\eta_5 &= \frac{5}{16} e^3 c_1;
\end{aligned} \tag{16}$$

$$\left.\begin{aligned}
\xi_1 &= \frac{1}{4} e\left(3 + \frac{1}{2} e^2\right) c_2, \\
\xi_2 &= \left(1 + \frac{3}{2} e^2\right) c_2, \\
\xi_3 &= \frac{9}{4} e\left(1 + \frac{1}{4} e^2\right) c_2, \\
\xi_4 &= \frac{3}{2} e^2 c_2, \\
\xi_5 &= \frac{5}{16} e^3 c_2;
\end{aligned}\right\} \tag{17}$$

$$\left.\begin{aligned}
\varepsilon_1 &= s\left(1 + \frac{1}{4} e^2\right) + \frac{1}{4}(1 + 3e^2) c_1, \\
\varepsilon_2 &= se + \frac{5}{2} ec_1, \\
\varepsilon_3 &= \frac{1}{4} se^2 + \frac{1}{4}\left(7 + \frac{17}{14} e^2\right) e_1, \\
\varepsilon_4 &= \frac{3}{2} ec_1, \\
\varepsilon_5 &= \frac{5}{16} e^2 c_1;
\end{aligned}\right\} \tag{18}$$

$$\left.\begin{aligned}
\zeta_1 &= \frac{1}{4}\left(1 + \frac{10}{4} e^2\right) c_2, \\
\zeta_2 &= \frac{5}{2} ec_2, \\
\zeta_3 &= \frac{1}{4}\left(7 + \frac{17}{4} e^2\right) c_2, \\
\zeta_4 &= \frac{3}{5} \zeta_2, \\
\zeta_5 &= \frac{1}{8} e\zeta_2.
\end{aligned}\right\} \tag{19}$$

/86

Here

$$s = 1 - \frac{3}{2} \sin^2 i; \quad c_1 = \sin^2 i \cos 2\omega; \quad c_2 = \sin^2 i \sin 2\omega. \tag{20}$$

Integrating expressions (14) and (15), and considering that for the perigee u = ω, we get the final expressions for determining the periodic fluctuations of parameters a and l:

$$\Delta a_{\text{пер}} = -2 \frac{\varepsilon}{\mu} \frac{1}{a(1-e^2)^3} \sum_{k=1}^{5} \frac{1}{k} [-\eta_k (1 - \cos k\omega) + \xi_k \sin k\omega], \tag{21}$$

$$\Delta e_{\text{пер}} = -\frac{\varepsilon}{\mu} \frac{1}{a^2 (1-e^2)^2} \sum_{k=1}^{1} \frac{1}{k} [-\varepsilon_k (1 - \cos k\omega) + \zeta_k \sin k\omega]. \tag{22}$$

The methodological error in determining h_π based on formulas (7), (21), and (22) is not more than 5%.

Long-periodic fluctuations in orbital elements. We will consider long-periodic fluctuations of elements of orbits whose attitude changes determine the lifetime of the satellite, i.e., the semimajor axis and the eccentricity.

Long-periodic fluctuations have been analyzed in several studies. In particular, Kozan and Brauer derived analytic expressions for orbital perturbations caused by the influence of zonal harmonics up to 14, inclusively. Kaul has developed an analytic theory of tesseral harmonics. A compilation of the formulas derived by these authors and a description of a program for the differential refinement of orbits DOI used in the United States are given in [5]. In the study [6], convenient formulas for long-periodic perturbations owing to the second harmonic were obtained on the basis of the problem of two fixed centers. A similar analysis of long-periodic perturbations for the case of near-circular orbits with reference to six harmonics is given in [7], and with reference to tesseral and sectorial harmonics -- in [8].

With reference to the stringent requirements on the speed of the computations, we limited ourselves to examining only the most essential perturbations caused by the effect of two, three, and four zonal harmonics, which in general cases is applicable for near Earth satellites.

Long-periodic oscillations of the semimajor axis a and eccentricity e in the proposed method are used in the form of the corrections Δa_g and Δl_g as the integration step.

Near-circular orbits ($e \leq 0.02$). For near-circular orbits, the following formulas were adopted [7], yielding the change in the parameters a and e in a single revolution: /87

$$\left.\begin{aligned} \frac{dq}{dN} &= A_4 - (A_2 - A_3)k, \\ \frac{dk}{dN} &= A_1 + (A_2 + A_3)q, \\ \frac{d\bar{a}}{dN} &= A_5 q, \end{aligned}\right\} \qquad (23)$$

where

$$q = e\cos\omega; \quad k = e\sin\omega; \quad \bar{a} = \frac{a}{R_e}; \qquad (24)$$

$$
\left.\begin{aligned}
A_1 &= \frac{3}{4}\frac{\pi}{\bar{p}^4}(5s_1-4)(3-2s_1)C_{20}^2,\\
A_2 &= \frac{3}{2}\frac{\pi}{\bar{p}^2}(5s_1-4)C_{20}+\frac{3}{32}\frac{\pi}{\bar{p}^4}(380s_1-445s_1^2)C_{20}^2+\\
&+\frac{15}{16}\frac{\pi}{\bar{p}^4}(16-62s_1+49s_1^2)C_{40},\\
A_3 &= \frac{3}{16}\frac{\pi}{\bar{p}^4}(-48+46s_1+15s_1^2)C_{20}^2+\frac{15}{16}\frac{\pi}{\bar{p}^4}(6s_1-7s_1^2)C_{40},\\
A_4 &= \frac{3}{4}\frac{\pi}{\bar{p}^3}\sin i\,(4-5s_1)C_{30},\\
A_5 &= \frac{9}{2}\frac{\pi}{\bar{p}^3}(5s_1-4)C_{20}^2;
\end{aligned}\right\} \qquad (25)
$$

$$
\bar{p}=\bar{a}(1-e^2);\quad s_1=\sin^2 i; \qquad (26)
$$

N is the integration step by revolutions.

The eccentricity and the argument of the latitude of the perigee of a perturbed orbit are computed in terms of q and k using the formulas

$$
e=\sqrt{q^2+k^2};\quad \omega=\arcsin\frac{k}{e}. \qquad (27)
$$

Elliptical orbits (e > 0.02). The following formulas [5, 6] were adopted for elliptical orbits:

a) owing to the second zonal harmonic

$$
a_B=a\left[1+\varepsilon_1^2\frac{(1+e\cos\omega)^3}{1-e^2}(\mu_1^3-1)\right]; \qquad (28)
$$

$$
e_B=\sqrt{e^2+\varepsilon_1^2(1+e\cos\omega)^2\left[(1+e\cos\omega)(\mu_1^3-1)-\sin^2 i\,(1-e^2)(\mu_1^2-1)\right]}, \qquad (29)
$$

where

$$
\mu_1=1+\frac{e(\cos\omega_N-\cos\omega)}{1+e\cos\omega};\quad \varepsilon_1=\frac{1}{p}\sqrt{\frac{2}{3}\frac{\varepsilon}{\mu}}, \qquad (30)
$$

a and e, and a_B and e_B are the unperturbed and perturbed values of the orbital parameters, respectively; ω and ω_N are the argument of the latitude of the orbital perigee at the initial point and at the endpoint of the integration step, respectively;

b) owing to the third zonal harmonic

$$
-\Delta e_3=-\frac{1}{2}\frac{C_{30}R_\oplus}{C_{20}a}\sin i\sin\omega. \qquad (31)
$$

The methodological error in formulas (23), and (27) - (29) does not exceed approximately 5%.

Equations of motion. The expressions obtained above for the representation of the flight altitude of AES in a revolution, and for the long-periodic oscillations in orbital elements, as well as the results of the work [1] make it possible to represent the changes in the orbital elements in a single revolution in the form: /88

$$\Delta Q = \Delta Q_g + \Delta Q_\rho; \quad (Q = \Omega, \omega, i, a, e, x, l), \tag{32}$$

where ΔQ_g and ΔQ_ρ are the perturbations of the orbital elements owing to the noncentrality of the Earth gravity field and the atmospheric drag, respectively.

For convenience in analysis, in addition to the orbital eccentricity e, we bring into consideration the linear eccentricity x = ae.

The increments of individual elements owing to each perturbing factor are defined by the formulas:

$$\Delta\Omega_g = -\frac{2\pi}{p^2}\frac{\varepsilon}{\mu}\cos i; \quad \Delta\Omega_\rho = 0, \tag{33}$$

$$\Delta\omega_g = \frac{\pi}{p^2}\frac{\varepsilon}{\mu}(5\cos^2 i - 1); \quad \Delta\omega_\rho = 0, \tag{34}$$

$$\Delta i_g = \Delta i_\rho = 0, \tag{35}$$

$$\Delta a_g = \begin{cases} \frac{da}{dN}, & e \leqslant 0{,}02, \\ \frac{a_в - a}{N}, & e > 0{,}02, \end{cases} \tag{36}$$

$$\Delta a_\rho = -a^2\delta\int_0^{2\pi}\frac{(1+e\cos E)^{3/2}}{(1-e\cos E)^{1/2}}\rho dE, \tag{37}$$

$$\Delta e_g = \begin{cases} \sqrt{\left(q+\frac{dq}{dN}\right)^2 + \left(k+\frac{dk}{dN}\right)^2} - e, & e \leqslant 0{,}02 \\ \frac{e_в + \Delta e_з - e}{N}, & e > 0{,}02, \end{cases} \tag{38}$$

$$\Delta t = \frac{2\pi}{\sqrt{\mu}} a\sqrt{a}, \tag{38a}$$

$$\Delta t_g = -\frac{2\pi}{\sqrt{\mu a}}\frac{\varepsilon}{\mu}\left[3 - \frac{5}{2}\sin^2 i - e\cos\omega(1 - 5\sin^2 i) + \right.$$
$$\left. + \frac{17}{2}e^2\left(1 - \frac{10}{17}\sin^2 i\right) + \frac{9}{2}e^2\cos 2\omega\left(1 - \frac{5}{6}\sin^2 i\right)\right], \tag{39}$$

$$\Delta x_\rho = -a^2\delta\int_0^{2\pi}\frac{(1+e\cos E)^{1/2}}{(1-e\cos E)^{1/2}}(\cos E + e)\rho dE, \tag{40}$$

where

$$\delta = \frac{FS_M C_x}{m}; \tag{41}$$

$$F = \left(1 - \frac{r_n \omega_a}{V_n} \cos i\right)^2; \tag{42}$$

ω_a is the angular rate of rotation of the atmosphere.

The quantities $a_в$, $e_в$, Δe_3, $\frac{dq}{dN}$, $\frac{dk}{dN}$, $\frac{da}{dN}$ are defined by formulas (23) and (29) - (31).

Equations (37) and (40) are the principal ones, defining the secular changes in orbit under the effect of atmospheric deceleration. An analysis of these equations for different types of orbits, with allowance for the effects of atmospheric compression and altitude scale variability, is given in [1]. However, one of the main assumptions in this work is the neglect of short-periodic oscillations in the instantaneous flight altitude owing to the noncentrality of the Earth gravity field. The effect of field noncentrality shows up most strongly for near-circular orbits; for elliptical orbits, the results of D. King-Healey are wholly suitable if the perigee altitude is used in the calculation, with allowance for the short-periodic effects (4) and (7). /89

Elliptical orbits -- $\nu = \frac{ae}{H} > 3$ $(e \geqslant 0{,}02)$. The formulas from the study [1] were taken for elliptical orbits; these formulas correspond to the case of deceleration in a compressed atmosphere with a variable altitude scale:

$$\Delta a_\rho = S_1 (\Delta_1 a + \Delta_2 a + \Delta_3 a), \tag{43}$$

$$\Delta x_\rho = S_1 (\Delta_1 x + \Delta_2 x + \Delta_3 x), \tag{44}$$

where

$$S_1 = 2\pi\delta a^2 \rho_\lambda Q^{-1} \exp\left[-(\nu_1 + c\cos 2\omega)\right] \exp\left(-\frac{\Delta a_\rho}{H_n}\right); \tag{45}$$

$$\Delta_1 a = I_0 + 2eI_1 + \frac{3}{4} e^2 (I_0 + I_2) + \frac{1}{4} e^3 (3I_1 + I_3); \tag{46}$$

$$\Delta_2 a = \frac{1}{2} bx^2 [3I_0 - 4I_1 + I_2 + e(-4I_0 + 7I_1 - 4I_2 + I_3) + \frac{3}{8} e^2 (7I_0 - 12I_1 + 8I_2 - 4I_3 + I_4)]; \tag{47}$$

$$\Delta_3 a = c\left[I_2 + 2eI_3 - \frac{1}{8} e^2 (3I_0 + 2I_2 - 17I_4)\right] \cos 2\omega + \frac{1}{4} c^2 [I_0 + 2eI_1 + [I_4 - e(I_3 - 3I_5)] \cos 4\omega]; \tag{48}$$

$$\Delta_1 x = I_1 + \frac{1}{2} e(3I_0 + I_2) + \frac{1}{8} e^2(11I_1 + I_3) + \frac{1}{16} e^3(7I_0 + 8I_2 + I_4); \quad (49)$$

$$\Delta_2 x = \frac{1}{4} bx^2\Big[(-4I_0 + 7I_1 - 4I_2 + I_3) + \frac{1}{2} e(19I_0 - 28I_1 + 12I_2 - 4I_3 + I_4) + \frac{1}{8} e^2(-44I_0 + 78I_1 - 48I_2 + 17I_3 - 4I_4 + I_5)\Big]; \quad (50)$$

$$\Delta_3 x = \frac{1}{2} c\Big[I_1 + I_3 - \frac{1}{2} e(I_0 - 6I_2 - 3I_4) - \frac{1}{8} e^2(16I_1 - 29I_3 - 11I_5)\Big]\cos 2\omega + \frac{1}{8} c^2\Big\{2I_1 + e(3I_0 + I_2) + \Big[I_3 + I_5 - \frac{1}{2} e(3I_2 - 6I_4 - 5I_6)\Big]\cos 4\omega\Big\}; \quad (51)$$

$$c = \frac{1}{2}\alpha H_{\pi}^{-1} r_{\pi} \sin^2 i; \quad (52)$$

$$H_{\pi} = -\frac{d\ln\rho}{dh_{\pi}}; \quad \nu_1 = aeH_{\pi}^{-1}; \quad b = \frac{\mu_a}{2H_{\pi}^2}; \quad (53)$$

$$Q = \frac{1 + \frac{1}{2}\mu_a\lambda^2 s^2}{\sqrt{1 + \frac{3}{4}\mu_a}}\sqrt{s}\exp(-\lambda s); \quad (54)$$

$\mu_a = \frac{dH_{\pi}}{dh_{\pi}}$ is the rate of change of the altitude scale;
is the atmospheric density at the altitude

$$h_{\lambda} = h_{\pi} + \lambda H_{\pi}; \quad (55)$$

$I_i = I_i(\nu_1)$ are the Bessel functions of the imaginary argument;
and s the relative error in specifying the scale of altitudes H.

The coefficients Q and λ were selected so as to minimize the errors in Δa_{ρ} and Δx_{ρ} owing to imprecise knowledge of the altitude scale characterized by the relative error s. For the interval /90

$$0.8 < s < 1.25 \quad (56)$$

the optimal values of Q and λ are determined by the formulas

$$\lambda = 0.5 + 0.33\mu_a, \quad (57)$$

$$Q = 0.596 - 0.25\mu_a. \quad (58)$$

Near-circular orbits, $\nu = \frac{ae}{H_{\pi}} \leqslant 3$ $(e \leqslant 0{,}02)$.

For near-circular orbits, the change of parameters a and x in a revolution is represented as the sum of the principal term that allows for deceleration in a spherically symmetric atmosphere with

a variable altitude scale, and a small correction that allows for the noncentrality of the Earth gravity field and the nonsphericity of the Earth:

$$\Delta a_\rho = S_2 \Delta_1 a + \Delta_k a, \tag{59}$$

$$\Delta x_\rho = S_2 \Delta_1 x + \Delta_k x, \tag{60}$$

where

$$S_2 = 2\pi\delta a^2 \rho_\lambda Q^{-1} \exp(-\nu_1) \exp \times \left(-\frac{\Delta a_\rho}{H_\pi}\right). \tag{61}$$

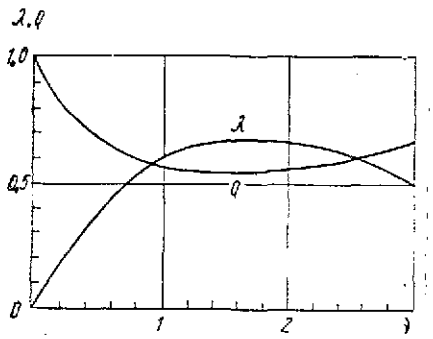

Optimal values of the coefficients Q and λ for the range of relative error $0.8 < S < 1.25$ as a function of ν.

On analogy with the case of elliptical orbits, the parameters Q and λ are introduced to compensate for possible errors in the assignment of the altitude scale. Their optimal values are shown in the figure for the range of relative error (56).

Based on formulas (37) and (40), the expressions for the corrections $\Delta_K a$ and $\Delta_K x$ can be represented as:

$$\Delta_k a = a^2\delta\left[\int_0^{2\pi} \frac{(1+e\cos E)^{3/2}}{(1-e\cos E)^{1/2}}\,\bar{\rho}\,dE - \int_0^{2\pi} \frac{(1+e\cos E)^{3/2}}{(1-e\cos E)^{1/2}}\,\rho\,dE\right], \tag{62}$$

$$\Delta_k x = a^2\delta\left[\int_0^{2\pi} \frac{(1+e\cos E)^{1/2}}{(1-e\cos E)^{1/2}}(\cos E + e)\,\bar{\rho}\,dE - \right.$$

$$\left. - \int_0^{2\pi} \frac{(1+e\cos E)^{1/2}}{(1-e\cos E)^{1/2}}(\cos E + e)\,\rho\,dE\right], \tag{63}$$

where

$$\bar{\rho} = \rho_n \exp\left(\frac{r_n - r}{H_\pi}\right); \tag{64}$$

$$\rho = \bar{\rho}\exp(\beta); \tag{65}$$

$$\beta = -\frac{\Delta h_{\text{per}}}{H_\pi}. \tag{66}$$

Expanding in a power series and considering only the linear and quadratic terms in β, we can represent expressions (62) and (63) as:

$$\Delta_k a = -a^2\delta \int_0^{2\pi} \frac{(1+e\cos E)^{3/2}}{(1-e\cos E)^{1/2}} \bar{\rho}\left(\beta + \frac{\beta^2}{2}\right) dE, \tag{67}$$

$$\Delta_k x = -a^2\delta \int_0^{2\pi} \frac{(1+e\cos E)^{3/2}}{(1-e\cos E)^{1/2}} (\cos E + e)\,\bar{\rho}\left(\beta + \frac{\beta^2}{2}\right) dE. \tag{68}$$

Converting, in formulas (67) and (68), to a new independent variable -- the true anomaly η -- after integration and subsequent transformations, we get to a precision of about 2%: /91

$$\Delta_k a = \pi a^2 \delta\rho_n (1+e) \frac{\exp(-\nu_2)}{H_\pi} \varphi, \tag{69}$$

$$\Delta_k x = \pi a^2 \delta\rho_n \frac{\exp(-\nu_2)}{H_\pi} [2e\varphi + (1-e) f], \tag{70}$$

where

$$\nu_2 = \frac{ae}{H_\pi} \frac{1-e}{1+e}; \tag{71}$$

$$\varphi = I_0(B-2C) + 2I_1 C\cos\omega - BI_2\cos 2\omega - \frac{1}{2H_\pi}\left\{\frac{1}{2} I_0\left[(B-2C)^2 + \right.\right.$$
$$+ \frac{1}{2}(B^2+4C^2)\Big] + B^2\left(\frac{1}{4} I_4\cos 4\omega - I_2\cos 2\omega\right) + 4C\left[C\left(\frac{1}{4} I_2\cos 2\omega - \right.\right.$$
$$\left.\left.\left. - I_1\cos\omega\right) - \frac{1}{2} B\left[\frac{1}{2}(I_1+I_3)\cos\omega\cos 2\omega - I_2\cos 2\omega - I_1\cos\omega\right]\right]\right\}; \tag{72}$$

$$f = CI_0\cos\omega + I_1\left[B\left(1-\frac{1}{2}\cos\omega\right) - 2C\right] - CI_2\cos\omega - \frac{1}{2} I_2 B\cos\omega -$$
$$- \frac{1}{4H_\pi}\left\{2\left[\frac{3}{4} B^2 + C(3C-2B)\right] I_1 + [C^2 - B(B-2C)](I_1+I_3)\cos 2\omega + \right.$$
$$\left. + 2C(B-2C)(I_0+I_2)\cos\omega + \frac{1}{4} B^2(I_3+I_5)\cos 4\omega - BC(I_0+2I_2 + \right.$$
$$\left. + I_4)\cos\omega\cos 2\omega\right\}; \tag{73}$$

$$I_i = I_i(\nu_2); \tag{74}$$

See (5) and (6) for B and C.

We must note that since the origin of reference of the short-periodic fluctuations in flight altitude (4) corresponds to the

instant the ascension node is traversed, to compute the increments $\Delta_k a$ and $\Delta_k x$ by formulas (69) and (70), we must use as the starting data the orbital elements for this same instant of time. In particular, the perigee altitude is computed by the formulas

$$h_p = a(1-e) - R_e . \tag{75}$$

REFERENCES

1. King-Healey, D., Teoriya orbit iskusstvennykh sputnikov v atmosfere [Theory of orbits of artifical satellites in the atmosphere], "Mir," Moscow, 1966.

2. El'yasberg, P.Ye., Vvedeniye v teoriyu poleta iskusstvennykh sputnikov Zemli [Introduction to the theory of the flight of artificial Earth satellites], "Nauka," Moscow, 1965.

3. Okhotsimskiy, D.Ye., T.M. Eneyev, and G.P. Taratynova, UFN 63(1) (1957).

4. Taratynova, G.P., Iskusstvennyye sputniki Zemli, No. 4 (1960).

5. Gaposhkin, Ye.M., in the book: Standartnaya Zemlya [Standard Earth], "Mir," Moscow, 1969.

6. Kislik, M.D., Iskusstvennyye sputniki Zemli [Artificial Earth satellites], Nos. 4 and 13, USSR Academy of Sciences Press, Moscow, 1960.

7. Kugayenko, B.V. and P.Ye. El'yasberg, Kosmicheskiye issledovaniya 6(3) (1968).

8. Ustinov, B.A., Kosmicheskiye issledovaniya, No. 2 (1967).